BERICHTE
aus dem Fachbereich Geowissenschaften
der Universität Bremen

No. 217

Kallmeyer, J.

SULFATE REDUCTION IN THE DEEP BIOSPHERE

Berichte, Fachbereich Geowissenschaften, Universität Bremen, No. 217.
161 pages, Bremen 2003

ISSN 0931-0800

The "Berichte aus dem Fachbereich Geowissenschaften" are produced at irregular intervals by the Department of Geosciences, Bremen University.
They serve for the publication of experimental works, Ph.D.-theses and scientific contributions made by members of the department.

Reports can be ordered from:

Monika Bachur

Forschungszentrum Ozeanränder,

RCOM

Universität Bremen

Postfach 330 440

D 28334 BREMEN

Phone: (49) 421 218-8960

Fax: (49) 421 218-3116

e-mail: *MBachur@uni-bremen.de*

Citation:

Kallmeyer, J.

Sulfate reduction in the deep Biosphere.

Berichte, Fachbereich Geowissenschaften, Universität Bremen, No. 217, 161 pages, Bremen, 2003.

ISSN 0931-0800

Sulfate reduction in the deep biosphere

Dissertation zur Erlangung des Doktorgrades
eingereicht am Fachbereich 5, Geowissenschaften
an der Universität Bremen

vorgelegt von Jens Kallmeyer
Bremen, Juni 2003

Tag des Kolloquiums: 7. August 2003
Gutachter: B. B. Jørgensen, J. Peckmann
Prüfer: K. Hinrichs, M. Zabel

Inhalt

Abstract

Dissimilatory sulfate reduction is the quantitatively most important terminal electron acceptor process in marine sediments. Sulfate reducing microorganisms are known to be able to live under almost all pressure and temperature conditions that allow life.

Sulfate reduction rates (SRR) in the deep sub-seafloor biosphere are several orders of magnitude lower than in shallow sediments. In most cases SRR in the deep biosphere were too low to be detected by standard radiotracer techniques. Therefore, a new radiotracer technique was developed that allows the detection of very low rates of sulfate reduction. This new technique was used to measure sulfate reduction rates in samples from the Peru continental margin to depths > 100 mbsf.

Additionally to the measurements, rates were mathematically modeled. In many cases where no sulfate reduction could be measured, the model suggest rates that are lower than the minimum detection limit of the radiotracer technique.

By calculating cumulative rates of sulfate reduction over depth it was shown that over 99 % of all sulfate reduction happens in the upper four meters of the sediment where methane is usually not occurring. It can therefore be concluded that in these sediments methane is not a significant carbon source for total sulfate reduction.

To incubate multiple samples under elevated pressure over a wide range of temperatures, a high-pressure thermal gradient block was developed. Samples from the hydrothermal vents of Guaymas Basin were incubated and analysed for rates of sulfate reduction and anaerobic oxidation of methane. The sulfate reducing microorganisms are thermophilic ot hyperthermophilic and show a strong increase in metabolic activity at higher pressure, the sulfate reduction rates increase by about an order of magnitude. Anaerobic oxidation of methane was shown at temperatures > 60 °C. However, the quantitative importance of methane as a carbon source for sulfate reduction is only minor.

Zusammenfassung

Dissimilatorische Sulfatreduktion ist der quantitativ wichtigste terminale Elektronenakzeptorprozeß. Sulfatreduzierer können unter fast allen Druck- und Temperatur Bedingungen unter denen Leben überhaupt bekannt ist, vorkommen. Sulfatreduktionsraten (SRR) in der tiefen Biosphäre sind um mehrere Größenordnungen geringer als in Oberflächensedimenten.

In vielen Fällen sind die SRR in der tiefen Biosphäre zu gering um mit den normalen Radioaktiv-Meßmethoden gemessen zu werden. Aus diesem Grunde wurde eine neue Methode entwickelt, welche es erlaubt sehr geringe SRR zu messen. Diese neue Methode wurde benutzt,um SRR in Proben aus Teufen > 100 m vom peruanischen Kontinentalhang zu messen.

Zusätzlich zu den Messungen wurden SRR auch mathematisch modelliert. In vielen Fällen wo auch die neue Meßmetode keine SRR feststellen konnte, waren die modellierten Raten unter der Nachweisgrenze der Radioaktiv-Meßmethode. Durch Berechnung der kumulativen Sulfatreduktionsrate über die Teufe konnte gezeigt werden, daß über 99 % der Sulfatreduktion in den oberen vier Metern des Sediments ablaufen, einer Teufe in der Methan normalerweise nicht auftritt. Daraus kann gefolgert werden, daß Methan keine signifikante Kohlenstoffquelle für die Gesamtmenge der Sulfatreduktion ist.

Um mehrere Proben gleichzeitig unter hohem Druck und über einen großen Temperaturbereich zu inkubieren wurde ein Hochdruck-Thermogradientenblock entwickelt und gebaut. Proben von den hydrothermalen Quellen vom Guaymas Becken wurden inkubiert und Sulfatreduktionsraten und Raten anaerober Methanoxidation bestimmt. Die Sulfatreduzierer sind thermophil und hyperthermophil und zeigen einen starken Anstieg ihrer metabolischen Aktivität unter erhöhten Drücken. Die SRR erhöhen sich um ungefähr eine Größenordnung. Anaerobe Methanoxidation konnte nachgewiesen werden bis zu Temperaturen > 60 °C. Die quantitative Bedeutung von Methan als Kohlenstoffquelle für Sulfatreduktion ist allerdings nur gering.

1 Introduction

Parkes et al., (1994) estimated that the biomass of the entire sub-seafloor biosphere would account for only 0.004 % of the global sedimentary organic carbon but it would account for ca. 10 % of the living biomass in the global biosphere. The fact that 10 % of the global biosphere is located in deep sub-seafloor sediments is surprising, as only just a few years ago it was not commonly agreed that a deep biosphere actually exists. Since those pioneering studies many advances have been made but still research in the deep biosphere remains problematic due to technical difficulties and limited access to samples.

Like in shallow environments, microorganisms in the deep biosphere are diverse and well adapted to their environment. They have considerable impact on their physical and chemical environment, including environments of commercial interest e.g. gas hydrate deposits, oil and gas reservoirs, and potential sites for nuclear waste storage.

Microorganisms from these environments are extremophiles in terms of optimum temperature range and pressure adaptation, and might have considerable biotechnological application (e.g. bioremediation, waste treatment, new biomolecules like enzymes, and for microbially enhanced oil recovery).

However, the deep subsurface sediment layers were deposited thousands to millions of years ago and microbial processes which take place in them are extremely slow. The rates of degradation of organic matter or of microbial metabolism are near or below the limit of detectability with many of the present experimental methods.

Deep-sea hydrothermal vents were discovered before the deep sub-seafloor biosphere. The discovery of such vents and their inhabitants revealed that a large portion of microorganisms could flourish at extreme conditions, including very high temperatures, low or high pH, high salt concentrations, elevated hydrostatic pressure or ionizing radiations.

The recent discovery of extensive microbial populations beneath the deep ocean floor and in other extreme environments has far reaching implications. In spite of the progress made in identifying physiochemical and locational frontiers of life on Earth, the true limits are still unknown.

These affect not only our immediate understanding of the biosphere, but also many other branches of science, as well as industrial processes. The discovery that bacteria

survive in far more extreme conditions than previously thought possible is causing us to revise our theories of how life began on Earth. These findings also provide the impetus for studying remote objects in the solar system where life could not be seriously imagined just a few years ago.

1.1. Biological Sulfate reduction and the marine sulfur cycle

Most organic matter that reaches the sea floor is remineralized via oxic respiration (see Wenzhöfer and Glud, 2002, and references therein). The quantitatively largest part of organic matter that becomes buried below the oxic zone of the sediment is oxidized through sulfate reduction (Jørgensen, 1982b). Canfield (1989) showed that in near-shore sediments about equal amounts of organic matter are re-mineralized via oxic respiration and sulfate reduction.

Froelich et al. (1979) showed that those electron acceptors that have the highest energy yield are preferentially utilized by the microorganisms and are therefore depleted at a shallower depth than others. Based on the energy yield a typical zonation occurs in the sediment, with the electron acceptors used in the following sequence: oxygen, nitrate, manganese, and iron.

Depending on the availability of electron donors, those electron acceptors with a higher energy yield are usually depleted within the top few millimeters (coastal sediments) to meters (open ocean) of the sediment (Froelich et al., 1979, Jørgensen, 1982b).

Froelich et al. (1979) however, did not recognize the importance of sulfate reduction as their reaction scheme did not cover sulfate reduction. At the sediment-water interface, dissolved sulfate concentrations are over 50 times higher than all electron acceptors with higher standard free energies (e.g. nitrate, iron, manganese) together (D'Hondt et al., 2002). Jørgensen (1982b) was the first to highlight the quantitative importance of sulfate reduction in marine sediments. Since then, the importance of sulfate reduction in the degradation of organic matter in marine sediments has been shown in numerous studies.

The dissimilatory reduction of sulfate to sulfide by bacteria at the sea floor is a key process in the oceanic sulfur cycle (Jørgensen, 1982b). In this process, sulfate is utilized as an electron acceptor for energy generating processes, in most cases the oxidation of organic material. Many organisms, like higher plants, algae, fungi, and

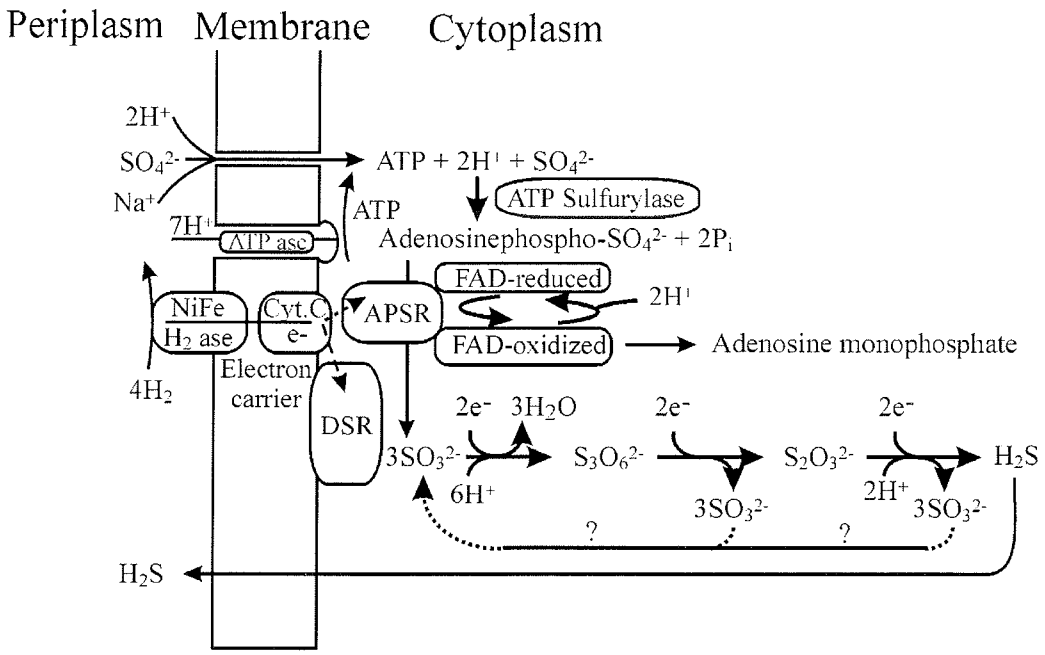

Fig. 1.1.1: The cellular mechanisms of sulfate reduction (from V. Brüchert)

many bacteria, use sulfate as a source of sulfur for biosynthesis; however, assimilatory sulfate reduction is of little quantitative importance as sulfur comprises only 1 % of the dry mass of organisms.

1.1.1 The cellular mechanisms of sulfate reduction

The sulfate reducing microorganisms occur among the bacteria and archaea (Canfield and Raiswell, 1999; Canfield and Teske, 1996) and are key players in the connection between carbon and sulfur cycle. They utilize inorganic sulfur compounds as extracellular electron carriers to convert organic to inorganic carbon. For each sulfate that is reduced to hydrogen sulfide eight electrons are transferred.

According to Cypionka (1989) sulfate is transported into the cell via a symport, taking up two sodium ions for marine sulfate reducers and with protons in freshwater sulfate reducers (Fig. 1.1.1). This so-called symport takes up two positive charges for each transported sulfate ion. The transport of sulfate through the cell membrane is depending on and proportional to a proton potential (the outside of the cell has lower pH) or a cross-membrane gradient of sodium ions. 3 protons are consumed per sulfate ion imported, which corresponds to the consumption of 1/3 ATP if sulfate accumulation is in equilibrium with the proton motive force (Widdel, 1988). Freshwater species

can concentrate sulfate within the cell up to 5000-fold (Cypionka, 1989) Different transport mechanisms have been described and there is indication of membrane impermeability to preserve the proton motive force for ATP synthesis because sulfate transport is reversible. The details of membrane transport regulation are still under investigation, but it is clear that a fine-tuned regulation of transport at the genetic and activity level is required to prevent the loss of membrane potential due to the reversible transport of sulfate (Cypionka, 1994). The regulation of transport is important as without the proton motive force to retain a positive charge on the outside of the cell, no new ATP could be synthesized and the cell would be deactivated.

After transporting the sulfate ion into the cell, the second step during sulfate reduction proceeds, the intracellular activation of the sulfate molecule by an ATP sulfurylase to produce adenosine phosphosulfate (APS) and pyrophosphate (PP_i). This is an energy-consuming process that requires one mole ATP per mole of sulfate (Cypionka, 1995). At high concentrations of APS and pyrophosphate this step is reversible, therefore the APS concentration has to be kept at < 0.1 mM to pull the reaction towards APS through further reduction steps. In a parallel reaction PPi is hydrolyzed to phosphate (2 P_i) (Rabus et al., 2000).

In the third step, the activated APS complex is reduced by a cytoplasmic APS reductase to release sulfite. In step four the sulfite is further reduced to sulfide by the cytoplasmic enzyme dissimilatory sulfite reductase (DSR). The exact electron donor for the APS and DSR for the different sulfate reducing-bacteria is not known (Hansen, 1994). The end product, hydrogen sulfide, is finally transported out of the cell.

1.1.2 Sulfide oxidation

H_2S is an important electron carrier between the anaerobic and the aerobic part of the sulfur cycle. Numerous bacteria have the metabolic potential to oxidize hydrogen sulfide with various electron acceptors, and to gain energy by this process (Jørgensen, 1982a).

One of the most impressive manifestations of sulfide oxidizing bacteria are the giant nitrate-storing species from the genus Beggiatoa, Thioploca, and Thiomargarita, the latter one being the largest bacteria ever found (Fossing et al., 1995; Ferdelman et al., 1997; Schulz et al., 1999).

Aller and Rude (1988) showed that in anoxic marine sediments manganese oxides can be utilized by bacteria to anaerobically oxidize elemental sulfur and reduced

sulfur compounds to sulfate. Through this process sulfate can be re-generated and thereby allow further sulfate reduction. Mixtures of manganese oxides and reduced sulfur species can occur close to the sediment-water interface where burrowing organisms rework the sediments continuously. Through this process oxidized particles are brought into deeper anoxic layers of the sediment. Aller and Rude (1988) also showed that sulfide is not oxidized to sulfate with iron oxides as electron acceptors. Thamdrup et al. (1993) showed that marine chemolithotrophic bacteria are able to disproportionate elemental sulfur to sulfate and sulfide in the presence of iron oxides. The products were sulfate, ferrous sulfide (FeS) and pyrite (FeS_2). When incubating the cultures with manganese oxides instead of iron oxides, then Mn^{2+} and sulfate was produced. A few very detailed studies give a description of the biogeochemical pathways of sulfide oxidation in marine sediments (Schippers and Jørgensen, 2001; Schippers and Jørgensen, 2002). They used radiolabelled ^{55}Fe to trace the reduction of iron monosulfides and pyrite by manganese oxides.

Hydrogen sulfide is not directly re-oxidized to sulfate but via thiosulfate ($S_2O_3^{2-}$) as an intermediate (Jørgensen, 1990). The two sulfur atoms in thiosulfate have different valence states, +6, the same as in sulfate, and -2, like in sulfide. There are three possibilities for thiosulfate to further react, either oxidized to sulfate (Eq. 1.1.1), reduced with organic matter as an electron donor (Eq. 1.1.2), or disproportionated to sulfate and sulfide (Eq. 1.1.3)

$$2\ S_2O_3^{2-} + 5O_2 = 4\ SO_4^{2-} \qquad \text{Eq. 1.1.1}$$

$$S_2O_3^{2-} + CH_3COO^- + H^+ = 2HS^- + 2\ CO_2 + H_2O \qquad \text{Eq. 1.1.2}$$

$$S_2O_3^{2-} + H_2O = HS^- + SO_4^{2-} + H^+ \qquad \text{Eq. 1.1.3}$$

All three reactions are biologically mediated and do not occur spontaneously under environmental conditions. The disproportionation of thiosulfate does not require electron donors or acceptors, but the products (sulfate and hydrogen sulfide) have oxidation states that differ from the mean oxidation state of thiosulfate. By using thiosulfate as an intermediate the electron flow between the oxidative and the reductive part of the sulfur cycle can be regulated. Depending on the environmental conditions, thiosulfate can be used as either an electron donor or acceptor.

It also acts as a "shunt" in the sulfur cycle as it partially decouples the oxidation of organic matter from the reduction of electron acceptors. Through disproportionation of

thiosulfate the large isotopic fractionation between sulfate and sulfide can be explained. While the inner S-atom (valence +6), which is relatively enriched in ^{34}S is converted to sulfate, the outer S-atom (valence -2) is converted to sulfide. By this mechanism isotopically lighter sulfur will be enriched in sulfide.

While the aforementioned bacteria are generally chemotrophic, there are also phototrophic genera, like Chlorobium, Chloroflexus, Chromatium etc. (e.g. Brock and Madigan, 1984). These organisms have unique metabolic pathways, allowing them to fix CO_2 while oxidizing hydrogen sulfide or thiosulfate.

1.1.3 Organiclastic vs. methanotrophic sulfate reduction

Sulfate reduction (SR) can broadly be divided into two main pathways: (1). Organoclastic SR that utilises low molecular weight substrates derived from fermented particulate or dissolved organic matter (Jørgensen, 1982a), and (2) methanotrophic SR that is driven by methane utilising consortia involved in the anaerobic oxidation of methane (AOM) (Boetius et al., 2000; Orphan et al., 2001).

The two reactions can be expressed by the following reactions .

Organoclastic SR:	$2\ CH_2O + SO_4^{2-} = 2\ HCO_3^- + H_2S$	Eq. 1.1.4
Methanotrophic SR:	$CH_4 + SO_4^{2-} = HCO_3^- + HS^- + H_2O$	Eq. 1.1.5

In the upper centimeters to meters of the sediment column, organiclastic SR is normally the dominant anaerobic process for the degradation of organic matter, due to the abundance of easily degradable organic matter. With increasing depth the fraction of recalcitrant organic matter becomes larger and SR decreases (Jørgensen, 1982a; Jørgensen, 1982b). The recalcitrant organic matter that is not utilised by sulfate reducers is then further degraded by different, mostly acetogenic and methanogenic, microorganisms (Parkes et al., 1993). The biologically produced methane diffuses upwards and finally reaches the zone where sulfate is available. In the narrow zone where sulfate and methane overlap, the sulfate-methane transition zone (SMZ), methanotrophic SR takes place. It was shown in several studies, that in this zone a narrow band of high SRR occurs before sulfate is depleted and therefore SR stops (Iversen and Jørgensen, 1985; Hoehler et al., 1994; Niewöhner et al., 1998; Adler et al., 2000). However, through the influx of brines or lateral fluid flow, sulfate may increase again at greater depth, and in such cases microbial SR can take place again

in the presence of a suitable electron donor (Böttcher et al., 1999; Böttcher et al., 1998; Worthmann et al., 2001).

Martens and Berner (1974) described the accumulation of methane in marine sediments only after sulfate is approaching depletion. Iversen and Jørgensen (1985) showed the 1:1 stoichiometry of sulfate reduction and methane oxidation in the sulfate-methane transition zone. However, methanotrophic SR remained elusive, as it was not clear which organism is responsible for the reaction. Hoehler et al. (1994) proposed a consortium of several different microorganisms responsible for the process and Boetius et al. (2000) finally identified aggregates that are capable of anaerobic methane oxidation. These clusters consist of archaea that apparently do reverse methanogenesis, surrounded by sulfate reducing bacteria. Orphan et al. (2001) additionally confirmed the methanotrophic metabolism by isotope analysis of the biomass. The isotopic signal of carbon was extremely negative and could only be derived from methane.

Although much progress has been made on the biology of these aggregates, the details of the overall reaction are still not fully understood. The archean metabolic products that are transferred to the sulfate reducers who then produce CO_2 and HS^- are still to be identified, H_2 or acetate being the most likely candidates.

The sulfate-methane transition zone is generally between 0.3 and 1 meter thick but can extend to up to tens of meters. As a rule of thumb Jørgensen et al. (2001) suggests the lower 10 % of the sulfate penetration depth for the estimated thickness of the transition zone. The thickness of the transition zone is surprising, considering the resulting long turnover times. It is still not clear why the process is so sluggish but may partly be explained by the small energy yield of only 25 kJ mol^{-1} under in situ conditions (Valentine and Reeburgh, 2000). In comparison, the reaction
$2\ CH_2O + SO_4^{2-} = 2\ HCO_3^- + H_2S$ yields 77 kJ mol^{-1}.

1.2 Thermochemical Sulfate reduction

Thermochemical Sulfate reduction (TSR) is the abiological, thermally driven reaction between organic carbon compounds and sulfate.

The geological settings in which TSR occurs are considerably different to those of biological sulfate reduction (BSR). TSR is most common at Mid Ocean Ridges (MOR), in Mississippi Valley Type (MVT) ore deposits, and in sour gas and oil reservoirs (Machel, 2001).

The main organic reactants for TSR are branched n-alkanes, followed by cyclic and mono-aromatic species. Sulfate is normally derived from the dissolution of gypsum ($CaSO_4 * 2H_2O$) and/or anhydrite ($CaSO_4$) (Machel, 2001).

The overall and simplified TSR reaction is given in Eq. 1.2.1.

$$CaSO_4 + CH_4 = CaCO_3 + H_2S + H_2O \qquad \text{Eq. 1.2.1}$$

Under almost all natural geochemical conditions, anhydrite and methane are thermodynamically unstable with respect to H_2S and oxidised carbon compounds like CO_2 and carbonates. Based on their modelling results Amurskii et al. (1977) state that TSR should take place in a direct chemical reaction (Eq. 1.2.1) at temperatures higher than 23 – 25 °C.

While the chemical reaction pathway has widely been accepted, the minimum temperature at which TSR starts is still discussed. There are numerous sweet (non H_2S-bearing) hydrocarbon reservoirs in different geological settings around the world bearing sulfate-containing minerals and having experienced temperatures > 25 °C, which contradict the results of Amurskii et al. (1977)

Experimental data suggest a much higher minimal temperature than 25 °C (see Trudinger et al., 1985; Machel, 2001, and references therein). However, it has to be noted that many of these experimental data have to be considered with caution, as the experimental set-ups often included stainless steel or glass reaction vessels, which at elevated temperatures can influence the reaction in many ways by reacting with the reagents of giving off compounds that influence the reaction. This problem was addressed by Cross (1999) who used annealed massive gold reaction vessels with titanium lids. His results deviate from previous experiments, which he partially attributes to the inert materials of his set-up.

The TSR reaction is fast on a geological timescale but orders of magnitude lower than biological sulfate reduction at shallow depths and low temperatures (< 100 °C). The half-life of sulfate increases with decreasing temperature, therefore experiments at low temperatures failed (Trudinger et al., 1985). At 200 °C, the half-life of sulfate in acetic acid is 5.75 years, and extrapolation to 100 °C suggests an increase to 3.9 million years (Kiyosu and Krouse, 1990). By adding small amounts of elemental sulfur the half-lives are reduced to 40 days and 395 years, for 200 °C and 100 °C, respectively.

In the presence of Toluene the half-life of sulfate at 250 °C is reduced to 94 hours (Goldhaber and Orr, 1995).

The lowest temperature at which TSR has been proven experimentally is 175 °C (Goldhaber and Orr, 1995). Geological field observations suggest a much lower temperature for TSR, the lowest temperature reported is 127 °C (Machel, 2001). The apparent contradiction between the modelled data on the one side and geological and experimental data on the other, have been explained by high activation energy. Through enzymatic reactions this energetic burden can be overcome by sulfate reducing microorganisms during biological sulfate reduction. TSR proceeds fast as soon as the required activation energy is overcome. In order to detect any TSR experimentally, high temperatures have been used to overcome the activation energy and the results were extrapolated to lower temperatures.

Most experimental studies have been carried out at pH values that are several units lower than those occurring naturally, but Cross et al., (submitted) have found that the TSR reaction is independent of the pH in the range of pH 4 – 6, which is normally found in hydrocarbon reservoir formation waters.

1.2.1 TSR mechanisms in hydrocarbon reservoirs.

H_2S in hydrocarbon reservoirs is economically undesirable as it is very corrosive and toxic. High H_2S concentrations (up to 78.1 mol % in the gas phase) in hydrocarbon reservoirs may be caused by TSR (for a review see Cross, 1999). Such high levels of H_2S can not be achieved by BSR as concentrations above ca. 10 % poison the microorganisms and thereby inhibit any further reaction (Widdel, 1988).

Additionally TSR can lead to the redistribution of porosity within the reservoir due to anhydrite dissolution, precipitation of carbonates and solid sulfides, and the formation of pyrobitumen. TSR can cause dilution of hydrocarbon gases with H_2S and CO_2 (Cross et al., submitted) or even complete destruction.

The reaction pathway and the stoichiometry of the TSR reaction was long debated (see Cross, 1999, for a review)

Worden et al. (2000) proposed a five-step model for the TSR reaction.

1) Dissolution of the solid phases to pass into the aqueous phase for reaction.
2) Transport of the reactants to the site of reaction
3) The actual chemical reaction of sulfate to sulfide. This step may involve several reaction steps

4) Transport of the product away from the reaction site to prevent them from inhibiting further reaction
5) Precipitation from solution may occur if the conditions are favourable.

1) Dissolution of the solid phases to pass into the aqueous phase for reaction.
A direct reaction between solid anhydrite and liquid or gaseous hydrocarbons is unlikely for several reasons. Even in the hydrocarbon-bearing zones of a reservoir, there is still some residual water. Anhydrite is a hydrophilic mineral, its surface has a greater affinity to polar water than to apolar hydrocarbons and therefore a thin layer of water separates the anhydrite from the hydrocarbons. This film of water forms an effective barrier to prevent a direct reaction to take place. The modelling results of Simpson (1996) suggest that the TSR reaction is endothermic, which would make the reaction between solid anhydrite and liquid hydrocarbon even less favourable. Moreover, Stasiuk (1996) found TSR reaction textures in solid pyrobitumen. In case solid anhydrite was the source of sulfate, it would be a solid-solid reaction, which is kinetically even less favourable than a solid-liquid reaction.

Reactions between solid anhydrite and gaseous hydrocarbons were, if they ever occurred, extremely slow because they would be inhomogeneous reactions which are orders of magnitude slower than homogenous reactions that occur in solutions (Lasaga and Kirkpatrick, 1981).

Worden et al. (2000) concluded that the thin layer of water around the mineral can not be the site where the TSR reaction takes place because it would not account for the large scale of the reaction in some reservoirs. The only possible way for TSR to occur is with sulfate in aqueous solution originating from anhydrite dissolution. Because of the limited miscibility of hydrocarbons and water, such an reaction may not account for the large scale of TSR in certain reservoirs as the available reaction surface is only small. Therefore a single solution which contains all reactants is favoured as the major mechanism for TSR. Bildstein et al. (2001) used a multi-disciplinary approach to identify the rate limiting step during the TSR reaction. Based on their modelling results and petrographic observations they concluded that the rate-controlling step evolves initially from (1) the rate of aqueous redox interaction between sulfate and hydrocarbons and (2) the rate of diffusion-controlled dissolution of anhydrite. (Bildstein et al., 2001) used this two-step rate control mechanism to explain the high minimum temperature found in TSR experiments as well as the

coexistence of anhydrite and hydrocarbons in reservoirs where TSR is already at an advanced stage.

2) Transport of the reactants to the site of reaction.
The current state of research suggests that at least in hydrocarbon reservoirs TSR takes place in very close proximity to solid anhydrite. Transport occurs mainly by diffusion and on such small distances differences in the diffusion rates of the reactants are negligible. Cross (1999) lists several case studies from hydrocarbon reservoirs, where solid anhydrite has been replaced by secondary calcite. Apparently the entire five-step reaction scheme of Worden et al. (2000) occurred within less than a milimeter.

3) The actual reduction of sulfate to sulfide.
This step may involve several reaction steps because TSR is significantly more complicated than Eq. 1.1 suggests. There is little doubt that Anhydrite is the major source for sulfate species in hydrocarbon reservoirs. However, methane is unlikely to be the only reducing agent when other hydrocarbons like ethane, propane, and organic acids are present. Worden and Smalley, (1996) showed that elemental sulfur can be found in many if not all hydrocarbon reservoirs that have undergone TSR, but in some cases only in very small amounts. It is not possible to convert all sulfate to hydrogen sulfide with hydrocarbons of a higher mass than methane, because there is a decrease in the H:C ratio with increasing mass. Therefore reactions with hydrocarbons of higher mass are important for the generation of elemental sulfur.

Equation 1.2.2 shows a more general way of describing the stoichiometry of the TSR reaction.

$$n\ CaSO_4 + CnH2n+2 = n\ CaCO_3 + H_2S + (n-1)S^0 + n\ H_2O \qquad \text{Eq. 1.2.2}$$

With methane as hydrocarbon (n = 1) no elemental sulfur is produced. For higher hydrocarbons (n > 1) the fraction of produced elemental sulfur becomes increasingly larger.

However, equation 2 does not indicate how the reduction of sulfate to sulfide occurs and how and why there is strong TSR in certain reservoirs although only tracer amounts of elemental sulfur have been found.

All successful TSR experiments had sulfide and/or elemental sulfur initially present in the reaction. Without those two reagents it was not possible to initiate the reaction (Trudinger et al., 1985). Based on the experimental work of Toland (1960), Orr (1992) suggested the following combination of reactions.

$$SO_4^{2-} + 3\ H_2S = 4\ S^0 + 2\ H_2O + 2\ OH^- \qquad \text{Eq. 1.2.3}$$

$$4\ S^0 + 1.33\ CH_2 + 2.66\ H_2O = 4\ H_2S + 1.33\ CO_2 \qquad \text{Eq. 1.2.4}$$

When combining the two reactions the net reaction can be expressed as follows:

$$SO_4^{2-} + 1.33\ (CH_2) + 0.66\ H_2O = H_2S + 1.33\ CO_2 + 2\ OH^- \qquad \text{Eq. 1.2.5}$$

There are several notable factors in the above reactions:

1) The reaction produces H_2S but much of it is used to initiate the further reaction.
2) The H_2S reacts directly with sulfate. This requires an initial presence of H_2S of non-thermogenic origin.
3) Elemental sulfur is an important intermediate in the reaction but it does not accumulate.
4) A base is formed, but the TSR reaction is know to proceed under acidic conditions.
5) Water is consumed, but according to Worden et al. (1996) the TSR reaction is known to produce water.
6) The replacement of anhydrite by calcite is not addressed.

To account for the facts that the TSR reaction proceeds under acidic conditions and a net production of water takes place, equation 1.2.5 was re-written by Worden et al. (1996)

$$3SO_4^{2} + 4\ (CH_2) + 6\ H^+ = 3\ H_2S + 4\ CO_2 + 4H_2O \qquad \text{Eq. 1.2.6}$$

Equation 1.2.6 does not explain the replacement of anhydrite to calcite. By combining Eq. 1.2.3 to 1.2.6, an overall reaction scheme, consisting of two equations can be derived (Eq. 1.2.6 and 1.2.8)

$$3n+1S^0 + 2n+H_2O + CnH_{2n+2} = 3n+1H_2S + nCO_2 \qquad \text{Eq. 1.2.7}$$

$$nCaSO_4 + 3nH_2S + nCO_2 = nCaCO_3 + 4nS^0 + 3nH_2O \qquad \text{Eq. 1.2.8}$$

$$nCaSO_4 + CnH_{2n+2} = nCaCO_3 + H_2S + 3nH_2O + (n-1)S^0 \qquad \text{Eq. 1.2.2}$$

When added together equations 1.2.7 and 1.2.8 reduce to Eq. 1.2.2. Equation 1.2.7 allows for the formation of H_2S that will react with sulfate in Eq. 1.2.8. H_2S and water are produced in the net reaction and anhydrite is replaced by calcite. If higher hydrocarbons are the reducing agent, S^0 will accumulate. To start the TSR reaction either sulfide or elemental sulfur have to be present.

The results of Worden et al. (1996) show that there is no reaction between aqueous sulfate and sulfide in the range of possible reservoir conditions without the presence of a catalyst. They also showed that without a catalyst there is no reaction between toluene and aqueous sulfate. The reduction of sulfate to sulfide might proceed via several low-valence sulfur intermediates, like thiosulfate, elemental sulfur and sulfite (e.g. Goldhaber and Orr, 1995; Ohmoto and Lasaga, 1982).

Eq. 1.2.8 shows the formation of elemental sulfur as an intermediate, but through slight changes in composition of the reactants or the reaction conditions other intermediates can be used instead. The modelling results of Amurskii et al. (1977) suggest that an assemblage of methane and sulfate is unstable under most diagenetic conditions. The TSR reaction is thermodynamically impossible at temperatures < 20 °C and becomes favourable at temperatures above 23 °C. The findings of Cross (1999) and Worden and Smalley (1996) from the Khuff formation, Abu Dhabi, suggest that the TSR reaction is kinetically, not thermodynamically controlled. The reaction is not governed by thermodynamic favourability, but rather is limited to situations where a relatively high rate of reaction is possible.

4) Transport of the reaction products away from the reaction site to avoid inhibition of further reaction.

Amurskii et al. (1977) demonstrated that in almost all cases there is a higher concentration of H_2S dissolved in the liquid hydrocarbon phase than is present in the gas phase that is in equilibrium with it. This mechanism could account for an

effective removal of a large fraction of H_2S from the aqueous phase and therefore allow the TSR reaction to proceed.

5) Precipitation of reaction products

Most hydrocarbon reservoirs that have undergone TSR are carbonate-evaporite reservoirs that have rather low concentrations of iron and other metals. In such cases a precipitation of solid sulfide minerals is rather rare and H_2S remains in solution. Machel (2001) describes the association of secondary calcite formed by TSR and unreacted anhydrite in many reservoirs. This suggests that there is little transport of the products away from the site of reaction. In cases where secondary calcite forms close to anhydrite it may affect the access of fresh reactants to the site of reaction. Although the precipitation of the reactants is desirable to allow the reaction to proceed, it may ultimately limit the rate of the reaction. The production of water provides an increased medium for the reaction to take place and a proportion of the produced sulfide may react with sulfate, thereby creating more low-valence sulfur compounds that catalyse the reaction but finally the build-up of calcite will cause the reaction to cease.

1.2.2 TSR mechanisms in hydrothermal vents

Thermochemical sulfate reduction does not only take place on a large scale in hydrocarbon reservoirs but also in hydrothermal vent systems, mainly located on the spreading axes of mid-oceanic rifts. However, the mechanisms that control TSR in such environments are considerably different. As a simplyfied model the hydrothermal systems that evolve around mid ocean ridges can be described as follows.

In the cold limb of the hydrothermal convection cell seawater is either convectively or diffusely draw down into the ocean crust where it is subsequently heated. The hot fluids penetrate the magmatic ocean crust and a number of water-rock interactions occurs which greatly modify the chemical composition of the water (Einsele et al., 1980; Fischer and Becker, 1991; Magenheim and GIeskes, 1992; Mottl et al., 1979).

During the circulation process, seawater sulfate is reduced to sulfide by TSR reaction. Based on measurements of the exit velocity of the hot sulfidic water in Black smokers (1 – 5 m s^{-1}) Cann and Strens (1982) calculated the length of time the seawater spends inside the convection cell. Depending on the geometry of the recharge system, the time can be as short as several hours, much shorter than the residence time of water in a hydrocarbon reservoir.

The chemical composition of Black smoker fluids depends on many different factors, like temperature and composition of the host rock. The presence of organic matter in the recharge zone (e.g. Guaymas Basin) has also great effect on the chemistry of the emanating fluids.

Cross (1999) compared the main physicochemical parameters of TSR in hydrocarbon reservoirs and Mid Ocean Ridge hydrothermal vent systems (Table 1.2.1). The most important differences are temperature and pH at which the TSR reaction proceeds. Also the reducing agents are much different.

	Hydrocarbon reservoir	Mid Ocean Ridge system
Source of sulfate	Solid anhydrite	Seawater
Reducing Agent	Hydrocarbons	H_2, Fe, Mn, or other?
Pressure (bar)	500 — 1500	< 500
Temperature (...C)	140 — 210	250 — >350
pH	5—6	3—5
Residence time of sulfate	1000 s years	Hours-days
Products	$H_2S + CO_2$	$FeS + CH_2O$

Table 3.1: Comparison of the main parameters of TSR in hydrocarbon reservoirs and mid-ocean ridge systems (Cross, 1999)

Through the much higher reaction temperatures, lower pH, and different reactants the pathway and the mechanisms of the the TSR mechanism in hydrothermal vents is considerably different to that of hydrocarbon reservoirs. Based on previous work and own data, Cross (1999) suggested a reaction model for the TSR reaction in hydrothermal vent systems.

The mechanism for the reduction of sulfate relies on the combination of hydrogen sulfide with sulfate to generate reactive intermediate species that undergo further reduction upon reaction with a reducing agent (organic matter or reduced ions). Biological sulfate reduction (BSR) and thermally induced cracking of organo-sulfur compounds form the hydrogen sulfide that initiate TSR in hydrocarbon systems. As in Mid Ocean Ridge (MOR) settings there is usually little organic matter available BSR may be quantitatively more important.

For MOR systems Cross (1999) assumed that aqeous sulfate and sulfide are likely to be available to initiate TSR. Sulfate is brought into the reaction not through anhydrite dissolution, but provided by seawater. The source of sulfides can either be BSR in the cooler part of the ridge circulation system (< 110 °C, see Jannasch et al., 1989; Jannasch et al., 1988; Jørgensen et al., 1992; Jørgensen et al., 1990) or massive sulfide deposits that may have formed in the hydrothermal reaction zone beneath the MOR.

At high temperatures sulfate and sulfide can form thiosulfate which is metastable at temperatures above 200 °C (Goldhaber and Orr, 1995). Under acidic conditions thiosulfate decomposes under acidic conditions to form sulfite and elemental sulfur. Any of the produced species (thiosulfate, sulfite and elemental sulfur) are able to further react with reducing agents to cause net sulfate reduction.

While in petroleum reservoirs hydrocarbons form the largest pool of reducing agents, the situation is much different in MOR settings. In seawater there is usually very little organic carbon, except in some special cases like Guaymas Basin where organic rich sediments directly react with the hydrothermal fluids. Therefore, other species are more probable candidates for oxidation, inlcuding iron and maganese that are leached from basalt by the hot fluids. Also hydrogen can be present in appreciable amounts due to degassing from the mantle. Cross (1999) demonstrated the TSR reaction between sodium sulfide and hydrogen under conditions commonly found in hydrothermal vents (250 – 350 °C, 500 bar). It is still not known which of the possible reducing agents is the most important one or if a combination of all is responsible for the TSR reaction.

1.3. The deep biosphere

1.3.1 Definitions of the deep biosphere

There is no consistent definition about what the deep biosphere is and where it starts. One could use the high pressure or high temperatures as an indicator, but for example in sediments with a low thermal gradient temperatures are still low in more than one kilometer depth. High pressure alone also does not necessarily describe a deep biosphere as in the deep Ocean trenches pressure exceeds 1000 bar at the sediment-water interface and the microbial community found there is not significantly different to much shallower habitats (ZoBell, 1952).

The cut-off from the energy supply of the sun and therefore relying entirely on chemolithotrophic metabolism would be perhaps a good definition of the deep biosphere.

It will be shown later that even one of the best studied deep biosphere environments, the sediments of the Peru Continental Margin, would not qualify by this definition. The most flexible definition would most probably be that the deep biosphere does not have any direct and immediate contact with the surface world.

1.3.2 Surface manifestations deep biosphere

One of the major problems when studying the deep biosphere is its inaccessibility, especially in the marine environment. While one way of getting access to the deep biosphere is to develop better tools for deep drilling that avoid sample contamination etc. Another way is to look for surface manifestations of the deep biosphere. Several environments have been recognized as "windows to the deep biosphere" and considerable research has been put into the exploration of these environments and their influence on global biogeochemical cycles. Such environments are hydrocarbon (oil and gas) seeps, fluid seeps, and mud volcanoes.

However, it remains questionable that the organisms found in these environments originate from the deep biosphere or if they are rather surface ecosystems fuelled by substances that originate from deeper strata. In seeps and mud volcanoes there is a good chance that at least some of the organisms have been transported from deeper layers to the surface as the temperatures in such environments are in the biological range. However, the majority of the organisms do not originate from the deep biosphere. Nonetheless, seeps and mud volcanoes provide insights into deep-seated processes and the hydrological and geochemical conditions at depth. The environmental conditions in such ecosystems may be models for the conditions in deeper layers.

1.3.2.1 Seeps

Seeps in general represent an important link in geochemical cycles between lithosphere, biosphere, hydrosphere, and atmosphere. Greenhouse gases like methane and carbon dioxide emanating from the seeps can also affect the biosphere by causing atmospheric changes leading to global warming. The emanating fluids are chemically diverse and can consist of various aqueous mixtures of liquids, gas, and oil. The more common gases in seeps are CH_4, CO_2, N_2, and H_2S. Methane dominated seeps have been studied most extensively. Seeps of shallow and/or deep sources, cold or warm, saline to fresh, have been characterized. The relative global importance and distribution of each type is, however, unknown.

Seeps alter the water and sediment chemistries as well as the sediment physical properties. At seepage sites where especially CH_4, CO_2, and H_2S discharge, the water chemistry, particularly concentrations of dissolved oxygen and inorganic carbon (DIC), and thus the pH, are strongly affected, and the $\delta^{13}C$ of the DIC altered. In gas hydrate deposits this is reflected not only in the $\delta^{13}C$ of authigenic carbonates but also in the biomass of the organisms living there, for example the microbial consortia that mediate anaerobic oxidation of methane (Orphan et al., 2001). Other important seep-related authigenic minerals are barite, and sulfides (mostly Fe sulfides). Tar and gas hydrates may also precipitate under favourable conditions. Precipitates can seal seeps and change patterns of fluid flow. Especially carbonates and barite can be useful tools in mapping paleo-seeps sites, the work of Peckmann et al. (2001a, 2001b, 2002) shows the use of mapping the authigenic mineral deposits and associated fossil assemblages to identify paleo-seep settings.

Hydrocarbon seeps, which consist of oil and/or hydrocarbon gas have been used in petroleum prospection and have led to the discovery of major oil and gas fields (e.g. Gulf of Mexico). Understanding the inventory of hydrocarbon seeps is important to estimate the magnitude and effect of petroleum pollution resulting from human activities. For example, the amount of oil that is naturally seeping into the Gulf of Mexico each year is in the same order of magnitude as the amount that was spilled during the Exxon Valdez disaster in Alaska, where it caused severe ecological damage (S. Joye pers. comm.). A thriving chemotrophic microbial community which is fuelled by hydrocarbons can be found in many areas, like in the Black Sea, and in the Gulf of Mexico (Joye et al., 2003, in press; Michaelis et al., 2002; Orcutt et al., 2003, in press). Hydrocarbon gas seeps also affect the atmosphere by adding an unknown component of greenhouse gases. Locations of heavy hydrocarbon seepage are known on the continents as well, for example in the Caspian Sea region (Hovland et al., 1997). Except for a few very well studied regions, little is known about the rate of seepage, and the flux of hydrocarbons from seeps is difficult to measure because many seeps are small, episodic, and ephemeral. Even on land the integrated rate of hydrocarbon seepage is not known.

Seeps in the ocean influence the distribution and reaction pathways of major and trace compounds, (i.e. dissolved gases, nutrients, halogens, and others), thereby effecting their geochemical mass balances, and global fluxes. The transfer of greenhouse gases to the atmosphere is mostly through volcanic activity, and the transfer

of material and volatile elements to the deep mantle is through subduction. Meteroic water seeps are important in the global hydrologic cycles because they transport solutes from the continents into the ocean. Submarine-, together with subaerial seeps, play a key role in coupling between the hydrologic and atmospheric fluid cycles on the one side and the carbon cycle on the other.

1.3.2.2 Hydrothermal vents

In hydrothermal vents the situation is much different than in seeps. The emanating fluids from the vents are so hot (e.g. up to 350 °C in Guaymas Basin (Jannasch et al., 1989) that they are effectively sterilized. Although these environments do not harbor organisms that originate from the deep biosphere, they still remain interesting for deep biosphere research. The ecosystems around such hydrothermal vents bear thermophile to hyperthermophile organisms, and harbor chemolithotrophic communities. The primary producers do not gain energy from sunlight. In terms of chemical- and temperature gradients hydrothermal vents are among the most extreme of all known environments. Because hydrothermal systems have prevailed throughout Earth's history, the organisms in these systems and their genomes may have changed little over geological time. The deeply branching lineages of the universal tree of life all contain thermophiles, although this is still controversial (Canfield and Raiswell, 1999). The Aquificales are one of the deepest bacterial lineages, and the metabolic plasticity exhibited by representatives of the group, such as the chemolithoautotrophic *Persephonella marina*, may thus be a relic of their evolution on a dynamically changing planet. Members of this lineage might have initially evolved using the limited redox couples available in the absence of molecular oxygen. Once photosynthesis drove the shift to an oxic atmosphere, near-surface redox chemistry changed dramatically, and other acceptors such as nitrate would have been available. To develop a better understanding of how such organisms thrive in their ecological niches, and what the mechanisms are that control their fossilization, are all essential in our interpretation of the early rock record and putative fossils from elsewhere in the solar system (Brasier et al., 2002; Schopf et al., 2002).

1.3.3 Terrestrial deep biosphere

Not only in the marine environment but also on land, the deep biosphere is currently explored. Biogeochemical investigations have been carried out in several environ-

ments for example deep mines and aquifers. Though advanced mining techniques it is now possible to mine in depths of several kilometers, like in the gold mines of South Africa (for a review see Baker et al., 2003). The advantage of working in such environments is their accessibility. One does not have to rely on cores with all their uncertainties like contamination, poor recovery etc., but can physically reach the sampling site and take larger samples and can specifically decide where to sample. However, working in deep mines creates a different set of problems. The rocks found in the gold mines are magmatic or metamorphic and do not possess significant pore space. Biological activity is mostly confined to rather narrow fracture zones where groundwater or brines circulate. Sampling these specific points is technically difficult. Moreover, working is deep mines is physically very demanding and access to such locations is mainly provided through industrial collaboration, possibly causing problems with the distribution of scientific results.

1.3.4 The deep marine biosphere

Morita and ZoBell (1955) defined the end of the marine biosphere at 7.47 mbsf because of their inability to culture bacteria from greater depths. Although this statement has been proven wrong in subsequent studies their paper contains some noteworthy statements:

1) They used cores from the organic poor sediments from the central Pacific, an area with a very low sedimentation rate (2 – 3 mm ky^{-1}). They concluded that the bacteria they found in several meters depth must have been viable for hundreds of thousands to millions of years.
2) The number of bacteria decreases with depth, reflecting decreasing availability of carbon.
3) They already speculated about the possible importance of hydrogen as an energy source for the deep biosphere and even postulated sources for hydrogen that have only recently been shown to play an important role, e.g. radioactivity (Lin et al., 2002).

Whelan et al. (1985) postulated that microbial life reaches much further into the sediment than previously thought. They conducted experiments where they amended sediment from ODP cores with radiolabeled substrates and detected the formation of radiolabeled products down to depths of 167 mbsf. The turnover rates in the deep

cores were several orders of magnitude lower than in surface sediments. They identified sulfate reduction, methanogenesis, and fermentation. CO_2 reduction by hydrogen was suggested as an important pathway of for methane production in deep sediments.

Parkes et al. (1994) proved the existence of a deep marine biosphere by identifying intact baterial cells down to depths of 518 mbsf. Based on the bacterial counts they estimated that the biomass of the entire sub-seafloor biosphere would account for only 0.004 % of the global sedimentary organic carbon but it would account for ca. 10 % of the living biomass in the global biosphere. The profiles of bacterial distribution are consistent between cores from different locations in the Pacific. This database was later extended to other oceans (see Parkes et al. (2000) for a review). The bacterial population profiles are remarkably similar at all locations sampled. In cases where there were significant deviations from the average distribution they could be assigned to specific environmental conditions, like organic carbon content or fluid flow.

Additionally to counting bacterial cells they measured several metabolic processes like acetogenesis, methanogenesis, and sulfate reduction. By measuring metabolic activity under different pressure/temperature conditions on pure cultures obtained from deep sediments, Parkes et al. (1994) reported a barophilic response of the organisms, indicating a deep-biosphere origin.

As already pointed out, one of the major obstacles when studying the deep biosphere is its inaccessibility and therefore the need to use highly specialized equipment. This is especially true for the deep marine biosphere because at the moment there is only one research vessel available that has the capability for drilling (JOIDES Resolution). In the future there might be more vessels available, but their number will remain limited.

1.4. Earth's History and the evolution of the sulfate cycle

The evolution of life on Earth has dramatically influenced the evolution of our planet. Earth is believed to be over 4.5 Gyr old, its origin still under debate (e.g. Bizarro et al., (2003). Theories about the formation of the Earth and our neighbouring planets are plentiful. The most widely accepted goes back on the work of Laplace (1796) and suggests an accumulation of dust and smaller planetesimal bodies through collision, leading to the formation of a number of planets of different sizes and distance from the sun. (see also Nisbet and Sleep, 2001, and references therein).

Over the first 500 to 700 Myr Earth experienced frequent impacts of large bodies, causing occasional heating of the Earth's surface and effective sterilization. During those times Earth already had a solid surface. The oldest rocks date back to about 4 to 3.8 Gyr (Acasta, Canada; Isua, Greenland). There are even older minerals, zircons now found in younger sediments in western Australia that date > 4 Gyr (Amelin et al., 1999). The oldest known emerged continental crust is about 3.5 Gyr old (Buick et al., 1995).

Around 4 Gyr temperatures were generally in the biological range but occasional impacts might have heated the oceans to > 100°C. There is geological evidence that life existed on this planet for at least 3.5 Gyr (Brocks et al., 1999), but most probably life existed before. The oldest known biomarkers suggest that oxygen producing cyanobacteria were present. The metasediments of the Isua belt suggest biological activity even before that time but remain controversial (Appel and Moorbath, 1999; Honma, 1996).

The most fundamental difference between the Earth and all other planets in our solar system is the accumulation of oxygen in the atmosphere and the presence of liquid water. During Earth's history not only did the atmosphere become oxygenated at some point in time, but also the oceans, even the deep oceans. These are two fundamental requirements for the biological and geological evolution of this planet to its present-day state.

Oxygen as a product of oxygenic photosynthesis by plants and cyanobacteria causes oxidative weathering on land, thereby creating oxidised species like metal oxides (mostly iron oxide) and sulfate that are subsequently transported into the ocean. There are no direct ways of estimating the oxygen content of the atmosphere or the sulfate concentration in the oceans over geologic times. However, the stable isotope composition of sulfate in seawater and its changes over time are preserved in evaporites like anhydrite and gypsum and other sulfate containing minerals like barite. In order to estimate the oceanic sulfate concentration throughout the history of the Earth, which reflects the accumulation of oxygen in the atmosphere, the stable isotope record can be used. Habicht et al. (2002) suggest that during the Archaean (> 2.5 Gyr) sulfate concentration in the ocean was > 200 µM which is less than 1 % of the present day value (28 mM). The low levels of sulfate in the Archaean Ocean were not only supplied through oxygenic weathering but also through volcanic SO_2 outgassing.

The now most commonly believed theory about the timing of the oxygenation of the atmosphere suggests that already in the early Archaean there were low levels of sulfate and atmospheric oxygen present (Canfield et al., 2000).

The formation of banded iron formations (BIFs), which consist of layered iron oxides was thought to be a result of the oxygenation of the oceans. However, the long time over which BIFs formed remained an enigma as the evolution of the atmosphere was thought to have proceeded much faster. Bjerrum and Canfield (2002) noted that upon the oxidation of reduced iron the freshly formed iron oxyhydroxides scavenge large amounts of phosphate. Based on this observation they concluded that through removal of this essential nutrient the growth of algae was phosphorus limited and therefore the oxygenation of the atmosphere was suppressed as long as there was enough reduced iron available to scavenge free oxygen and adsorp available phosphates. Only after the pool of reduced iron was depleted, phosphate could accumulate in the water, allowing algae to grow on a larger scale and therefore oxygen concentrations were able to rise to higher levels.

Sedimentary sulfide deposits are known to exist over almost the entire geological record, they date back to at least 3.5 Gyr. There are two different ways of formation, either by biological activity, i.e.sulfate reduction, or by hydrothermal venting.

Through studies of pure cultures and natural marine sediments, the isotopic fractionation during biological sulfate reduction was determined for many different sulfate reducing organisms (for a review see Habicht and Canfield, 2001). In general, there is a positive correlation between isotopic fractionation and sulfate reduction rate, the higher the rate, the higher the fractionation. There is not a fixed rate of isotopic discrimination but a rather wide range of fractionation coefficients, ranging from 30 to 55 ‰(PDB) (Habicht and Canfield, 2001). In case the isotopic difference between sulfate and sulfide minerals is larger than the maximum fractionation that is possible in one reduction step, there is an indication of an oxidative part of the sulfur cycle, where sulfide becomes re-oxidised to sulfate again. Through this recycling from sulfide to sulfate and back a larger isotopic fractionation can be achieved. During Earth's history the isotopic signature of seawater changed between approximately 0 and + 30 ‰ (PDB) but the sulfide minerals range from about -50 to + 40 ‰ (Canfield and Teske, 1996).

Based on the sulfur isotope record Canfield (1998) developed a model for Proterozoic ocean chemistry. Between 2.5 to 2.3 Gyr oxidation of the atmosphere started to

increase through increased rates of sedimentary burial of organic matter, leading to a significant oxidation of the Earth's surface around 2 Gyr ago. However, the oceanic bottom waters remained anoxic much longer. Aerobic conditions developed much later in the Neoproterozoic era, around 1 to 0.54 Gyr ago. At this time a second large increase in the atmospheric oxygen concentration happened.

The accumulation of appreciable amounts of oxygen to allow for metazoan life to develop happened in the early Proterozoic (2.5 to 0.54 Gyr). The oldest known metazoan fossil deposits are the Ediacara Fauna from South Australia and date back about 0.7 Gyr (Wade, 1968). Not only did metazoans evolve after oxygen concentration reached higher levels, also reoxidation of reduced chemical species started, thereby creating an oxidative part in global biogeochemical cycles.

Canfield and Teske (1996) used a dual approach to track back the development of atmospheric oxygen concentration in the Neoproterozoic. The differences between the isotopic signal of marine sulfate minerals, which reflect isotopic composition of the seawater and sedimentary non-hydrothermal sulfides and a phylogenetic study were combined. They suggested that until 1.05 and 0.64 Gyr ago oxygen concentrations were between 5 and 18 % of present day level. During this time interval the isotopic fractionation between sedimentary sulfate minerals and biogenically produced sulfides becomes much larger than what has been found in older deposits. This large isotopic fractionation can only be explained by operation of an oxidative sulfur cycle. In a second line of evidence Canfield and Teske (1996) argue that the appearance of non-photosynthetic sulfide-oxidising γ-proteobacteria falls into the same time-interval as the increase in atmospheric oxygen concentration inferred from the isotopic record. These sulfide oxidizers require oxygen, they can therefore not have evolved earlier.

The results of Shen et al. (2001) indicate that sulfate reduction is an ancient metabolic pathway, at least 3.47 Gyr old. Most probably sulfate reduction has evolved even earlier, but the stable isotope record is unequivocal. At low sulfate concentration isotopic fractionation during biological sulfate reduction becomes too small to discriminate the produced sulfides from those of hydrothermal origin.

1.5. Metabolic and phylogenetic diversity in the deep biosphere

The most important pathway of production of reduced carbon compounds, photosynthesis, is not existing in the deep biosphere due to the lack of light. Without photosynthetic primary production other pathways of electron transfer are used. By using

different geochemical energy sources and exploiting different oxidation-reduction reactions microorganisms can gain energy. Not only the electron donors but also the electron acceptors change with increasing sediment depth. Several studies measured subsurface activity and showed that chemolithotrophic communities exist and (see Phelps et al., 1994, and Parkes et al., 1999, for a review).

1.5.1 Models for carbon utilization in marine sediments

D'Hondt et al. (2002) postulated that in the Deep Biosphere (> 1.5 mbsf) methanotrophic sulfate reduction is the dominating terminal electron acceptor process. Their conclusion is based on an in-depth review of available sulfate and methane porewater data from the Ocean Drilling Program (ODP) and its predecessor the Deep-Sea Drilling Program (DSDP). They broadly distinguished two different zones:

1) Ocean margins, with sulfate being depleted within meters to tens of meters below the seafloor and high methane concentrations.
2) Open ocean settings, with much deeper sulfate penetration and low methane concentrations. At many open ocean sites high concentrations of sulfate and low concentrations of methane coexist over long depth intervals, a fact that contradicts the commonly accepted redox sequence.

In ocean margin settings, D'Hondt et al. (2002) postulate that most of the sulfate flux below 1.5 mbsf is used to oxidise upwards diffusing methane. Because there is normally no methane above the sulfate methane transition zone, the total sulfate flux into the sediment can be used as a measure for total carbon turnover in the entire sediment column. Like in some earlier case studies of sulfate reduction coupled to methane oxidation at DSDP sites (Canfield, 1991) the continental slope of Namibia (Niewöhner et al., 1998), and the Amazon Fan (Adler et al., 2000), these findings are all based on flux calculations and numerical modelling. In light of the results of Fossing et al. (2000) and Jørgensen et al. (2001) however, sulfate reduction exclusively based on modelling tends to underestimate the total areal SRR and thereby the total carbon turnover of the sediment (see chapter 5).

At open ocean sites, where methanotrophic SR can be neglected due to low methane concentrations, the depth-integrated rate of sulfate reduction can be used as a measure of total dissimilatory activity (Canfield, 1991; D'Hondt et al., 2002).

Some ecosystems exist without light but rely at least in part on photosynthetic production of oxygen and/or reduced carbon compounds. Examples are the communities on the sea floor of the deep sea.

Even some "real" deep biosphere environments, like the deeper layers of the sediments in the Peru Margin are at least in part fueled by organic compounds that were produced by photoautotrophic organisms. The organic carbon utilized in these sediments originates from planktonic and/or terrestrial material that was deposited on the sea-floor millions of years ago. Therefore these ecosystems do not operate completely independent from sunlight. Kallmeyer et al. (Chapter 5) address the question if and how much the oceanic productivity during time of deposition influences microbial activity in deep sediments today.

There are, however, ecosystems that are completely de-coupled from the surface world. Notable are those based on H_2, which is a constituent of magmatic gases but can also be a product of the geochemical reduction of H_2O at high temperatures or of radiogenic origin (Lin et al., 2002).

Metabolic strategies that use H_2 to reduce CO_2, sulfur, or O_2 fuel chemolithoautotrophic primary production and represent energy conservation strategies that can operate entirely independent from sunlight. Such metabolic pathways are found mostly in hydrothermal ecosystems but can also be present in other deep biosphere environments.

All of these strategies can be traced deeply into the universal tree of life. Methanogenesis [$CO_2 + 4\ H_2 = CH_4 + 2\ H_2O$] is confined to the Archaea, but both Archaea and Bacteria gain energy from sulfate reduction with hydrogen

[$SO_4 + 4H_2 + H^+ = HS^- + 4H_2O$] (Widdel, 1988). Both reactions are kinetically sluggish, even when there is thermodynamic potential for the reactions to proceed. Several studies have shown that sulfate reduction and O_2 reduction do not proceed measurably in the absence of life at hot spring temperatures, and CO_2 reduction to methane fails to equilibrate rapidly even at 500 °C (Machel, 2001; Reysenbach and Shock, 2002; Trudinger et al., 1985). Thermochemical sulfate reduction (TSR) is known to proceed fast on geological timescales at temperatures > 150 °C, but up to about 100 °C biological sulfate reduction is orders of magnitude faster than TSR (see Chapter 1.2).

Organisms use enzyme catalysts to lower the activation energy of these thermodynamically favorable reactions and tap into the free energy released as the reactions are allowed to proceed. The possibility that these reactions can supply energy

depends on the availability of the reactants. Outside hydrothermal vent systems with its active fluid flow, diffusion limits the availability of the reactants. Therefore many processes are confined to small horizons in the sediment because only there all necessary reactants are available. The relatively narrow sulfate-methane transition zones are a good example of how diffusion of the necessary reagents limits the spatial distribution of a metabolic process.

Over the past two decades, there has been an enormous increase in the number of isolated thermophilic microorganisms (see Reysenbach and Shock (2002) for a review). These organisms have special and highly diverse metabolic strategies to take advantage of the number of different geochemical energy sources associated with continental and deep-sea hydrothermal vents. The isolates include microaerophiles, aerobes, and anaerobes; heterotrophs that use organic carbon as their sole energy and carbon source, sometimes coupling this with for example iron reduction and chemolithoautotrophs that use inorganic energy sources and fix CO_2 (Reysenbach and Shock, 2002). Many of these organisms can use several different electron acceptors and donors, like *Pyrococcus fumarii* (Blöchl et al., 1997), who oxidizes H_2 with nitrate, thiosulfate, or oxygen.

Through the use of culture-independent approaches based on molecular phylogenies of the small 16S rRNA, our view of microbial and potential metabolic diversity in the deep biosphere has vastly increased. Classical microbiological enrichment and cultivation techniques fail in many cases or are extremely time-consuming, due to the slow growth rate of these organisms. Only a small fraction of the diversity of life in the deep biosphere is well characterized and in pure culture. By using molecular assessments, a huge number of novel lineages can be discovered in little time, many of them will most probably never be grown in pure culture because of, for example, syntrophic requirements.

1.6 Adaptation to the deep biosphere: Thermophilic and barophilic organisms

Organisms living at great depth have to be adapted to elevated temperatures and pressures. Not only in hot environments like hydrothermal vents it is necessary for the organisms to develop special strategies to survive high temperatures but also in deep sedimens as temperatures increase with increasing sediment depth. The normal geothermal gradient is around 30 °C per kilometer depth but can strongly deviate from this value. In the Nankai Trough, for example, the gradient is in the range of

180 °C/km (see ODP database) and in Guaymas Basin it is even more extreme, up to 475 °C/km (Fischer and Becker, 1991).

Hydrothermal vents, first on land and much later in the marine environment, have been of interest since long time ago. Davis (1897) described the "vegetation" of hot springs at Yellowstone National Park, including observations of life at 85 °C. Setchell (1903) carefully extended these observations to 89 °C. He also identified a problem that still plagues biochemists: "What is it that enables the protoplasm of the thermal organisms to withstand a temperature which coagulates, and consequently kills, the protoplasm of the majority of organisms"

Now with the upper temperature limit of life being currently set by *Pyrolobus fumarii* (Blöchl et al., 1997) at 113 °C, the question raised by Setchell, (1903) becomes even more important. How do these organisms survive such hostile conditions, and where is the absolute upper temperature limit for life?

Teske et al. (2002), Schouten et al. (2003) and also Kallmeyer & Boetius (Chapter 4) found evidence that in the hydrothermal vent sediments of Guaymas Basin anaerobic oxidation of methane (AOM) takes place at elevated temperatures. Up to now the upper proven temperature limit for AOM was around 10 to 15 °C, like in Hydrate Ridge, off Oregon, USA (Boetius et al., 2000; Nauhaus et al., 2002). Michaelis et al. (2002) suggests that AOM is a process that might have been one of the first metabolic pathways developed by early life. There is geological and geochemical evidence that hydrothermal vents have been existing for almost 4 billion years. In almost all hydrothermally altered rocks, as well as in active hydrothermal ecosystem traces of biological activity can be found. Now with more and more genomic information available showing that the most deeply branching organisms are thermophiles and hyperthermophiles it appears at least possible that life has started around hydrothermal vents (Reysenbach and Shock, 2002).

Organisms adapted to high temperature remained curiosities until the molecular, phylogenetic, and genomic revolutions of the past two decades moved them to the center of debates about the mechanisms of evolution, the depths of the biosphere, mineral-microbe relations, the origins of ecosystems, the emergence of life, and the potential for life on other planets. Many of the questions driving current research puzzled the pioneers as well. Already Davis (1897) speculated that "Perhaps ... these organisms resemble more closely the primitive first forms of life than any other living types", and wondered about their evolution, dispersal, and ecology. Since the

early studies of Davis (1897) and Setchell (1903) the hot springs of Yellowstone and their microbial population have been a major point of interest. In a recent study of the microbial diversity of Obsidian Pool, a hot spring at Yellowstone National Park, 86 novel lineages were found, 32 within the Archaea (Barns et al., 1996) and 54 within the Bacteria (Hugenholtz et al., 1988). Within the Bacteria alone, 12 novel division-level lineages were proposed. Assessment of the Archaea in Obsidian Pool revealed the presence of sequences that branched deeply within the archaeal kingdom Crenarchaeota or below the bifurcation between the Crenarchaeaota and the Euryarchaeaota. This discovery led to the proposition of a third kingdom within the Archaea, the Korarchaeota (Barns et al., 1996; Burggraf et al., 1997). Reysenbach and Shock (2002) see this as additional evidence for hydrothermal vent systems being some of the focal points of the earliest evolution of life on this planet.

In addition to the high diversity of thermophilic organisms, culture-independent phylogenetic studies also reveal the widespread occurrence of certain lineages found in many different locations around the world. For example, among samples from actively venting submarine hydrothermal chimneys an archaeal lineage (DHVEG) endemic to vents is prevalent in clone libraries from samples from the western Pacific (Manus Basin, Okinawa Basin sediments, and Myojin Knoll in the Izu-Ogasawara arc); along the East Pacific Rise, Juan de Fuca Ridge, in the Indian Ocean; and from an in situ growth chamber experiment on the Mid-Atlantic Ridge (see Reysenbach and Shock, 2002, and references therein). Some of these diversity assessments also yielded 16S rRNA sequences most closely related to sequences previously associated with zones of anaerobic methane oxidation in sediments the so-called ANME-1 group (Orphan et al., 2001).

High pressure has also been regarded as a characteristic feature of the deep biosphere. While over the last few years the number of isolated thermophiles and hyperthermophiles has increased drastically, much less barophilic organisms have been cultivated. One of the main reasons for this are the much more complicated (and expensive) techniques that are necessary to meet the requirements of the organisms (Kallmeyer et al., 2003; Parkes et al., 1995). While there are several facultative barophiles in pure culture, strictly obligate barophilic organisms are much rarer. They are very difficult to isolate from natural samples as all handling, from sampling to pure culture, has to be done under pressure (see Jannasch and Taylor, 1984; Yayanos, 1995; Kato and Bartlett, 1997, for reviews).

Because most measurements of microbial activity in deep biosphere samples are carried out at atmospheric pressure there has been considerable debate about the effects of decompression on the rates of microbial activity in deep-sea samples. (Parkes et al., 1995, 1999) shows that storage of samples from deep drilling cores at 4° C and atmospheric pressur over long periods (> 1year) does not influence the rates of methanogenesis and sulfate reduction, when brought back to the in-situ p/T conditions. However, effects in both directions, either increasing (Jannasch and Taylor, 1984) or decreasing (Bianchi and Garcia, 1993), or little to no effect (Martens, 1998) are reported in the literature. Ferdelman et al. (1999) give an overview about the work on pressure effects with special emphasis on sulfate reduction and conclude that decompression has apparently no effect on sulfate reduction. Weber et al. (2001) however, conclude that based on their results they cannot give a consistent explanation for the differences between SRR measured in situ and in the laboratory. Kallmeyer et al. (2003) and Kallmeyer & Boetius (subm.) (Chapter 3 and 4) show that in Guaymas Basin there is a strong response of the sulfate reducers to increased pressure.

As the several studies show different effects upon decompression even for the same process, it seems as if much more work on sampling and handling techniques is necessary to finally obtain a comprehensive picture of life under high pressure.

1.7 Quantification of sulfate reduction rates

Two different methods for the determination of sulfate reduction rates are commonly in use; mathematical modeling based on interpretation of chemical gradients, and radiotracer incubations followed by distillation. In a pioneering study the different methods were compared (Jørgensen, 1978a; Jørgensen, 1978b; Jørgensen, 1978c). Since then few studies have been conducted where modeling and tracer measurements were directly compared (Fossing et al., 2000; Jørgensen et al., 2001). Both studies show that in deeper layers where the distribution of sulfate is only affected by molecular diffusion, modeling can be a powerful tool for the estimation of sulfate reduction rates. However, in shallow sediments where advective transport and re-oxidation are influencing the distribution of sulfate, models tend to underestimate the true sulfate reduction rates.

Kallmeyer et al. (Chapter 5) compare the results of radiotracer measurements and model results calculated with the procedure of Berg et al. (1998) from cores taken at

the Peru continental margin during ODP Leg 201. Their results are similar to Fossing et al. (2000) and Jørgensen et al. (2001); in shallow sediment depth the model tends to underestimate SRR whereas deeper in the sulfate-methane transition zone the model results provides a more realistic picture. Moreover the model is able to reliably calculate rates that are too low to be detected by the radiotracer technique.

1.7.1 Mathematical modeling based on interpretation of chemical gradients

This approach was used in many different studies, covering many different oceanographical settings (Berner, 1964; Jørgensen, 1978b; Schulz et al., 1994; Adler et al., 2000).

Modeling provides information about the net sulfate reduction rates. The concentration gradient is assumed to be a function of diffusion and consumption. If not specifically quantified and included in the model, other processes influencing the concentration profile, like re-oxidation, bioturbation, or advective transport are not taken into account. In such cases modeling may not provide reliable results. Several modeling programs have been used for calculations of consumption rates, (see Adler et al. (2000) for an overview of the most recent models). Berg et al. (1998) introduced a numerical modeling procedure that takes into account factors like biodiffusivity and irrigation. By inclusion of such parameters a better estimate of turnover rates in shallow sediment-depth was possible but still the sulfate reduction rates were considerably underestimated compared to the rates measured with radiotracer (Fossing et al., 2000). However, in deeper sediment layers where transport processes other than molecular diffusion can be ruled out, the models may even provide a better estimation than radiotracer measurements.

In the sulfate-methane transition zone, methanotrophic sulfate reduction can be difficult to measure because degassing due to pressure release upon retrieval of the core on board ship can significantly decrease the availability of methane and therefore influence the SRR. The sulfate gradient is normally not affected by the degassing and can therefore be used as a more robust tool for estimation of SRR.

1.7.2 Direct measurements with radiotracer

Such techniques provide information about the gross rates. Much of our current understanding of sulfate reduction has been derived from experiments conducted with $^{35}SO_4^{2-}$ radiotracer (among others Elsgaard et al., 1994; Fossing, 1990). $^{35}SO_4^{2-}$ tracer is

relatively inexpensive and can be obtained with high specific activity in carrier-free from. Ivanov (1956) first described radiotracer $^{35}SO_4^{2-}$ incubations for determination of SRR. His work was later adopted and modified by others to accommodate the different experimental needs.

When working with sediments, two different ways of mixing the tracer with the sediment have been applied, mechanical mixing by stirring under anoxic conditions (e.g. (Sorokin, 1962) and direct injections into undisturbed cores (e.g. Jørgensen, (1978a). The first technique tends to underestimate the true SRR while the direct injection technique has proven to give more reliable results (Jørgensen, 1978a, Skyring, 1987). In this case the sediment cores are retrieved in acrylic or polycarbonate tubes (2 – 3 cm diameter) with small silicone cemented holes in the side. Through these holes a small volume of radiotracer is injected (usually 10 to 100 µL). In practice the tracer can be injected while withdrawing the needle from the sediment, thereby leaving a line of tracer that will then diffuse further into the sediment. Due to the small distance between the injections (normally 1 cm) the tracer is evenly distributed in the sediment by diffusion.

After incubation for hours to days, the incubation can be terminated in two different ways: Either by quickly freezing the entire core followed by slicing the frozen sediment into the desired resolution; or by pushing the sediment stepwise out of the liner, slicing it in the desired resolution and transferring the slices into zinc acetate (ZnAc) solution (usually 20 % w/v). The freezing technique has an advantage when stopping many cores simultaneously. Fast freezing is critical to avoid redistribution of radiotracer through migration of porewater caused by ice formation. The ZnAc technique has now been widely accepted and proven to be robust (see King, 2001, for a review). However great care has to be taken to completely homogenize the sediment with the ZnAc as otherwise SR can proceed for an unknown length of time inside the block of sediment, causing wrong estimation of the SRR.

1.7.2.1 Distillation techniques

After incubation the radiolabelled reduced sulfur species have to be separated from the sediment. In many earlier studies it was assumed that all radiolabelled reduced compounds formed by the bacteria during incubation are free or acid volatile sulfur (AVS, i.e. hydrogen sulfide and ferrous sulfide). Therefore several authors acidified the sediment in order to retrieve the bacterially produced hydrogen sulfide

(Jørgensen, 1978a, and references therein). Howarth and co-workers (e.g. Howarth and Giblin, 1983) concluded that radiotracer measurements solely based on AVS determinations might underestimate the true SRR by showing that the bacterially produced H_2S also reacts to form pyrite and other non-AVS phases.

Zhabina and Volkov (1978) introduced the hot acidic chromous chloride distillation procedure for separating reduced sulfur species comprising hydrogen sulfide, ferrous sulfide, pyrite, and elemental sulfur. The extracted sulfur species were liberated as hydrogen sulfide and subsequently trapped as solid metal sulfide. Later studies have modified this technique according to their needs.

Based on the work of Zhabina and Volkov (1978) and Canfield et al. (1986), a single-step chromium reduction method was introduced by Fossing and Jørgensen (1989). The method of Fossing and Jørgensen (1989) is now widely used by many workers and has shown to be robust albeit fairly labor-intensive. This single-step method retrieves all reduced inorganic sulfur species (total reduced inorganic sulfur, TRIS) by boiling the sample in hot acidic chromous chloride solution.

The chromium reducible sulfur (CRS) includes pyrite and elemental sulfur (ES). AVS can either be extracted in a step prior to CRS extraction by acidifying the sample or together with the CRS when the sample is boiled in hot acidic chromous chloride solution. Heating is necessary because only at elevated temperatures the Cr^{2+} is able to transfer an electron to one of the S atoms, thereby reducing the strength of the very stable S-S bond in ES (Luther, 1987). Fossing and Jørgensen (1989) showed that the recovery of granular and colloidal ES is low, even with boiling. Contrarily, ES dissolved in acetone is recovered almost entirely even with cold chromium solution.

When using the hot chromium distillation, a minute amount of radioactivity distils over causing a certain background signal that can not be attributed to sulfate reduction or carry-over from the previous distillation. This background is negligible as long as the SRR are high enough to produce enough radiolabelled TRIS to give a signal well above the background. When measuring low rates of sulfate reduction, this blank determines the minimum detection limit. This blank is inherent to the hot chromium distillation.

Several studies have used passive distillation procedures by which the sample and all reagents were mixed in one container with a trap hanging in the gas phase above the solution in order to trap all produced sulfides (Hsieh and Yang, 1989; Ulrich et al., 1997). The passive distillation procedures work at cold or at sub-boiling temperatures.

In theory, a carry over of non-reacted sulfate is limited or even absent by this procedure. Passive distillation is less labor intensive and allows processing a larger number of samples at one time. However, the experimental designs used so far (Hsieh and Yang, 1989; Ulrich et al., 1997) have certain practical disadvantages for the recovery of radiotracer-labelled sulfide:

1) The trap hangs inside the reaction flask, therefore $^{35}SO_4^{2-}$ containing aerosols can reach the trap. By this way non-reacted sulfate radiotracer can be carried over and increase the blank.
2) The trapping vial will be contaminated on the outside, requiring either extremely thorough cleaning or transfer of the trapping solution into a new vial.
3) CO_2 produced during the acid dissolution of carbonate-containing samples creates high pressure and can cause the reaction flask to leak or burst. Sample size either has to be kept to a minimum, a step to remove the carbonates prior to distillation is required, or a pressure-compensation has to be installed.

Furthermore, some of the passive distillation methods may suffer from low recovery (Howarth and Giblin, 1983), especially for ES (Ulrich et al., 1997). Although ES may not form a significant fraction of the total TRIS pool, a significant fraction of the labeled sulfide often ends up in this fraction during an SRR experiment.

In order to improve the recovery of ES, Hsieh and Yang (1989) used N, N-Dimethylformamide (DMF). Not only does DMF solubilizes ES rapidly, but DMF is also an organic solvent commonly used to promote reaction rates. This reagent destabilizes the S-S bonds and therefore allows the chromium to reduce it to sulfide. Kallmeyer et al. (Chapter 2) have developed a cold chromium technique that allows the recovery and detection of very small amounts of radiolabelled TRIS. The carry over of unreacted radiotracer is almost completely stopped.

1.8 Outline of the project

The project was part of the EU project DeepBUG (Deep Bacteria Under Ground).

The main objectives of DeepBUG were

1) To develop new, and refine existing, techniques to quantify the presence and activity of procaryotic microorganisms in sub-seafloor sediments.
2) To explore the phylogenetic diversity and physiological potential of the deep biota.
3) To demonstrate the fidelity of new and improved procedures by integrated studies, using different but complementary techniques and by comparison of the geochemical data with the results from model experiments.
4) To develop sensitive indices for distinguishing thermogenic and biogenic processes and hence their interaction in deep sediments.
5) To use these techniques and approaches on future ODP Legs of specific deep biosphere interest.

The different sub-project presented in this thesis focused on sulfate reduction, one of the quantitatively most important anaerobic terminal electron acceptor processes. The aims of the projects were:

1) To develop a much more sensitive technique for the detection of sulfate reduction rates.

This was a key part of the project as without a sufficiently sensitive technique sulfate reduction rate measurements on samples from the deep biosphere would have been impossible. The new technique will be described in detail in Chapter 2.

2) To develop a tool for incubating multiple samples under high pressure along a thermal gradient.

A high-pressure thermal gradient block was developed. It will be described in Chapter 3. A study about the influence of pressure on microbial activity will be presented, as an application of the high-pressure thermal gradient block.

3) To use the developed techniques on samples from the deep biosphere.

Several sets of samples have been analyzed, originating from different sources. The geographic focus point of this study was the upwelling region off Peru. In this area Parkes et al. (1994) first provided evidence for the existence of a deep bacterial biosphere. During RV SONNE cruise SO 147 in June 2000 this area was extensively

sampled down to sediment depths of about 5 mbsf with multicores and gravity cores. In spring 2002, during ODP Leg 201, deep sediment cores (> 100 m long) on the Peru continental margin were taken. Sulfate reduction rates measured on samples from the Peru continental margin are presented in Chapter 5.

Another set of deep biosphere samples that was analyzed originated from the Nankai Trough, off the coast of Japan, taken during ODP Leg 190. Samples from several cores reaching down to > 1000 mbsf were analyzed for sulfate reduction. With the exception of one core, only the shallowest samples showed detectable activity. The results from this set of samples will not be addressed in any greater detail in this thesis

4) Quantification of rates of sulfate reduction and methane oxidation in hydrothermal sediments.

In collaboration with the University of North Carolina at Chapel Hill sediments from the hydrothermal vent field of Guaymas Basin were obtained. These sediments were deposited in an environment with very high heat flow and very steep thermal gradients. The results of Teske et al. (2002) suggest that methane is an important electron donor in those sediment. The quantitative importance of methane as a carbon source and the role of temperature on the utilization of certain carbon sources were tested, see Chapter 4 .

5) Other projects etc.

Another major point of focus was to combine the obtained data with those from the other members of DeepBUG in order to create a more comprehensive conceptual model about the mass balances and metabolic pathways in the deep biosphere.
The data produced during this project have been distributed among the members of DeepBUG and other co-workers. At the time of writing no peer-reviewed journal publication has been submitted including the results of several members of DeepBUG.

There has been a close collaboration with the Microbiogeochemistry group of the Institute for Chemistry and Biology of the Marine Environment (ICBM) in Oldenburg. Members of this group participated in the SONNE 147 cruise and a joint publication was submitted. A manuscript that describes the connection between microbial activity and its influence on the distribution of major and trace elements in surface sediments of the Peruvian Shelf was not included in this thesis (see Chapter 6).

During RV SONNE cruise SO156 in April 2001 numerous multicores and gravity cores from the Chilean continental margin were taken and analyzed for sulfate reduc-

tion. During this cruise not only sulfate reduction rates (SRR) were measured by $^{35}SO_4^{2-}$ radiotracer but also rates of anaerobic oxidation of methane (AOM) by using $^{14}CH_4$. The results of this study will not be covered in this thesis but published somewhere else. During this cruise, substantial amounts of sediment have been taken according to the various needs of the DeepBUG members for method testing and other purposes.

1.9 Contributions to publications

Evaluation of a cold chromium distillation procedure for recovering very small amounts of radiolabeled sulfide related to sulfate reduction measurements
Jens Kallmeyer, Timothy G. Ferdelman, Andreas Weber, Henrik Fossing, Bo Barker Jørgensen

Previously unpublished data from A. Weber and H. Fossing were used.
In close collaboration with T. Ferdelman and B. B. Jørgensen, I carried out the development of the new distillation procedure and wrote the main parts of the paper.
T. Ferdelman wrote the part about the statistical treatment of the data. H. Fossing provided much input during all stages of the project.

A high-pressure thermal gradient block for investigating microbial activity in multiple deep-sea samples
Jens Kallmeyer, Timothy G. Ferdelman, Karl-Heinz. Jansen, Bo Barker Jørgensen

All authors were involved in developing the conceptual model of the high pressure system. K.-H. Jansen did the final technical layout of the pressure system. Based on existing models I solely designed the gradient block myself. The entire set-up was build and operated by me. I wrote the publication, with input and comments from all co-authors.

The effects of temperature and pressure on rates of sulfate reduction and anaerobic oxidation of methane in hydrothermal deep-sea sediments of Guaymas Basin
Jens Kallmeyer, Antje Boetius

A. Boetius and myself jointly developed the idea about the investigation of thermophilic anaerobic oxidation of methane (AOM). I carried out the incubations and all sulfate

reduction rate analysis. A. Boetius and technical staff did the analysis of the AOM samples. The interpretation of the results and the preparation of the manuscript were done jointly.

Pathways of organic carbon turnover in deep sediments from the Peru continental margin
Jens Kallmeyer, Timothy G. Ferdelman, Tina Treude, Ivano W. Aiello Bo Barker Jørgensen

All samples from the SONNE cruise SO 147 were taken and analysed by me. T. Ferdelman I. Aiello, and B. B. Jørgensen were on board Leg 201 of JOIDES Resolution. T. Ferdelman did all SRR incubations. He and myself carried out all distillations. The numerical modeling was carried out by me. The AOM incubations and analysis was done by T. Treude. I wrote the manuscript with input from the co-authors.

2 Evaluation of a cold chromium distillation procedure for recovering very small amounts of radiolabeled sulfide related to sulfate reduction measurements

Jens Kallmeyer, Timothy G. Ferdelman, Andreas Weber, Henrik Fossing, Bo Barker Jørgensen

Intended for submission to Biogeochemistry

Abstract

A method that is specifically optimized for the determination of very low sulfate reduction rates (SRR) with the $^{35}SO_4^{2-}$ radiotracer method is presented. The separation and detection of extremely small amounts of radiolabeled reduced sulfur species is greatly improved by optimization of the entire distillation and detection process. By reducing the amount of background radioactivity, the threshold from which turnover of radiotracer can be detected, was lowered considerably.

Reduction of the background radioactivity could be achieved in two ways,

1) reducing cross-contamination between distillations by modifying the distillation setup
2) preventing an unidentified ^{35}S-containing compound which greatly contributes to the background from reaching the final trap by lowering the distillation temperature

With the method presented here background radioactivity could be lowered by about an order of magnitude, allowing the measurement of low SRR, shorter incubation times, and the use of less ratiotracer. Experiments with pure sulfur minerals and a variety of sediments verified that the efficiency of the new method is equal to the hot single-step chromium reduction method. Furthermore, the reproducibility is also greatly improved through reduced standard deviation.

1. Introduction

Dissimilatory sulfate reduction (DSR) is a key process in the anaerobic degradation of organic matter in marine sediments. The overall reaction can be written as $2CH_2O + SO_4^{-2} \rightarrow 2HCO_3^- + H_2S$. Sulfate reducing bacteria reduce sulfate to sulfide that either remains in solution as hydrogen sulfide or precipitates as various forms of metal mono- and disulfides or elemental sulfur (ES). These combined inorganic end products of sulfate reduction are termed Total Reduced Inorganic Sulfur (TRIS). The importance of DSR as a terminal electron acceptor process in marine sediments has been established through measurements of sulfate reduction rates (SRR) by using carrier-free radiolabeled $^{35}SO_4^{2-}$ as a tracer. The volume of tracer that that is added is in the range of 2 to 10 microliters and contains only negligible amounts of sulfate, ca. 1 nmol sulfate per injection of ca. 50 kBq $^{35}SO_4^{2-}$. Therefore no change in the amount of porewater or sulfate concentration occurs. Radiotracer incubations are generally done

by injecting carrier-free $^{35}SO_4^{2-}$ radiotracer into the undisturbed sediment followed by incubation for hours to days. Incubations may be terminated by transferring the radiolabeled sediment into 20% (w/v) zinc acetate solution.

The rate of sulfate reduction in sediments can be calculated by Equation. 1:

$$SRR = [SO_4] \times P_{SED} \times \frac{a_{TRIS}}{a_{TOT}} \times 1/t \times 1.06 \times 1000 \qquad \text{Eq. 1}$$

SRR	Sulfate reduction rate (nmol cm^{-3} d^{-1})
$[SO_4]$	sulfate concentration of the porewater of the sediment sample (mmol l^{-1})
P_{SED}	porosity of the sediment ($ml_{porewater}$ cm^{-3}_{sed})
a_{TRIS}	radioactivity of TRIS (cpm or dpm)
a_{TOT}	total radioactivity used (cpm or dpm)
t	incubation time (days)
1.06	correction factor for the expected isotopic fractionation (Jørgensen and Fenchel, 1974)
1000	factor for the change of units from mmol l^{-1} to nmol cm^{-3}

By comparing the activity of the radiolabeled TRIS to the total sulfate radiotracer a reduction rate can be calculated from Eq. 1, assuming that only a small fraction of the sulfate is reduced during incubation. The detection limit of the radiotracer method for measuring SRR depends on the efficient separation of a minute amount of radiolabeled reduced sulfur (a_{TRIS}) from an overwhelming background of unreacted $^{35}SO_4^{2-}$ radiotracer. If we wish to measure a rate of 1 pmol cm^{-3} d^{-1} at 10 mM SO_4^{2-} pore water concentration, a porosity of 0.8, 10 days of incubation, and a tracer addition of 1 MBq then the amount of TRIS produced is only about 1.2 Bq. This would generate a radioactive count rate of 71cpm, assuming a distillation and counter efficiency of 100 %.

The vast majority of SRR measurements have been restricted to the upper centimeters to meters of the seafloor and sediments from marine environments with high turnover rates of 10 – 200 nmol cm^{-3} day^{-1} (e.g. Martens and Klump, 1984; Albert, 1985; Jørgensen et al., 1990; Ferdelman et al., 1997; Schubert et al., 2000; Jørgensen et al., 2001). However, in less active sediments, where the rates are expectedly lower by several orders of magnitude, SRR measurements are more difficult to carry out.

Three factors can in theory be manipulated independently to increase the sensitivity of SRR measurements, 1) incubation time (t), 2) the total amount of radioactivity (a_{TOT}),

and 3) the detection limit of a_{TRIS}. With an increase in either time or a_{TOT}, a_{TRIS} proportionally increases. However incubation time cannot be increased infinitely. A theoretical maximum incubation time can be determined, as shown in Equation 2:

$$t_{MAX} = 1/\ln 2 * t_{1/2} \qquad \text{Eq. 2}$$

Where t_{MAX} is the maximum incubation time and $t_{1/2}$ the half-life of the isotope.

The half-life time of ^{35}S is 88 days placing an absolute maximum for ^{35}S incubations at 127 days. Longer times would lead to a decrease in a_{TRIS} because the decay of labeled TRIS becomes faster than the production of newly labeled TRIS. The maximum incubation time is independent of the rate of sulfate reduction and only controlled by the half-life of the isotope. However, long incubation times are not necessarily desirable. The prokaryotic community, the sediment chemistry and the turnover rates may radically change with time from the in situ state. To obtain representative rate measurements all parameters influencing the bacterial community in the sediment should be kept constant over the entire incubation time. The radioactivity of the reduced sulfur compounds must also increase linearly with incubation time in order to be able to calculate a true sulfate reduction rate. If some of the reduced sulfur pool is turned over during incubation these pools become saturated with ^{35}S i.e. the specific radioactivity stays constant and a reliable SRR cannot be estimated (see Fossing (1995) for a detailed discussion).

Increasing the amount of tracer creates another problem. We have observed that $^{35}SO_4^{2-}$tracers from different manufacturers (Risø, Amersham) contain a compound that contributes to the blank. The blank is defined as the amount of radioactivity that is found in the TRIS fraction without being produced by sulfate reduction. There are several sources of blanks, which will be discussed later. The blank that is associated with the tracer itself increases proportionally with the amount of tracer added. Furthermore, an increase in the amount of tracer (a_{TOT}) has practical limitations in matters of cost and safety. The amount of sample that can be efficiently processed is also a limiting factor. Upscaling of the entire distillation set-up, therefore, reaches practical limits very soon. The most promising way to increase the sensitivity of the method is to lower the detection limit of TRI^{35}S by lowering of the radioactive background.

2. Methods and Materials

2.1 Methods

Over the last decades, several methods have been developed to separate the reduced sulfur species from sediments. Sorokin (1962) first introduced direct radiotracer measurements of sulfate reduction rates. Most separations are based on the methods of Zhabina and Volkov (1978) who introduced the hot acidic chromous chloride distillation procedure for separating reduced sulfur species comprising hydrogen sulfide, ferrous sulfide, pyrite, and elemental sulfur. The extracted sulfur species were liberated as hydrogen sulfide and trapped in cadmium acetate solution as solid cadmium sulfide. Subsequent studies have modified this technique according to their needs. Based on the assumption that all H_2S produced by bacteria was retained in the sediment as free or acid volatile sulfur (AVS, i.e. hydrogen sulfide and ferrous sulfide), several authors acidified the sediment in order to retrieve all bacterially produced hydrogen sulfide (Jørgensen (1978) and references therein). Howarth and co-workers (e.g. Howarth and Giblin, 1983) showed that the bacterially produced H_2S also reacts to form pyrite and other non-AVS phases. They concluded that radiotracer measurements solely based on AVS determinations might underestimate the true SRR.

Based on the extraction scheme of Zhabina and Volkov (1978) and modified by Canfield et al. (1986), Fossing and Jørgensen (1989) developed a new single-step method that retrieves all reduced inorganic sulfur species by boiling the sample in acidic chromous chloride solution. The chromium reducible sulfur (CRS) includes pyrite and elemental sulfur (ES). AVS can either be extracted in a step prior to CRS extraction by acidifying the sample followed by degassing or together with the CRS when the sample is boiled in hot acidic chromous chloride solution. The reason for heating the sediment is the very stable S-S bond in ES. Only at elevated temperatures is the Cr^{2+} able to transfer an electron to one of the S atoms, thereby reducing the strength of the S-S bond (Luther, 1987). Fossing and Jørgensen (1989) showed that even with boiling the recovery of ES depends on its degree of crystallinity. While ES dissolved in acetone is recovered almost entirely even with cold chromium solution (91.4 % +/- 2.8 %), recovery drops close to zero for granular and colloidal ES.

The method of Fossing and Jørgensen (1989) has proven to be robust, albeit fairly labor-intensive. Nonetheless, when using the hot chromium distillation, even under stringently clean conditions, a minute amount of radioactivity distils over and creates

a signal that can not be attributed to DSR. This phenomenon, or "blank problem" is inherent to the hot chromium distillation. The sample blank, BS, which is the blank attributed to the radio-labeled sample. B_S can be lowered by washing the sample several times prior to the distillation in order to remove as much $^{35}SO_4^{2-}$ as possible. As long as SRR are high and produce enough radiolabeled TRIS to obtain a ^{35}S-sulfide signal well above B_S, this problem can be neglected. However, as soon as a_{TRIS} is low (< 100 cpm) it becomes crucial to keep B_S even lower in order to detect the actual signal. This blank, B_S, appears to be a function of reaction temperature and acid strength. Whereas acid concentration can be regulated to minimize B_S, heat is required to make the measurement fully quantitative. Eliminating heating would improve the method as long as all TRIS is quantitatively distilled. The sample blank is one of the key problems when a SRR is estimated after a relative short incubation or if SRR are generally low.

Several studies have used passive distillation procedures by which the sample and all reagents were mixed in one container with a trap hanging in the gas phase above the solution in order to trap all produced sulfides. The passive distillation procedures work at cold or at sub-boiling temperatures, are less labor intensive, and allow processing a larger number of samples at one time. However, some of the passive distillation methods may suffer from low recovery (Howarth and Giblin, 1983), especially for ES (Ulrich et al., 1997). Although ES may not form a significant fraction of the total TRIS pool, a significant fraction of the radioactively labeled sulfide may still end up in this fraction during an SRR experiment. In order to improve the recovery of ES, Hsieh and Yang (1989) used N, N-Dimethylformamide (DMF). Not only does DMF solubilizes ES rapidly, but DMF is also an organic solvent commonly used to promote reaction rates. This reagent destabilizes the S-S bonds and therefore allows the chromium to reduce it to sulfide (Hsieh and Yang, 1989). In theory, a carry over of non-reacted sulfate is more limited or even absent by this procedure due to the lower distillation temperatures. The passive distillation has certain practical disadvantages for the recovery of very low levels of radiotracer-labeled sulfide. Since the trap hangs inside the reaction flask, aerosols containing radiolabeled $^{35}SO_4^{2-}$ might reach the trap, carrying over non-reacted sulfate and thereby increasing B_S. Moreover, the trapping vial will be contaminated on the outside, requiring either extremely thorough cleaning or transfer of the trapping solution into a new vial. CO_2 produced during the acid dissolution of carbonate-containing samples creates high pressure and can cause the reaction flask

to leak or burst. Sample size either has to be kept to a minimum, a step to remove the carbonates is required prior to distillation, or a pressure-compensation has to be installed. We have adapted the use of DMF in the acidic chromium solution in order to run the active distillation at room temperature.

2.2 Hot single-step chromium reduction method

In the hot single-step chromium reduction method of Fossing and Jørgensen (1989), a sample containing sediment and zinc acetate (ZnAc) is centrifuged and the supernatant removed. Two to three grams of sediment are mixed with 20 ml of 50 % (v/v) ethanol-water solution and placed into a 3 neck round bottom flask that is connected to a reflux cooler. Nitrogen is introduced through one of the necks, the other one is used as a chemical port. The apparatus is gassed with N_2 for at least 10 minutes to remove any O_2. For a single-step distillation 8ml of 6N HCl and 16ml of a 1M $CrCl_2$ solution are injected through the chemical port and the slurry is boiled for 40 minutes. The produced volatile H_2S is bubbled through a disposable Pasteur pipette into a trap filled with 7 ml of 5% (w/v) ZnAc-solution to trap all sulfide as zinc sulfide. To prevent the trap from overflowing a drop of antifoam is added. In cases where samples contain only little sulfide, some carrier (zinc sulfide suspension) is added to enhance the efficiency of the method.

2.3 Cold single-step distillation

Figure 1 shows the cold distillation apparatus. The setup is similar to the hot distillation but with the following important modifications:

1) The reflux cooler is replaced by PEEK (Poly-Ether-Ether-Ketone) tubing (1/8" OD). PEEK is gas impermeable and non-reactive. It can easily be cleaned by flushing with water.
2) In between the PEEK tubing and the zinc acetate trap another trap with 7 ml of a 0.1 M Citrate solution (19. 3 g Citric acid, 4 g NaOH in 1 l H_2O, pH 4) is placed. This trap is necessary to prevent any aerosols from reaching the final trap. In the hot distillation this trap is not necessary as condensed water runs down the reflux cooler, stripping the aerosols from the upward flowing gas stream. Experience has shown that the citrate trap does not have to be replaced after every distillation. All connections between the glassware and the PEEK tubing are made from short pieces of Viton tubing, mechanically secured with silicone tubing placed over it.

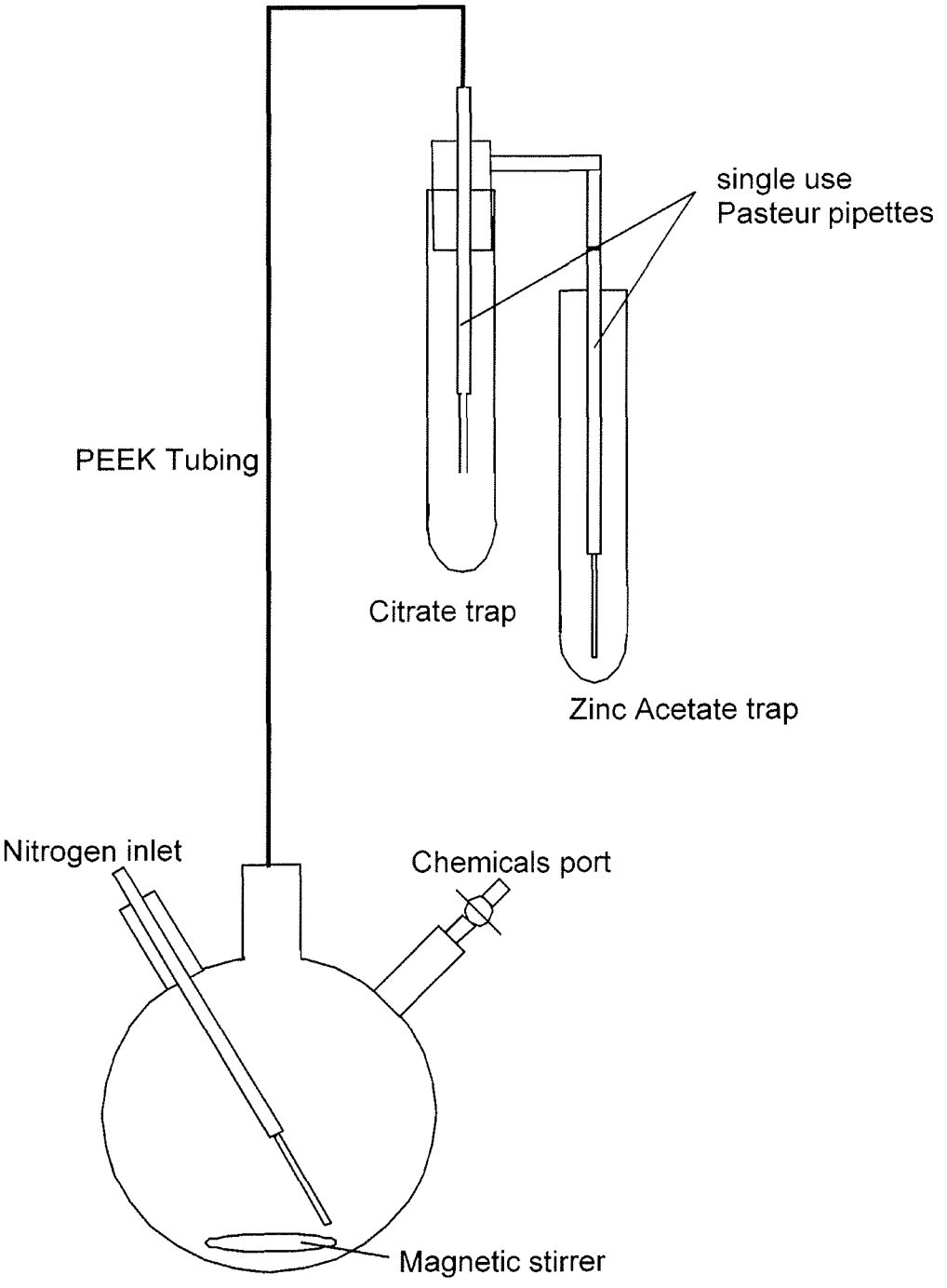

Fig. 1: Schematic view of the cold distillation apparatus. See text for description

The sample is transferred to a 3-neck round-bottom glass flask, 20 ml of N, N-Dimethylformamide (DMF) is added together with a magnetic stir bar to secure an efficient mechanical break-up of the sample. While DMF enhances the reactivity of reduced sulfur species, it also allows oxidation to take place at an enhanced rate. To prevent oxidation prior to distillation, contact of the sediment-DMF slurry with air should be avoided. As soon as the sample is mixed with DMF the reaction flask is connected to the gas line and flushed with N_2 for 10 minutes. Subsequently, 8 ml of 6 N HCl are injected through the chemical port, followed by 16 ml of 1 M $CrCl_2$ solution. The sample is then bubbled at a rate of 2 – 5 bubbles per second with N_2 for 2 hours and continuously stirred. Over the last 15 minutes the gas flow rate is increased to remove the last vestiges of sulfide from the system. In case the sample is rich in carbonate the acid has to be added slowly and stepwise to avoid heavy foaming during the liberation of CO_2. If the HCl concentration is too low, and consequently the pH too high, the Cr(II) solution will appear brick-red in color. With additional HCl the Cr(II) solution will revert to its characteristic blue color. Similar to the hot method, the liberated sulfide is trapped as zinc sulfide in 7 ml of 5% (w/v) ZnAc-solution with a drop of antifoam. Carrier should be added to samples with low sulfide content to enhance efficiency; we typically employ 500 µl of a 50 mM ZnS suspension.

2.4 Efficiency control experiments

To test the efficiency of the new method, pure mineral sulfur phases were prepared and then distilled using both the hot and cold chromium reduction method. The quantity of trapped sulfide was determined according to the method of Cline (1969).
The following minerals were prepared and investigated:

$BaSO_4$: 1 L of 0.25 M barium hydroxide solution (47.34 g $Ba(OH)_2{}^*H_2O$ in 1 L H_2O, pH adjusted to 7 with HCl) was mixed with 200 ml of 1.25 M sodium sulfate solution (177.55 g Na_2SO_4 in 1 L H_2O). The precipitated $BaSO_4$ was washed three times in deionized water and dried at 60 °C.

Dissolved Sulfur: An exact amount of flour of sulfur (10 to 100 mg) was dissolved in 20 ml of acetone.

Crystalline Sulfur: Flowers of sulfur (10 to 100 mg) was directly weighed into the reaction flasks.

FeS: 200 ml of 0.6 M ferrous sulfate solution (167 g $FeSO_4{}^*7H_2O$ in 1 L H_sO) was mixed with 200 ml of 0.6 M sodium sulfide solution (144 g $Na_2S{}^*9H_2O$ in 1 L H_2O).

The resulting precipitate was washed five times in de-ionized water to remove free sulfides.

Natural FeS_2: Originating from an ore-processing flotation plant (cf. Schippers and Jørgensen, 2001). The material was ground to 50 – 100 µm grain size.

Synthetic FeS_2: The mineral was prepared according to Fossing and Jørgensen (1989). It was cleaned of adhering elemental S by mixing several hundred milligram of material with 250 ml n-hexane in a stoppered glass bottle and placing it on a shaker overnight. The remaining grains were rinsed in acetone. The elemental sulfur that was dissolved in acetone could be precipitated as colloidal sulfur upon addition of water. Extraction was complete after no precipitation could be observed in the washing solution.

2.5 Tracer experiments

Radioactivity was determined by using a liquid scintillation counter (Packard 2500 TR) with a counting window of 4 to 167 keV, no luminescence correction, and high sensitivity mode turned off (we observed that this feature increased background variability of count rates without a meaningful gain in sensitivity or lowered detection limit). A cut-off of the low energy range (0 – 4 keV) eliminates a large fraction of low energy background counts, while only minimally reducing the count rate of ^{35}S, whose β-energy spectrum lies at higher energies (up to 167 keV). All activities presented in this study were recorded in the range of 4 – 167 keV. The scintillation cocktail used was Lumasafe Plus® (Lumac BV, Holland) mixed with the trapped ZnS 2:1, vol:vol. Results are given as counts per minute (cpm).

2.6 Background determination

When a distilled sample is counted on a scintiallation counter, background is an inherent part of the the total number of counts as shown in Equation 3:

$$a_s = a_{TRIS} + B_S \qquad \text{Eq. 3}$$

Where a_S is the amount of radioactivity in the distilled sample, a_{TRIS} are the activity due to the $TRI^{35}S$ formed during DSR, and B_S is the sample blank that is attributable to all background sources. The sample background, B_S, is composed of several factors as shown in Equation 4:

$$B_S = B_C + B_D + B_T \qquad \text{Eq. 4}$$

Where B_C, or counter blank, is the count rate inherent to the environment and scintillation fluid without addition of a radioactive sample; B_D, or distillation blank, is the background radioactivity resulting from the distillation equipment itself (e.g., traces of radioactivity in gas lines), and B_T, or tracer blank, is the count rate attributed to the ^{35}S radio-labeling and distillation, but not arising from bacterial sulfate reduction.

2.6.1 Counter blank and distillation blank

The counter blank, B_C, is equivalent to the number of cpm that are recorded by the scintillation counter when a non-radioactive sample is measured. It is independent of the method of distillation and might be lowered slightly by enforced cleanliness and thorough evaluation of the counting conditions. The distillation blank, B_D, can be determined by distilling a non-radioactive sample immediately after a radioactive sample has been treated in the distillation equipment. This type of blank takes into account ambient background radioactivity in the distillation apparatus and reagents. Most of this ambient radioactivity arises because of memory effects (carry-over) between distillations.

2.6.3 Tracer blank

The tracer itself contains a component, B_T, that can be distilled and thus contributes to the sample blank, B_S. To investigate this radioactive component, we separated the tracer using ion-chromatography (pump: Waters 510; column: Waters IC-Pak Anion 4.6 mm x 5 cm; detector: Waters 430 Conductivity detector; eluent: 1 mM Isophtalic acid; flow: 1.0 ml/min). The retention time for sulfate was about 11 min. The outflow from the IC was collected using a fraction collector (time intervals 0 – 2, 2 – 6, 6 – 12, 12 – 18, 18 – 24, 24 – 40 min.). Those six fractions were distilled using the hot chromium reduction method of Fossing and Jørgensen (1989). The amount of radioactivity in each fraction prior to and after distillation was compared. In an identical experiment the outflow of the IC was collected in two-minute time-intervals and counted. The set of samples from the latter experiment was kept and counted bimonthly over a period of two years in order to establish whether the $^{35}SO_4^{2-}$ tracer contained any other radioisotope than ^{35}S as judged from the ^{35}S-half life of 88 days.

2.6.2 Sample blank

The sample blank (B_S) gives the total number of counts that are not associated with sulfate reduction (see Eq. 4). A sediment sample is first vigorously mixed with 20 % (w/v) ZnAc to cease sulfate reduction, after 30 minutes or more, radiolabeled $^{35}SO_4^{2-}$ is added in the same amount as used for sulfate reduction measurements. Because bacterial activity is stopped before the addition of the tracer, no turnover should take place, and accordingly no radiolabeled TRIS should form. The number of counts found in the trap should be equal to $B_D + B_C$. It is important to note that we only ever measure B_C, B_S, or $(B_C + B_D)$. There is no direct means of ascertaining B_D or B_T alone.

2.7 Preparation of radiolabeled sediments

Sediments from various sites were obtained for testing the new method. The types of sediments used for testing the method cover a variety of marine environments with respect to sediment type, salinity, sulfate reduction rate, and organic carbon content. In order to have a large amount of homogeneous material for the tests, several hundred grams of sediment were incubated with $^{35}SO_4^{2-}$ radiotracer in gas-tight plastic bags (Hansen et al., 2000) for 3 to 4 days. Transferring the mud into 20 % (w/v) ZnAc-solution terminated the incubation. The homogenized slurries were dispensed with a pipette and distilled using both the hot and cold distillation methods. The distillation time necessary to obtain reproducible results with the cold chromium distillation was determined from a time course experiment. Hence, after the distillation was initiated the ZnAc-trap was changed after 30, 60, 90, 120, 150, 210, and 300 minutes and the amount of radioactivity in each trap was measured. The sediments used were:

Namibia Upwelling (Nam): Taken with a Multicorer at 22°38.51S, 4°18.259E at a water depth of 70 m. The sediment is diatomaceous ooze deposited within the oxygen minimum zone. Sulfate reduction rates range from 100 to 2000 nmol cm^{-3} d^{-1}.

Makran Plateau off Pakistan (Mak): The sample consists of indistinctly laminated olive grey mud (A. Lückge, pers. comm.). It was taken with a box corer during the RV SONNE cruise SO 130 at 22°56'34" N, 66°38'77" E in 831 m depth below the oxygen minimum zone. Sulfate reduction rates were expected to be extremely low.

Peru (Pe): The sample was taken during the RV SONNE cruise SO 147 in summer 2000 in the coastal upwelling off Peru within the Oxygen Minimum Zone. Sulfate reduction rates are between 50 and 700 nmol/cm^3/d at the surface. The sediment is sandy clay.

Cold		
Mineral	recovery %	sd
Barite	0,014	0,005
S crystal	74,80	7,61
S dissolved	90,04	1,45
FeS	95,88	9,72
Pyrite crystals 50-100 µm	88,40	4,00
synthetic Pyrite	101,28	5,62

Hot		
Mineral	recovery %	sd
Barite	0,005	0,001
S crystal	10,35	3,82
S dissolved	84,47	5,42
FeS	98,36	2,10
natural Pyrite *	95,00	2,60
synthetic Pyrite **	100,00	8,40
*= data taken from Canfield et al. (1986)		
**=data taken from Fossing & Jørgensen (1989)		

Tab 1: Recovery of pure sulfur phases.

Weddewarden (WW): The sampling site is located in the intertidal zone of the estuary of the River Weser in northern Germany. Salinity ranges from 4 ‰ to 20 ‰, temperature from 3 °C to 30 °C. The sediment consists mostly of silt with ca. 10 % fine sand and 10 % clay. SRR are highly variable and range from 1 to 100 nmol $cm^{-3} d^{-1}$.

Sample blank (B_S): Makran Plateau sediment (Pak) was preserved in 20 % (w/v) ZnAc-solution to stop sulfate reduction prior to addition of $^{35}SO_4^{2-}$.

2.8. Application of the cold method

Samples from several cruises along the continental margin of Chile and Peru were analyzed by the cold chromium distillation technique. These samples cover a broad range of water-depths, sediment-depths, ages, organic matter content, sedimentological properties, and sulfate reduction rates.

3. Results

3.1 Pure sulfur phases

Control experiments with different pure sulfur-phases show that the cold chromium distillation technique produces results comparable to the hot distillation (see Table 1). The only value that differs significantly is the recovery of crystalline sulfur. With the cold distillation we extracted 74.8 % ± 7.6 of crystalline sulfur whereas the recovery

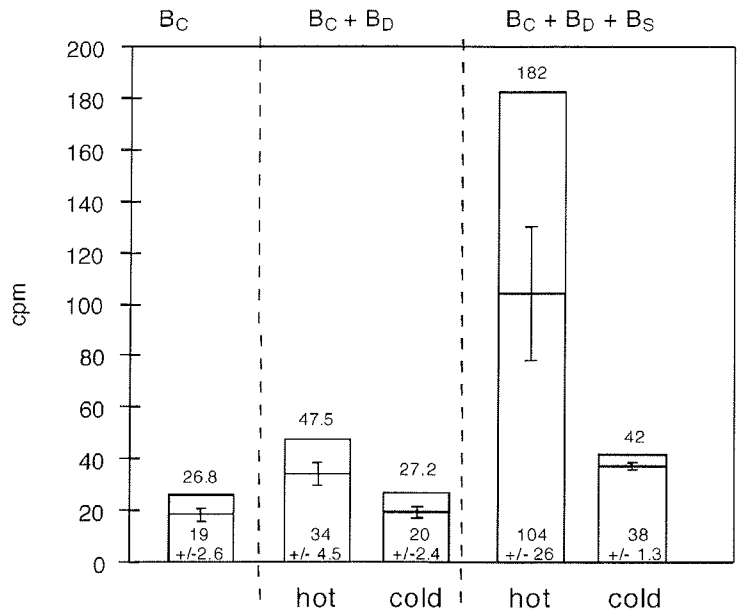

Fig 2: Counter blank, distillation blank, and sediment blank obtained with the single-step chromium reduction method and the cold distillation method. The error bars show one standard deviation. The upper number on each bar indicates the respective value plus three times standard deviation.

only averaged 10.4 ± 3.8 %for the hot method. $BaSO_4$ was not reduced during distillation by either method. For FeS both methods fell slightly short of 100 %, probably caused by oxidation of FeS during preparation and storage or inhomogeneities in the suspension. For natural FeS_2 the cold method recovered only 88.4 ± 3.5 %, slightly less than Canfield et al. (1986) found in their study (95 ± 2.6 %). The synthetic pyrite was completely extracted within 2 hours (recovery 101.3 ± 5.6 %), which is consistent with the results of Fossing and Jørgensen (1989) (100 ± 8.4 %).

3.2 Blanks

For the cold method the sum of counter blank and distillation blank ($B_C + B_D$) does not differ significantly from the counter blank (B_D). The amount of radioactivity found in the trap (20 +/- 2.4 cpm) after running a distillation blank exercise only differs slightly from BC (19 +/- 2.6 cpm, Fig. 2). For the hot method $B_C + B_D$ is significantly higher than for the cold method as it is significantly higher and has a larger standard deviation (34 +/- 4.5 cpm). For sample blank ($B_S = B_C + B_D + B_T$) the trend is the same: the cold method has a much lower B_S than the hot method (38 +/- 1.3 cpm and 104 +/- 26 cpm, respectively).

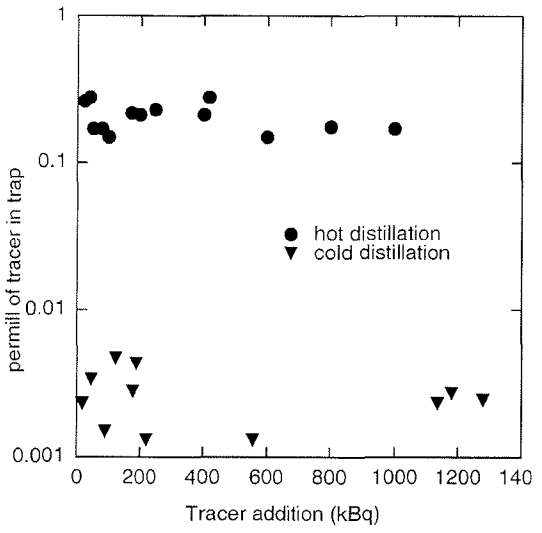

Fig. 3: Relationship between the amount of tracer added and the amount trapped as radiolabeled TRIS. Hot distillation is shown with circles, cold distillation with triangles.

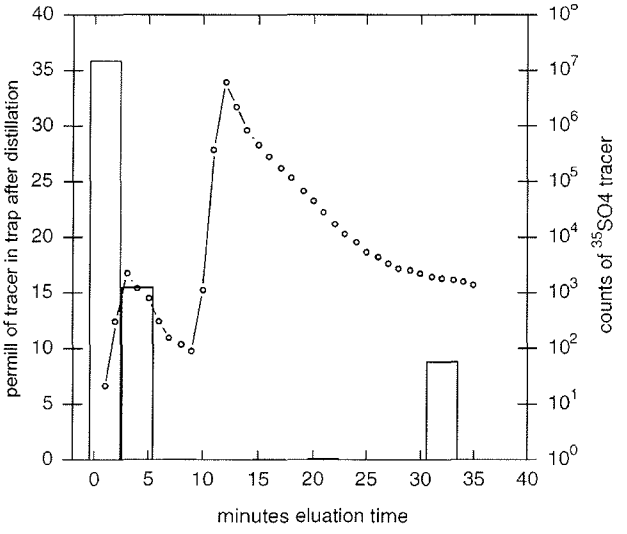

Fig. 4: Separation of the tracer with ion chromatography. The curve shows the distribution of radioactivity over time. The first small peak at 4 minutes is the contaminant compound, the large one at 12 minutes is sulfate. The bars show the fraction of the eluted tracer that distilled over in a hot distillation. Note the log scale for $^{35}SO_4^{2-}$ radioactivity.

3.3. Tracer distillations

The distillation of pure $^{35}SO_4^{2-}$ tracer shows that the tracer blank (B_T) for both methods is proportional to the amount of tracer added (Fig. 3). As B_C is independent from the amount of tracer added, B_C can be subtracted from the amount of radioactivity found in the trap after distillation. By this way B_T can be determined indirectly.

The cold method lowers the tracer blank by about two orders of magnitude, compared to the hot distillation. The tracer blank that is observed in both methods appears not to be caused by sulfate but by some other radioactive compound.

Separation of the tracer solution by ion-chromatography provides further evidence for the existence of a non-sulfate radioactive compound (curve in Fig. 4). Sulfate separates at about 11 min and 99.95 % of the radioactivity is found in the 6 to 24 minute fractions. The sample blank (bars in Fig. 4) from the separated sulfate fraction (6 – 4 min) is very low, < 0.01 ‰ of the total counts. A minor peak of radioactivity appears at 3 minutes (curve in Fig. 4). Nevertheless, this minor peak of radioactivity contributes to the major fraction of the sample blank. In the 0 to 6 min fraction about

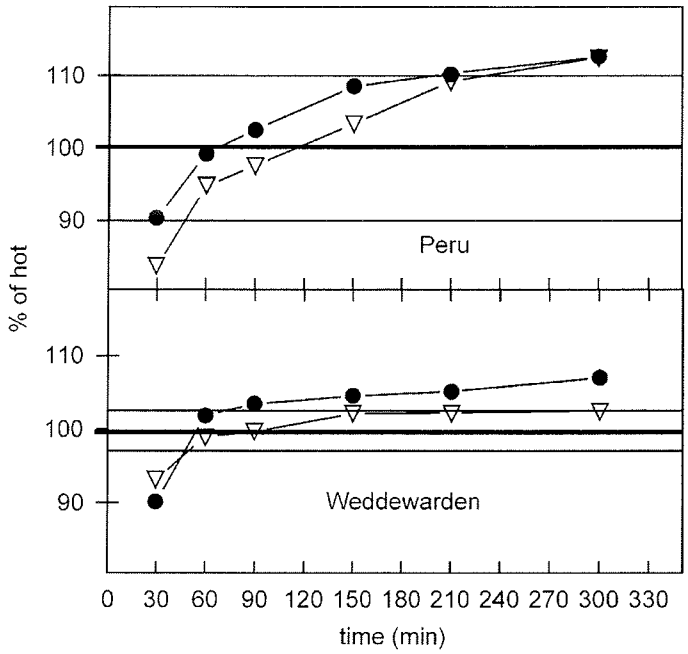

Fig. 5: Time course experiment to find the time needed for quantitative cold distillation, shown for two different sediments. The results are expressed as percent of the average of the hot distillation. The upper an lower vertical line show one standard deviation of the hot method.

35 ‰ of the total counts were measured as sample blank. This means that 0.05 % of the total radioactivity produce a blank that is 3500 times larger than the blank of the remaining 99.95% of the tracer. By counting the separated samples repeatedly over two years we could see that the decay followed the expected decay of ^{35}S (data not shown).

3.4 Incubated samples

The time needed for the complete cold distillation was determined in a time course experiment (Fig. 5). Performing a cold distillation on radiolabeled samples the distilled amount of aTRIS was within one standard deviation of the results of the hot method after 120 minutes. Therefore all subsequent experiments we distilled for 120 minutes. Figure 6 shows the results of the hot and cold distillation of the bag incubations of the different sediments. The results are given as counts per minute of the trapped sulfide per gram of sediment slurry dispensed (cpm/g). For all sediments tested the recovery of the cold distillation falls roughly within one standard deviation of the hot method.

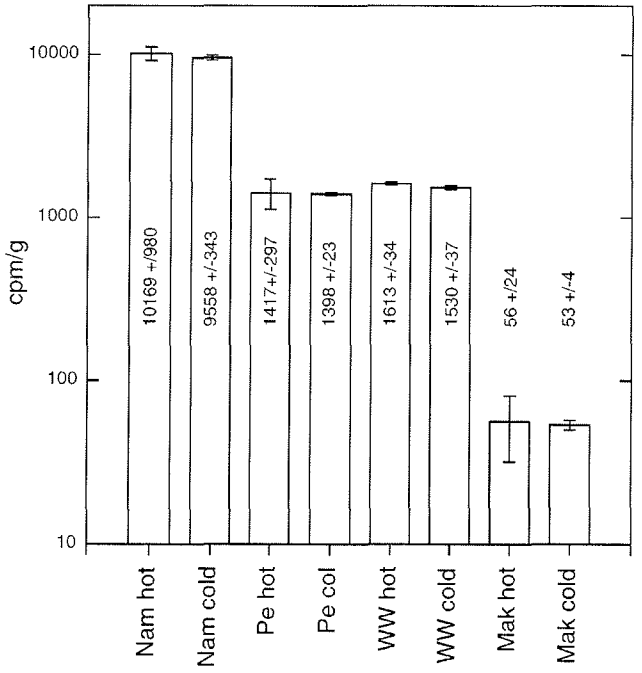

Fig. 6: Efficiency of the hot single-step chromium reduction method and the cold distillation method described in this paper. The error bars are one standard deviation (n=6). Note log scale on the y-axis.

4. Discussion

The techniques currently used for the determination of sulfate reduction rates are either active distillations and similar to the single-step chromium reduction method of Fossing and Jørgensen (1989) or passive techniques (Ulrich et al., 1997). The new cold chromium reduction method and the hot single-step chromium reduction method at a first glance show the same results (Fig. 6). However, the standard deviation is significantly less when the cold method is applied. What is also important, however, when deciding on the distillation method is the cpm g^{-1} of the sample blank. Figure 7 also shows the effect of the changing sample blank, BS, and sample blank standard deviation, sBS, on the minimum detection limit, MDL. For most analytical systems, the minimum detection limit (MDL) can be defined as the mean sample blank value (B_S) plus some factor (k) times one standard deviation (σ_{BS}) of the sample blank signal.

$$MDL = B_S + (k * \sigma_{BS}) \qquad \text{Eq. 5}$$

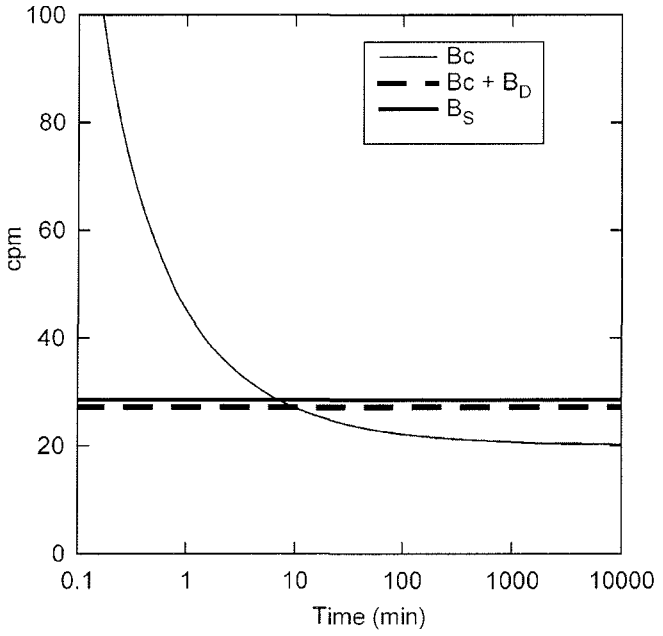

Fig. 7: The influence of counting time on the minimum detection limit (MDL). The black curve indicates the counter blank (BC), which can not be lowered. Assuming a counter blank of 20 cpm, and distillation blank (BC + BD), and sample blank (BS) of 2.4 and 2.9 cpm, this would result in MDL of 27.2 and 28.5 cpm, respectively. Both values do not change with counting time. After about 10 minutes the analytical detection limit exceeds BC, longer counting times would not limit the MDL.

Skoog and Leary (1992, and references therein, in particularly Kaiser, 1970) suggest that k = 3. Kaiser (1970) states that blank measurements are not normally distributed, and therefore we may only expect a confidence level of at least 89 %.

The hot method produces a sample blank of 104 ± 26 cpm (n = 6) but this value is reduced significantly to 38 ± 1.3 cpm when the cold method is applied (Fig. 2). The corresponding MDL is 182 cpm for the hot and 41.9 cpm for the cold method. The sample blank (B_S) must be subtracted from the total counts of a sample in order to calculate a realistic SRR. The Pak sediment for example reveals counts by the hot method (56 ± 24 cpm g^{-1}) that are significantly below the sample blank (104 ± 26 cpm g-1) and the MDL (182 cpm). A sulfate reduction rate cannot be calculated as subtraction of the sample blank results in a negative value. In this case a SRR in the Pak sediment can only be estimated by using the cold method (incubated sediment 53 ±4 cpm g^{-1}, B_S = 38 ± 1.3 cpm g^{-1}, MDL = 41.9 cpm, net TRIS radioactivity 15 ± 4.2 cpm g^{-1}).

When separating the tracer by ion chromatography (IC) a compound that perhaps is the cause of the sample blank (B_S) could be isolated by its shorter retention time. The bar graph in Fig. 4 shows that the fractions collected from 0 to 6 minutes produce the majority of the sample blank when the hot method is performed, whereas the increased values between 30 and 35 minutes cannot be explained. When counting the time fractions repeatedly over almost two years and comparing the decay with the expected decay for ^{35}S we can conclude that no other radioisotope was present in the $^{35}SO_4^{2-}$ tracer but ^{35}S. However, we could not determine whether this compound is a real ^{35}S-contamination, and therefore could possibly be removed one way or the other, or just in equilibrium with sulfate.

An increase in the amount of tracer, and thereby an increase in its specific activity (activity of tracer per mole of sulfate in the sample) has its limitations because of the sample blank that is associated with the tracer itself. As can be seen in Figure 1, 0.001 to 0.01 ‰ of the tracer is transferred to the ZnAc-trap when non-reduced $^{35}SO_4^{2-}$ is distilled by the cold method. With the hot method this value is two orders of magnitude higher. This means that the sample blank is still low when the cold method is applied even when the sample blank increases its total cpm when more $^{35}SO_4^{2-}$ is injected into the sediment (Fig. 3). By washing the sample prior to the distillation, the sample blank further decreases but preparation time increases considerably.

The sample blank might not only be caused by the compound that was separated by IC but also through thermochemical sulfate reduction (TSR). Figure 4 shows that most of the carry over is derived from the unidentified compound. Apparently this compound distils over at lower temperatures than sulfate because the sample blank is greatly reduced upon a reduction of the distillation temperature. Machel (2001) and Trudinger et al. (1985) have shown that TSR can take place in the presence of a strong reducing agent even at temperatures well below 200 °C. Divalent chromium is a strong reducer and the walls of the reaction flask certainly reach temperatures above 100 °C. When boiling the sediment slurry in acidic chromous chloride solution the conditions inside the reaction flask may allow TSR. By comparing the values of the sample blanks in Fig.2 it is evident that reduced distillation temperatures lead to a reduction of tracer being carried over. Although the unidentified compound causes the major part of the carry-over, TSR can not be completely ruled out.

The low distillation temperature of the cold method had also another positive effect. Metal parts such as heaters, clamps etc. used in the distillation set-up were usually

exposed to a very corrosive environment during the hot distillation. This is not the case with the cold method as hardly any acid vapor is produced. The analytical set up therefore has a much longer lifetime. A major drawback of the cold method is the use of DMF, which is a toxic organic solvent requiring careful storage and handling. Costs of DMF disposal may also be considerate.

Reduction of the distillation and tracer blank (B_D and B_T) are the keys to better sensitivity. Therefore in addition to lowering the temperature, we sought to improve the distillation setup. In order to keep the distillation blank to a minimum, all equipment in contact with the sample must be disposable or kept absolutely clean. Cross-contamination was considerably reduced by using only glassware that can either be put into a dishwasher or is disposable and PEEK tubing that does not absorb any chemicals and can easily be cleaned. Soaking the coolers of the hot distillation apparatus in acid and rinsing them thoroughly takes away some contamination but no constant background could be achieved (data not shown). Removal of the coolers contributed to a reduction of the distillation blank. The PEEK tubing has a much lower surface area (ca. 1500 mm^2) than the coolers (ca. 95000 mm^2). When comparing the numbers of the distillation blank from the hot method with those from the cold method (Fig. 2), the improvement can clearly be seen. Not only the distillation blank itself was reduced but also the standard deviation (from 34 +/- 4.5 cpm to 20 +/- 2.4 cpm).

In order to be able to measure low SRR all aspects of the procedure had to be optimized but there are limits to incubation length and total amount of radioactivity that might be used. The counting efficiency of modern scintillation counters is in the range of 95 %, leaving little space for improvements. We also considered whether longer counting times would lower detection limits by decreasing the variability of the counter blank signal (B_C). The treatment of background measurements and determination of detection limits in radiometric analysis has received an immense amount of attention. For this discussion, we use the treatment of Hurtgen et al. (2000) that is based on the seminal work of Currie (1968), where the lower limit of detection, LD, is defined as:

$$LD = 2.861 + \sqrt{4.78\ b_C + 1.36} \qquad \text{Eq. 6}$$

Where b_C = BC*t, the number of total counts of the counter blank over the measuring period, and where t = time in minutes . The $MDL_{counter}$ then becomes LD/t. Fig. 7 shows

the $MDL_{counter}$ for background count rates of 20 cpm, which is an upper value for the counter background. Figure 7 shows that longer count times lead to a correspondingly lower MDLcounter value.

However, increasing counting times only makes sense up to a certain point. The sums of distillation plus counter blank blanks ($B_C + B_D$) and distillation, counter, and sample blank ($B_C + B_D + B_S$) have standard deviations of 2.4 and 1.3 cpm respectively (Fig. 2) . Assuming a counter background of 20 cpm, this would give MDLs of 27.2 and 23.9 cpm (using Eq. 5). Our experience is that cpm values of the sample and distillation blanks vary independently from counting time. Thus, after 10 minutes of counting, these analytical detection limits exceed the MDLcounter. Longer counting times would not lower the detection limit. The real detection limits that we are likely to be facing are shown as the straight lines in Fig. 7.

The age of the sediment and thereby the crystalinity of the mineral phases influences the distillation time and the specificity of the method. Applying the hot method to sediment samples Canfield et al. (1986) report extraction times between one hour for modern sediments and two hours for ancient sediments (e.g. shales). For the rather young sediments in our study we found two hours to be sufficient to obtain results comparable with the hot distillation (Fig. 5). A time course experiment should be conducted for any sediment in order to evaluate the essential extraction time. We found that it is crucial to keep the sample as fine-grained as possible and in constant suspension, otherwise the reaction is slowed down considerably.

The distillation of pure mineral phases shows good agreement between the hot and the cold method except of ES (Table 1). Both methods completely extract AVS when FeS was chosen as a typical AVS mineral. As Duan et al. (1997) have shown, the sulfur pool sizes can differ based on the extraction scheme used, and terms like AVS and CRS are operationally defined rather than based on mineralogical properties.

Liberation of ferric iron through the addition of acid can cause oxidation of AVS to ES, thereby underestimating the amount of AVS (Berner, 1964). Albert (1985) solved this problem by addition of titanium chloride or stannous chloride to the AVS extraction and increased AVS recovery by 20 – 38 %. When a single-step distillation (either hot or cold) is performed, this problem is circumvented as all liberated ferric iron becomes immediately reduced to its divalent state by the chromium.

Dissolved ES is extracted with almost equal efficiency by both methods but for the hot method the recovery is low for crystalline ES (Table 1). Because DMF is added

during the cold method ES is rapidly brought into solution which allows the chromium to reduce it.

Pyrite is the quantitatively the most important chromium reducible sulfur (CRS) mineral. Canfield et al. (1986) reported a recovery of mineral pyrite of 95.9 % with the hot chromium reduction method. The cold method recovered only 88.4 %, perhaps we have used a coarser material. The synthetic pyrite resembles more closely the type of mineral that can play a role as a sink for sulfides produced during sulfate reduction. This mineral was extracted completely by both methods. Many workers have highlighted the differences between the extraction of freshly precipitated and sedimentary or metamorphic pyrite. According to Cornwell and Morse (1987) synthetic pyrite can be completely extracted with hot HCl and $SnCl_2$. Fossing and Jørgensen (1989) found that cold HCl and $CrCl_2$ have the same effect. Duan et al. (1997) divided the CRS fraction into a cold extractable (CCRS) and hot extractable (HCRS) fraction in order to separate two different classes of crystallinity of pyrite. The percentage of CCRS of the total CRS varied from about 20 % for Jurassic pyrite, 40 to 60 % for recent concretions and pyrite in recent black mud, to 100 % for synthetic pyrite. Such differentiation may be helpful for a mineralogical classification of sediments but for measurements of SRR, it seems unlikely that any highly crystalline mineral phases play a major role. Duan et al. (1997) also have shown that the sulfur pool sizes can differ based on the extraction scheme used, and terms like AVS and CRS are operationally defined rather than based on mineralogical properties. When comparing the results from the distillation of the different incubated sediments, no significant difference was found between the hot method and the cold method. Therefore it can be concluded that even if highly crystalline pyrite (or HCRS according to Duan et al., 1997) has formed during incubation, it was equally extracted by the two methods.

Isotope exchange reactions between labeled compounds can influence the distribution of ^{35}S between the different sulfur pools (Fossing and Jørgensen 1990). In cases where only specific sulfur fractions are extracted from the sediment this could be a possible source for errors. Fossing and Jørgensen (1989) however have not found any isotopic exchange between pyrite and other mineral phases within 24 hours. Therefore, it can be concluded that even if such reactions take place during long incubations, the loss of radioactivity due to the incorporation into recalcitrant mineral phases like highly crystalline pyrite would be only very small or not existent.

Only a few SRR measurements have been made in sediment samples from depths of several hundred meters below the sea floor (see Parkes et al., 2000, and references therein). Most probably because the SRR in these sediments often are at or below the detection limit of the hot methods, they were not able to pick up smaller differences in SRR that would reflect changes in specific environmental factors like lithology, porosity etc. Therefore, as long as we are not able to detect very low rates and continue to use the hot method, SRR measurement in the deep sub-seafloor biosphere will continue to be sparse and crude.

We have analyzed several hundred samples from cruises along the continental margin of Chile and Peru that cover SRR that decrease over ca. 7 orders of magnitude with depth (Kallmeyer et al. in prep.). The cold distillation method is able to give reproducible results over the whole range. The lowest numbers detected were in the range of ca. 0.1 pmol cm^{-3} d^{-1} and are thus up to 2 orders of magnitude lower than those of Parkes et al. (1994), measured at the same locations (Kallmeyer et al. in prep.). We therefore argue that SRR measured by the cold method not only result in more reasonable rates of the bacterial turnover in deep sediments but are also able to reveal sulfate reduction that cannot be detected when the hot method is applied.

5. Conclusions

We have established a distillation procedure for reduced sulfur and optimized for sensitive measurements of sulfate reduction which allows rate measurements over a broad range and down to levels previously not measurable (< 1 pmol SO_4^{2-} cm^{-3} d^{-1}). The method is optimized for the measurements of sulfate reduction rates with $^{35}SO_4^{2-}$ radiotracer, its use for the sequential extraction of different reduced sulfur phases based on their solubility in different reagents was not specifically tested. By combining the advantages of the hot single-step chromium reduction method of Fossing and Jørgensen (1989) with those from passive distillation procedures, we reduced cross contamination and lowered the background considerable to levels that make it possible to detect extremely low sulfate reduction. The improved sensitivity of the method can not only be used to measure SRR on deeply buried or inactive but also to reduce incubation length, thereby minimizing the artifacts caused by changes in the sample during incubation. Thus for obvious reasons the cold method should be preferred when low counts (i.e. close to the sample blank) are expected.

3 A high-pressure thermal gradient block for investigating microbial activity in multiple deep-sea samples

Jens Kallmeyer[1], Timothy G. Ferdelman[1], Karl-Heinz Jansen[2], Bo Barker Jørgensen[1]

Accepted for publication in Journal of Microbiological Methods

[1] MPI for Marine Microbiology, Celsiusstr. 1, 28359 Bremen, Germany
[2] SYKAM GmbH, Am Ährenfeld 13, 82256 Fürstenfeldbruck, Germany

Abstract

Details about the construction and use of a high-pressure thermal gradient block for the simultaneous incubation of multiple samples are presented. Most parts used are moderately priced off-the-shelf components that easily obtainable. In order to keep the pressure independent of thermal expansion of the sample vessels, a back-pressure system with a constant leak rate was installed. Pressure is applied through high-pressure liquid chromatography (HPLC) pumps that run in constant pressure mode with variable flow rate, thereby regulating any pressure fluctuations. The device allows incubations along a wide range of temperatures and pressures and can easily be modified to accommodate different experiments, either biological or chemical. As an application, we present measurements of bacterial sulfate reduction rates in hydrothermal sediments from Guyamas Basin over a wide range of temperatures and pressures. Sulfate reduction rates increase with increasing pressure and show maximum values at pressures higher than in situ.

1. Introduction

Microorganisms have been found in the deepest parts of the oceans (Tamegai et al., 1997), under hundreds of meters of sediment cover (Parkes et al., 1994), and their activity has been measured at temperatures of at least 100 °C (Weber and Jørgensen, 2002). However, the combined effects of temperature and pressure are rarely investigated because of the technical difficulties encountered. Since the 1950s, thermal gradient systems have been used to study the temperature dependence of microbial metabolism (for an overview of earlier work, see Battley, 1964). Most of the systems were complicated to handle, not suitable for the study of larger numbers of samples, difficult to keep sterile, and allowed incubation only over a limited temperature range of < 50 °C. The type of gradient block described by Elsgaard et al. (1994) is now widely used, and allows simultaneous incubation of more than 100 samples over a broad temperature range. The block itself is a thermally insulated aluminium block (150 x 150 x 2000 mm), with several rows of equidistant holes. One end of the block is heated with electrical heating elements while the other is cooled with a built-in cooling coil connected to the fluid circulation of a laboratory cooler. Each sample is

contained in a separate stoppered glass vial in a hole in the block. So far, these systems only allowed incubations at one to a few bars of pressure.

Parkes et al. (1995) describe an incubation system consisting of large pressure vessels that can be heated. Similar systems have been used for experiments with barophilic organisms over the last decades. The advantage of this system is the rather large volume (up to several litres) of each pressure container, allowing the incubation of many samples or large volumes in one experiment. The drawback, however, is that each setup can be used only at one combination of temperature and pressure. For combined investigations of the temperature and pressure limits of organisms, multiple experiments have to be carried out. In many cases, the high price prohibits the acquisition of a greater number of those systems.

Yayanos et al. (1984) developed a system that allowed incubation along a thermal gradient under pressure. Like the block of Elsgaard et al. (1994), an aluminium block was heated at one end and cooled at the other. The holes for the pressure containers were not drilled in one of the long sides but from the end and through the block. Pressure containersas long as the gradient block were filled with several small sample vials or with long glass tubes with gels, containing microorganisms, and inserted into the holes. The incubation temperature of a sample was determined by its position in the pressure container.

Depending on the maximum temperature, the insulation material for such blocks was either synthetic foam (e.g. Styrofoam) or mineral wool. Both materials have disadvantages: the synthetic foam has only limited temperature resistance and the mineral wool is not able to support the weight of the heavy thereby creating potential inhomogeneities in the insulation.

Our goal was to develop a system that is easy to build and to operate, consists mostly of standard off-the-shelf parts, and can incubate multiple samples under high pressure over a wide range of temperatures.

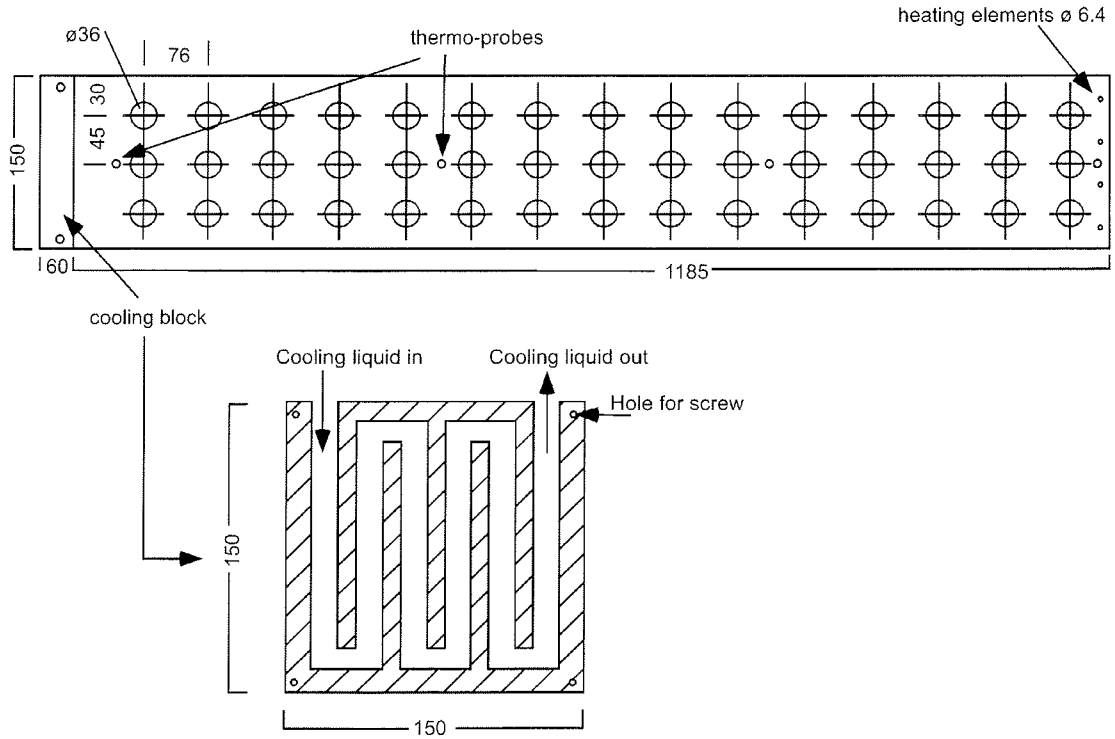

Fig. 1: Schematic view of the thermal gradient block and the cooling unit. All dimensions are in mm.

2. Methods and materials

The high-pressure thermal gradient system consists of two main units: the thermal gradient block (TGB) and the high-pressure unit.

2.1. The thermal gradient block

The TGB consists of an aluminium block (AlCuMgPb F34; 1185 x 150 x 150 mm) with three rows of 15 equidistant holes (140-mm deep x 36-mm diameter). A schematic view is given in Fig. 1. The block is insulated by a 20-cm-thick layer of Trolit (Trocellen, Troisdorf, Germany). This solid material is made from mineral fibres and has very good thermal insulation characteristics. The temperature gradient is almost linear, independent of the minimum and maximum temperatures and the gradient (Fig. 2). At incubation temperatures > 200 °C, the outside of the unit is not more than 25 °C. Trolit is available in blocks of different sizes and can easily be cut with a hacksaw and allows cutting of holes and groves. It is stable enough to hold the weight of

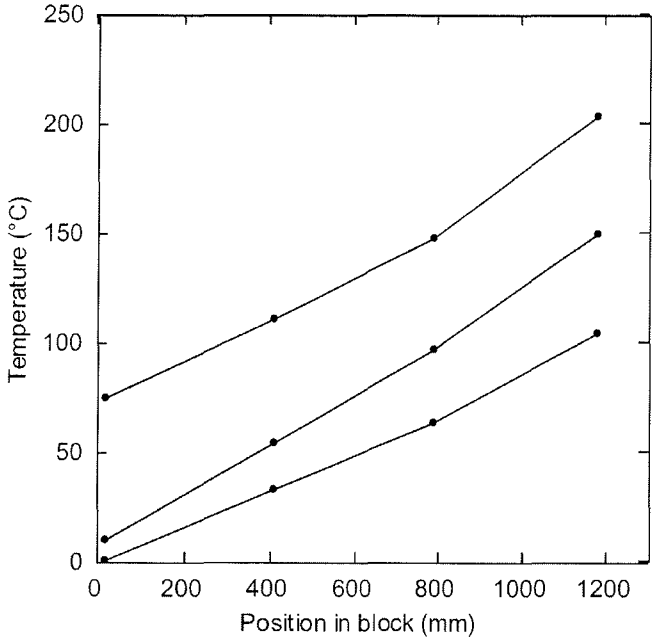

Fig. 2: Linearity of the thermal gradient block at different minimum and maximum temperatures and thermal gradients.

the aluminium block, thereby eliminating the need to use different materials as support. It is temperature resistant to over 1000 °C. The whole block is housed in a custom-made case on wheels (Kalms Flightcases, Hannover, Germany), allowing easy transport and the use also on ship cruises or remote laboratory situations. The Trolit and the aluminium block are held in place only by the case; the single blocks are not glued or fixed in any way to allow for thermal expansion of the material and easier dismantling. For better handling during construction, we first built the bottom of the case, then the actual thermal gradient block including the insulation and, finally, placed the sides of the case around the construction. The Trolit blocks that cover the top have not been fixed in the lid as otherwise it would have been too heavy for one person to handle. A schematic view is given in Fig 3. CAD construction files from the block and the cooling unit can be obtained from the corresponding author.

2.2. Cooling

At one end of the block, a cooling element is attached. This element was milled from a solid piece of aluminium (150 x 150 x 60 mm) and has a meandering internal channel where cooling liquid is circulated. The inlet and outlet are on top of the unit and

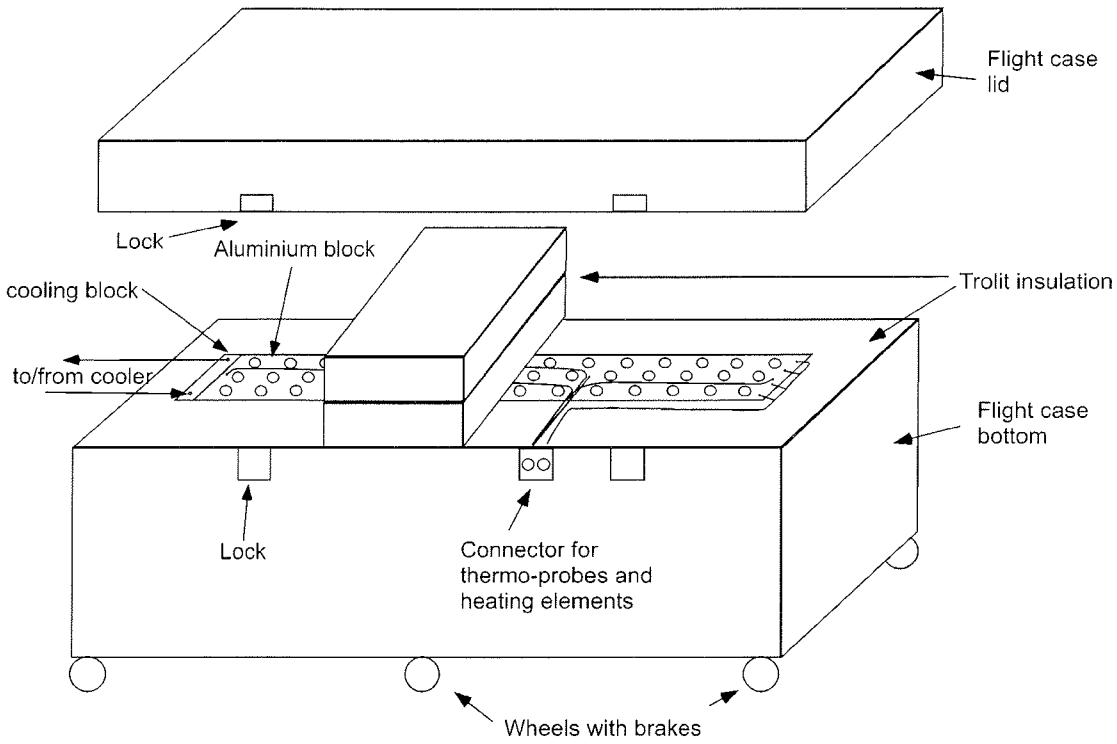

Fig. 3: Schematic view of the thermal gradient system. For better viewing, only part of the Trolit blocks that cover the top are shown. The case has eight heavy-duty handles (not shown)

connected to a laboratory cooler (Julabo RS 6, 4.5 kW). The cooling unit was mechanically fixed to the block with four screws, and sealed with heat-resistant elastic sealant (Surebond, BMW). The cooling liquid was chosen according to the desired temperature, ranging from oil for high temperatures (> 100 °C) over water (for 0 – 100 °C) to antifreeze for sub-zero temperatures. In case very low temperatures were desired, the hoses from the laboratory cooler to the TGB and back were thermally insulated to avoid precipitation of moisture and, eventually, the buildup of ice. We found insulation sleeves for hot water plumbing to be well suited.

2.3. Heating

At the opposite end of the TGB, four electrical heating elements (6.4-mm diameter x 88.9 mm, 200 W, RS Components, Germany) were placed into 6.5-mm-diameter holes in the block. The maximum temperature that can be achieved is 220 °C and the steepest thermal gradient is 160 °C, giving about 10 °C temperature difference between each row of containers.

2.4. Control

Over the length of the block, four thermo-probes (PT 100, - 60 to + 400 °C, RS Components) were installed to continuously monitor the temperature. The thermo-probes were connected to an electronic multi-controller (JUMO iTron, RS Components) that switched the heating elements on and off. Temperatures can thereby kept constant within ±0.5 °C over weeks (data not shown).

2.4. Pressure system

One of the key objectives when constructing the high-pressure thermal gradient system (HPTGS) was to use moderately priced off-the-shelf components to have a high degree of flexibility and good availability of the components. As the pressure containers are heated, the samples undergo thermal expansion. We therefore wanted a system that automatically regulates any pressure buildup in the containers. We chose a back-pressure system with a constant small leakage. Pressure is created by two high-pressure liquid chromatography (HPLC) pumps (SYKCAM S 1122) that were modified by the manufacturer with stronger motors and gear units for a higher pressure range (from 400 to 600 bar). This modification is registered by the manufacturer and may be ordered under the catalogue no. 10 10 046-22 VS. The pumps run in constant pressure mode with variable flow rate. In case any thermal expansion happens during the warm-up period, pressure will not exceed the desired value. A schematic view of the pressure system is given in Fig. 4. First, we used the pumps in parallel for increased safety. In case one pump fails, the other one will automatically increase its flow rate and maintain the pressure. However, we found the pumps to be so reliable that we abandoned this idea and now use the system without any backup pump. All high-pressure plumbing is made with standard 1/16" stainless steel HPLC tubing.

2.5. Back-pressure system

To create a suitable back-pressure system, we placed five used HPLC columns (250 x 4.6 mm, Hypersil or Spherisorb, 5 µm, Sykam, Fürstenfeldbruck, Germany) in line. At 450-bar pressure, about 0.7 – 0.8 ml leaks through. During the warm-up period, thermal expansion may cause the pressure to rise faster than the back-pressure system can release it. In such a case, opening of one of the connections between the HPLC columns smoothly increases the outflow of the system in a controlled manner. After thermal equilibrium is achieved, the connection is fastened again. The outflow

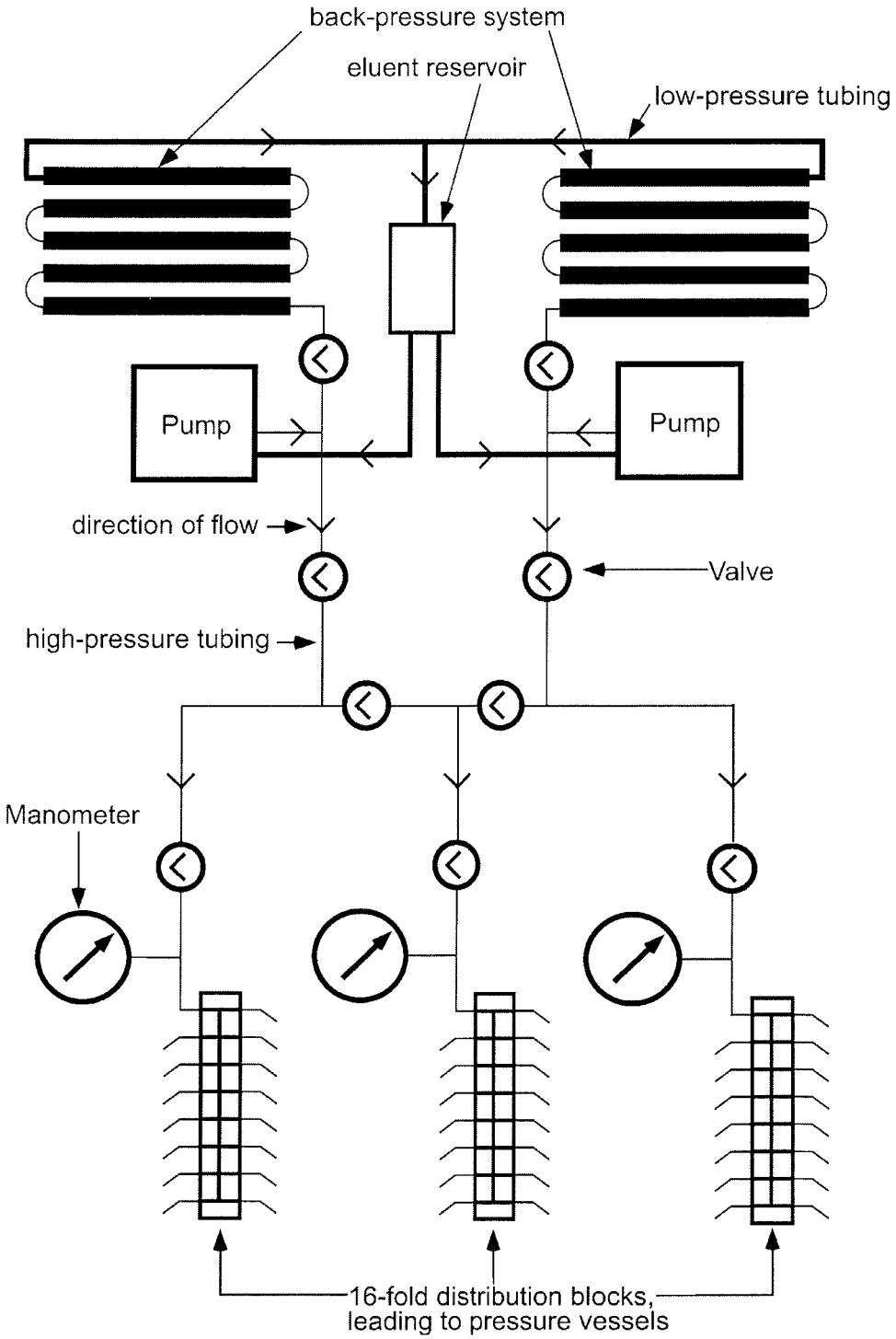

Fig. 4: Schematic view of the high pressure system. The thin lines are high-pressure connections, the bold lines are low pressure connections.

of the back-pressure system goes back into the eluent container to be reused. We found demineralised water to be a suitable liquid.

2.6. Pressure distribution system

The pumps connect to a manifold of valves. This manifold allows the connection of each pump to any of the three lines of pressure vessels, or to use the pumps in parallel. Each line has a Bourdon-type manometer (16-cm diameter, Sykam). Such large manometers were chosen to dampen the pulsation of the pump. Fluctuations in pressure are negligible; at 450 bar, the pulsation of the pumps leads to fluctuations of < 5 bar. A custom-made 16-fold distribution block (Sykam) connects the pressure containers of each line to the valve manifold. Small pockets in the Trolit insulation house the distribution blocks.

2.7. Pressure vessels

The vessels consist of large standard stainless steel HPLC columns (ID 20 mm, 120 mm long, Sykam). One end has a normal HPLC 1/16" fitting, the other end is closed with a steel cap. The pressure containers were delivered with Teflon seals, which however were unsuitable for high-temperature experiments. Now we have replaced the Teflon seals with copper rings (normal plumbing hardware). These seals last for several incubations but have to be exchanged on a regular basis.

2.8. Sample vials

Custom-made screw-cap Hungate tubes (OD 18 mm, 50-mm long, Glasgerätebau Ochs, Bovenden, Germany) proved to be the most suitable containers. Two of these vials fit in each pressure vessel, thereby producing exact duplicates in pressure and temperature. For incubations at temperatures up to 95 °C black rubber septa (6-mm thick, Glasgerätebau Ochs) can be used. Although the septa are thick, pressure is easily transmitted. Even with air bubbles of up to 5-mm diameter, the vials did not crack at 450 bar. For higher temperatures a different kind of septum has to be used. We found 2 mm thick Viton plates, covered with 0.2 mm thick PTFE lining (Thomaplast, Reichelt Chemie Technik, Heidelberg, Germany) on the side facing the sample to be suitable. This material is stable to 300 °C. Both kinds of septa are secured with aluminium screw caps with a hole in the centre (Glasgerätebau Ochs). The pressure vessels are placed in a bucket filled with demineralised water and the sample

vials dropped into them. The caps are screwed on the pressure vessel under water to avoid trapping of air bubbles. After all pressure vessels are connected to the distribution block, about 50 bar is applied to check for leaks. When no leak is observed, the vessels are inserted into the TGB and left for thermal equilibration. The buildup of pressure is carefully monitored and released if necessary. After 1 or 2 h, the pressure is set to the desired value.

3. Results and discussion

The HPTGS has proven to be a robust and reliable tool. In normal use, we incubate each line at a different pressure, one line being a no- or low-pressure control, the other two lines at higher pressure of up to 450 bar. When a greater number of replicates at one pressure is desired, two or three lines can be connected together, giving four or six replicates, respectively, at one temperature. In cases where the incubation temperature goes over 100 °C, pressure has to be applied also to the no-pressure controls to prevent boiling. The necessary pressure depends on the maximum temperature. For instance, 10 and 30 bar are required for temperatures of 180 and 230 °C, respectively. Normally, it is sufficient just to close the line as thermal expansion brings the pressure rapidly to values that eventually require some depressurising. For safety reasons, we normally apply 10 bar before closing off the line and carefully monitor the pressure increase to avoid any influence of pressure on the low-pressure control.

The caps of the pressure vessel have thicker walls and, therefore, a different thermal expansion than the tubes. To prevent ceasing of the threads of the pressure vessels, copper grease (Caramba C13) is applied and cooling has to be done slowly. We found that the best way to cool the pressure vessels is to take them out of the TGB and leave them under pressure at room temperature until they are only hand-warm, which takes about an hour. Then pressure is released and the vessels opened. To clean the pressure vessel from excess copper grease, they can simply be placed in a laboratory dishwasher.

Trolit has very good insulation characteristics. Moreover, it is robust, mechanically quite stable, and easy to cut and drill. Compared to synthetic foam and mineral wool, it is the superior material. One major disadvantage, however, is its open pore structure that acts like a sponge for any kind of liquids. Open surfaces should be covered with heat-resistant material that can be wiped clean in case hazardous substances such as

radioactive tracers are used. Furthermore, when Trolit becomes soaked with water, it looses its mechanical stability and starts to crumble.

3.1. Experiments with the high-pressure thermal gradient system

Our first application of the high-pressure thermal gradient system was to investigate the pressure and temperature characteristics of sulfate-reducing bacteria in hydrothermal vent sediments and to examine a possible overlap between bacterial and thermochemical sulfate reductions. To quantify the reduction of sulfate to sulfide, the $^{35}SO_4^{2-}$ radiotracer (Jørgensen, 1978) method was used. We incubated a slurry of hydrothermal sediments from Guaymas Basin along the thermal gradient under three different pressures (t = 75 – 200 °C, P=10, 220 and 450 bar). The slurry was prepared in an anaerobic glove box by mixing the sediment with anoxic sterile mineral salt solution to a final concentration of about 30 % sediment volume. The mineral salt solution had the following constituents (in grams per litre of deionized water): KH_2PO_4, 0.2; NH_4Cl, 0.25; NaCl, 25.0; $MgCl_2 \cdot 6H_2O$, 5.0; KCl, 0.5; $CaCl_2 \cdot 2H_2O$, 0.15, and the following additions: Resazurin, 0.1 w/v sol., 1 ml; $NaHCO_3$, 84 g/l, 30 ml; $Na_2S \cdot 9H_2O$, 12 g/l, 3 ml. The solution was adjusted to pH 7.5 with 1 M NaOH; SO_4^{2-}concentration was set to 10 mM with 1 M Na_2SO_4 solution. Incubation time was 4 days.

Before the sample vials were placed in the pressure vessels, 10 µl of carrier-free $^{35}SO_4^{2-}$ radiotracer (ca. 500 kBq) was injected into each sample. Incubation was terminated by transferring the slurries into 20% w/v zinc acetate solution to stop all bacterial activity and to precipitate any hydrogen sulfide. The glass vials were opened and the slurry immediately poured into the zinc acetate; the remaining slurry was flushed out with a few ml of zinc acetate. In our experience, the loss of hydrogen sulfide is negligible as long as the transfer is done quickly. The reduced inorganic sulfur species were subsequently separated from the rest of the sediment by cold chromium distillation (Kallmeyer et al., in preparation). The turnover of sulfate can be calculated by comparison of the amount of radiolabeled sulfate and the produced radiolabeled reduced sulfur species. The 10-bar incubation did not cover the whole temperature range but ended at 120 °C. Fig. 5 shows that high rates of sulfate reduction occur between 75 and 100 °C. Sulfate reduction rates (SRR) found in the 10-bar incubation are in the range of 100 – 200 nmol cm^{-3} day^{-1}, in good agreement with the results of Weber and Jørgensen (2002) and Elsgaard et al. (1994). Teske et al. (2002) suggest that hyperthermophilic archaeal sulfate reducers of the genus *Archaeoglobus* (Burggraf et

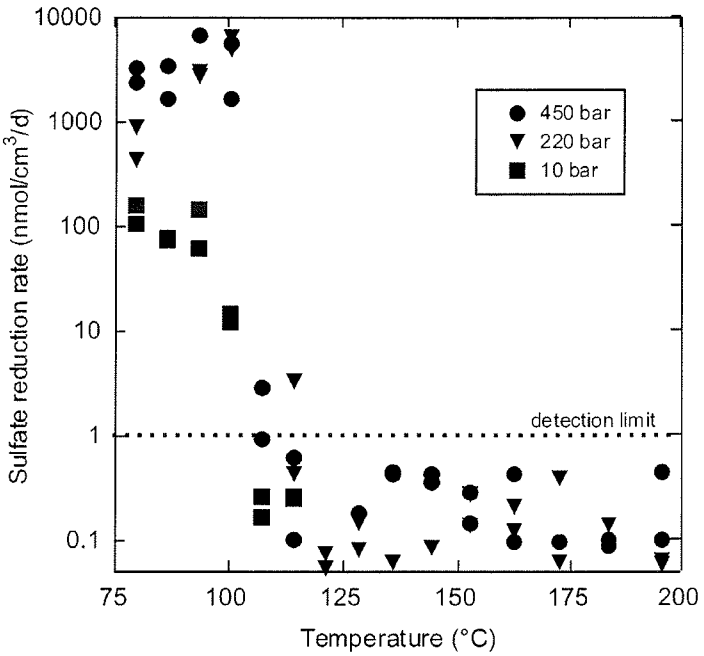

Fig. 5: Sulfate reduction rates in Slurries of Guaymas Basin sediments incubated at different pressure conditions.

al., 1990; Stetter, 1988) are the quantitatively most important sulfate reducing microorganisms in these sediments. Sulfate reduction rates of the two high-pressure incubations are the highest in the 75 – 100 °C range; they exceed the 10-bar incubation by more than an order of magnitude. The large difference in sulfate reduction rates between the 10-bar incubation and the 220- and 450-bar incubations suggests that barophilic organisms predominate in Guaymas sediments. Up to now, there are no published data about barophilic members of the genus *Archaeoglobus* (Boone and Castenholz, 2001). Sulfate reduction rates were not above the detection limit of about 1 nmol cm^{-3} day^{-1} at temperatures > 100.5 °C, independent of pressure. All samples were incubated in duplicates, and show good reproducibility.

3. Conclusions

The high-pressure thermal gradient system is easy to build and to use, and allows the incubation of samples over the entire biological temperature range and even beyond, and over a wide range of pressures. The high-pressure thermal gradient block provides a large number of data that cover a wide range of p/T conditions in a single

experiment. With slight modifications in the choice of vials, seals, etc., the high-pressure thermal gradient block can be used for a wide range of experiments, either biological or purely chemical.

Acknowledgements

We thank P. Färber, G. Herz, A. Kutsche, J. Langreder, V. Meyer, and A. Nordhausen from the MPI workshops for continuous support and helpful comments while building the system. This work is supported by the European Union under the FP. 5 Project DEEPBUG, contract no. EVK3-CT-1999-00017.

4 The effects of temperature and pressure on rates of sulfate reduction and anaerobic oxidation of methane in hydrothermal deep-sea sediments of Guaymas Basin

Jens Kallmeyer[1], *Antje Boetius*[2,3]

submitted to Applied and Environmental Microbiology

[1] Max Planck Institute for Marine Microbiology, Bremen, Germany
[2] Alfred Wegener Institute for Polar and Marine Research, Bremerhaven, Germany
[3] International University Bremen, Germany

Abstract

Rates of biological sulfate reduction and anaerobic oxidation of methane (AOM) were measured in hydrothermal deep-sea sediments from Guaymas Basin by means of radiotracer incubations. Experiments were conducted over a wide temperature range (5 – 200 °C). Additionally, sulfate reduction rates (SRR) were determined at different pressures (1, 220, 450 bar). SRR had an optimum activity between 60 – 90 °C and was detectable up to 101 °C at 1 bar. In 220 and 450 bar incubations SRR increased 20-fold, showing a strong barophilic response of the sulfate reducing microorganisms. AOM was detectable in the same sediments and maximal activities also occurred in the thermophilic range between 35 – 90 °C. This is in support of previous studies that proposed the existence of a thermophilic anaerobic methanotrophic community in Guaymas sediments. However, AOM rates were low over the entire temperature range, and accounted in no case for more than 5 % of the SRR. Apparently carbon sources other than methane are utilized preferentially by the thermophilic microbial communities of the Guaymas vents.

1. Introduction

Earth and life sciences alike aim at the identification of microbial cells and metabolic pathways which may serve as analogues of life on early earth. The strong interest in the functioning and diversity of today's microbes thriving in extreme environments is driven by our hypotheses about conditions and settings which have favoured the origin of life, about the primal cells and their first metabolic activities. Candidates for original life forms are microorganisms able to grow on elements, energy and electron acceptors provided by the deep earth, independent of sunlight, photosynthesis and its products. Although it remains a hypothesis, it is widely believed that hydrothermal vents, with their high temperatures and abundance of reduced, energy-rich elements derived from hot water-mineral interactions, are model systems of early earth (Reysenbach and Shock, 2002,Martin and Russel, 2002). The inhabitants of such hot environments – the thermophiles – are defined as microbes growing optimally at temperatures above 45 °C. They are represented in deeply branching phylogenetic lineages of all three domains of life, pointing to their early origin. The record of microbial growth at high temperature is currently set at 113 °C by *Pyrolobus fumarii*, a chemoautotroph using hydrogen oxidation to gain energy (Blöchl et al., 1997). Some "living

fossils" may be found among meso- and thermophilic anaerobic lithotrophs, which manage to thrive independent of oxygen based on deep earth's resources, potentially making up a significant proportion of the global biomass beneath the ocean's sediments and crusts (Cowen et al., 2003). Knowledge on the diversity and metabolic versatility of thermophilic bacteria and archaea is currently increasing rapidly due to large research efforts and the availability of new molecular methods circumventing the tedious cultivation of extremophiles.

Life on Earth started out under anaerobic conditions, and most ocean environments remained anoxic for at least the first 2000 million years of Earth's history (Canfield, 1998). Early element cycles included H_2, S, Fe, NH_3, PO_4, CO_2, hydrocarbons and abiotically produced organic molecules. When the first microbial mats evolved, the recycling of their biogenic materials could have supported fermentation and methanogenesis (Nisbet and Sleep, 2001) Recently it was proposed that another original biogeochemical process on early earth may have been the anaerobic oxidation of methane with sulfate by microbial consortia (Michaelis et al., 2002). At hydrothermal settings hot fluids percolate through rocks and deliver hydrogen, methane, and sulfur species abiotically. Such habitats may sustain populations of anaerobic methanotrophs independent of other biogenic processes. Hence, the question arises as to the existence of anaerobic thermophilic methanotrophs at hydrothermal vents as a potentially very original metabolic capacity. However, anaerobic methanotrophic archaea (named ANME–groups) and their syntrophic partners (sulfate reducing bacteria) have only been found in cold environments (-1.5 – +10 °C) where they occur in large numbers, performing high rates of anaerobic oxidation of methane of several µmol cm^{-3} d^{-1} (Boetius et al., 2000; Joye et al., 2003, in press; Michaelis et al., 2002; Orcutt et al., 2003, in press). Physiological experiments with ANME-groups from cold seeps have shown an optimum of the anaerobic oxidation of methane (AOM) at around 10 °C (Nauhaus et al., 2002). However, samples from warm or hot environments containing active populations of ANMEs have not been available to physiological experiments before this investigation.

Assumptions on the existence of anaerobic thermophilic methanotrophs have so far been based on findings of typical biomarker and 16S rDNA signatures in thermophilic environments such as chimneys of hydrothermal vents (Reysenbach and Shock, 2002) and sediments of the Guaymas basin (Schouten et al., 2003; Teske et al., 2002). Unfortunately, none of these recent investigations proposing the existence of active

anaerobic methanotrophs at hydrothermal vents included rate measurements of anaerobic oxidation of methane. The main aim of the present study was to test the activity and temperature optima of microbial populations from a hydrothermal vent system carrying signatures of ANME groups. Because the anaerobic oxidation of methane occurs in two steps (oxidation of methane to carbon dioxide and reduction of sulfate to sulfide), both carbon dioxide and sulfide production were measured by incubating environmental samples with radioactive methane and sulfate as trace substrates at a range of temperature settings from 5 – 200 °C.

2. Materials and Methods

2.1 Study site:

The Guaymas Basin is an actively spreading basin (5 – 6 cm/yr), located in the Gulf of California (Einsele et al., 1980). The most notable feature of Guaymas Basin is the rapidly deposited (1 – 2 mm/yr), organic-rich (2 – 4 % C_{org}) sediment cover of several hundred meters thickness (Einsele et al., 1980; Lonsdale and Becker, 1985; Simoneit and Lonsdale, 1982). Most of the organic matter is of planktonic origin, with only minor proportions of land-derived material (Jørgensen et al., 1992; Simoneit and Schoell, 1995). Sediment covers the spreading centers of the basin, while the ocean plate accretion process occurs by intrusion of sills and dykes into the soft sediment (Einsele et al., 1980). The interaction of hot magmatic rocks with the overlying sediment leads to formation and convective flow of acidic hydrothermal fluids, rich in H_2S and trace elements. While ascending, the hydrothermal fluids interact with the organic matter in the sediments, forming a range of different hydrocarbons and short chain fatty acids (Martens, 1990; Simoneit and Lonsdale, 1982).

A sediment pushcore (7.5 cm diameter, about 20 cm long) was retrieved by the submersible ALVIN (Dive 3780, cruise AT-07, 5.5.2002). The core was taken from a vented site covered with a *Beggiatoa* mat. The maximum temperature recorded at this site (27°00.53 N, 111°24.43 W, 2013 m water depth) ranged from 94 to 130 °C at 20 cm sediment depth (D. Albert, pers. comm.), representing a similar setting as for previous sampling of vent cores (Elsgaard et al., 1994; Schouten et al., 2003). The core was very gassy and expanded during retrieval. Immediately after recovery, the complete sediment sample was stored anaerobically in plastic bags in Argon filled containers at +4 °C until the experiment. Longer storage times at cold temperatures do not foster

experiment (No.)	rate measurement	temperature range (°C)	methane addition	pressure (bar)	pre-incubation (days)	incubation w tracer (days)
1	SRR	80 - 200	none	10	none	4
	SRR	80 - 200	none	200	none	4
	SRR	80 - 200	none	450	none	4
2	SRR	5 - 90	100 µM	1	1	1
	AOM	5 - 90	100 µM	1	1	1
3	SRR	5 - 90	100 µM	1	7	1
	AOM	5 - 90	100 µM	1	7	1
4	AOM	5 - 90	1 mM	1	7	1

Table. 1: Experiments on sulfate reduction and anaerobic oxidation of methane

the development of a mesophile bacterial community during storage (Jørgensen et al., 1990). Other experiments with sediments from gassy seeps showed that natural communities of sulfate reducing and methane oxidizing microbes can be stored cold and anaerobic for more than a year and still be reactivated to their original activity when field conditions are simulated in the experiment (Nauhaus et al., 2002).

2.2 Experimental design

Sediment from a single core was mixed and diluted with anaerobic mineral medium to approximately 1:3 to 1:6 sediment-medium slurries. These slurries were used for all experiments shown in Tab. 1. Sulfate reduction rates were measured at high temperatures and pressures to compare the sample activity to rates measured in earlier investigations (Exp. 1). To explore the effects of temperature and pressure on microbial activity in Guaymas sediment several temperature gradient experiments (Exp. 2 – 4) were carried out with different pre-incubations times (1 day or 7 days) and methane concentrations (0.1 mM or 1 mM). The temperature gradient block used in the experiments consists of a thermally insulated 2 m long aluminium block that is electrically heated on one side and cooled on the other side. The block has four replicate slots for each of 31 equidistant incubation temperatures. The temperature gradient in the block was checked regularly and remained constant within +/- < 1 °C. The effect of pressure on SRR was studied by using a high-pressure thermal gradient block (Kallmeyer et al., 2003). The block itself is comparable with the one used for the 1 bar incubations, but has only 3 slots for each of 15 equidistant temperatures. The pressure cylinders are modified HPLC columns (ID 20 mm, 120 mm long). Pressure is applied through HPLC pumps (Sykam, Germany) running in constant pressure mode.

3. Methods

3.1. Slurry preparation

All equipment or reagents that were in direct contact with the sample were either pre-combusted at 600 °C or autoclaved at 121 °C for 30 minutes. For the incubations we used "Mini Hungates", i.e. shortened Hungate screw-cap tubes with a total volume of about 5 ml (Glasgerätebau Ochs, Bovenden, Germany). For the low-temperature incubations (up to 90 °C) we used 6 mm thick black rubber septa (Glasgerätebau Ochs, Bovenden, Germany). For higher temperatures we used 2 mm thick Viton plates with 0.2 mm thick Teflon coating on the side facing the sample (Thomaplast®, Reichelt Chemie Technik, Heidelberg, Germany). Both kinds of septa were secured with aluminium screw-caps (Glasgerätebau Ochs, Bovenden, Germany) with a hole in the centre for tracer injection.

The sediment slurries were prepared using a mineral salts solution that contained the following constituents (in grams per litre of deionized water): KH_2PO_4, 0.2; NH_4Cl, 0.25; NaCl, 25.0; $MgCl_2*6H_2O$, 5.0; KCl, 0.5; $CaCl_2*2H_2O$, 0.15, and the following additions: Resazurin, 0.1 w/v sol., 1 ml; $NaHCO_3$, 84 g/l, 30 ml; Na_2S*9H_2O, 12 g/l, 3 ml. The solution was adjusted to pH 7.5 with 1 M NaOH; SO_4^{2-} concentration was set to 10 mM with 1 M Na_2SO_4 solution.

For the methane-free incubation experiments the slurry was prepared by dispensing the sediment inside a glove box under N_2/CO_2 atmosphere into a beaker and mixing it under constant stirring with the desired amount of mineral salts solution to a final concentration of 15 % to 30 % sediment content. Dispensing into the Mini Hungates was done with a 100 ml plastic syringe, leaving no headspace. For incubations with methane-saturated slurries, the slurry was prepared in the same way as for methane-free slurries, but instead of a beaker, a glass flask closed with a thick rubber stopper was used. After the slurry was prepared, the headspace of the flask was flushed with methane and pressurized to about 1.5 bar. The slurry was left under constant stirring for about one hour allowing equilibration with the headspace (final concentration 0.1 mM or 1 mM). After transfer back into the glove box the slurry was then dispensed with a syringe into the Mini-Hungate vials, which were closed immediately after filling to minimize degassing. All data were calculated back to activity per volume of undiluted sediment.

3.2. Rates of sulfate reduction (SRR) and anaerobic oxidation of methane (AOM)

After pre-incubation of sediment slurries 10 µl of $^{35}SO_4^{2-}$radiotracer (ca. 700 kBq, Amersham, Braunschweig, Germany) were injected through the septum into the 5 ml samples and incubated for 24 hours. Incubations were terminated by transferring the slurry quantitatively into 20 ml of 20 % (w/v) Zn-acetate solution. By mixing the sample with Zn-acetate, all free $H_2^{35}S$ is precipitated as solid $Zn^{35}S$. The glass vials were opened and the slurry immediately poured into the zinc acetate; the remaining slurry was flushed out with a few ml of zinc acetate. In our experience, the loss of hydrogen sulfide is negligible as long as the transfer is done quickly. The fixed samples were stored frozen until analysis. The thawed samples were centrifuged and the supernatant removed for analysis of $^{35}SO_4^{2-}$. Radiolabeled reduced sulfur species (S^0, FeS_2, FeS, H_2S), produced during incubation are liberated by a cold single-step chromium reduction method of Kallmeyer et al. (in prep). Quantification of radioactivity was done by liquid scintillation counting using a Packard Tri-Carb 2500 TR counter and Lumasafe Plus Scintillation liquid (Lumac LSC BV, Groningen, Netherlands). Two replicates were used in all experiments for each temperature setting. Blank values were determined by fixing a sample in Zn-acetate prior to adding the radiotracer. To inject the tracer into the pressurized samples, they had to be de- and re-pressurized. Therefore, the pressure experiments were carried out without pre-incubation but total incubation time was extended to 4 days to allow the bacterial communities to adjust.

In replicate samples 50 µl of $^{14}CH_4$ saturated anaerobic seawater (ca. 10 kBq) was injected through the septum. Incubations were terminated after 24 hours by transferring the slurry quantitatively into glass jars filled with 25 ml of 5 % (w/v) NaOH. Analysis of $^{14}CO_2$ production was carried out according to Treude et al. (submitted). Two replicates for AOM measurements were used in Exp. # 1 and 2, and 4 replicates in Exp. # 3. Blank values were determined by incubating samples that had no sediment but only sterile mineral salt solution and by fixing the sample prior to addition of tracer.

4. Results and discussion

Thermophilic sulfate reduction in hydrothermal sediments from Guaymas basin was shown before with an optimum of 63 – 83 °C and high rates of 30 – 140 nmol cm^{-3} d^{-1} (Weber and Jørgensen, 2002). A variety of thermophilic sulfate reducers were isolated from these sediments such as *Archaeoglobus* (Burggraf et al., 1990; Stetter, 1988),

Pressure	Temperature (°C)										
(bar)	73	80	85	95	100	105	115	120	130	...	195
1	154	90	76	n.d.	n.d.	n.d.	n.d.	n.d.	n.d.	...	n.d.
10	n.d.	128	75	100	13	0,2	0,3	n.d.	n.d.	...	n.d.
220	n.d.	645	n.d.	2786	5564	0	1,8	0,1	0,4	...	0,1
450	n.d.	2805	2465	6660	3619	1,8	0,4	0	0,3	...	0,3

Table 2: Effect of pressure on sulfate reduction rates at high temperatures (Exp. 1). Numbers are sulfate reduction rates in nmol ml^{-1} d^{-1}.

Desulfurococcus (Jannasch et al., 1988) as well as thermophilic methanogens such as *Methanococcus* (Zhao et al., 1988) Other studies of microbial activity in *Beggiatoa* covered, hot sediments from the Guaymas basin include the analysis of organic substrates in sediment porewater (Martens, 1990), the investigation of microhabitats in *Beggiatoa* mats (Gundersen et al., 1992; Jannasch et al., 1989), experiments on temperature and substrate effects on SRR (Elsgaard et al., 1994; Weber and Jørgensen, 2002), as well as analyses of microbial diversity and biomarker and stable isotope signatures (Schouten et al., 2003; Teske et al., 2002). In the present investigation, a sample of *Beggiatoa*-covered, gassy sediments from a hydrothermal area of the Guaymas basin was used to quantify temperature and pressure effects on rates of sulfate reduction (SRR) and anaerobic oxidation of methane (AOM).

4.1. Evidence for thermophilic and barophilic sulfate reduction

Sediments collected from *Beggiatoa* mats covering vented sediments were homogenized and incubated at different temperatures from 5 – 200 °C (Tab. 1). SRR > 100 nmol cm^{-3} d^{-1} were found in subsamples incubated for several days at high temperatures and a clear thermophilic reaction was observed (Tab. 2, Fig. 1). The temperature optimum of sulfate reduction was between 60 – 90 °C, with a peak at 80 °C. In all slurry experiments SRR dropped below < 1 nmol cm^{-3} d^{-1} at temperatures below 8 °C and above 101 °C. Intact sediment cores previously sampled from vented sediments covered by Beggiatoa mats had maximum sulfate reduction rates of 1500 nmol cm^{-3} d^{-1} at 70 °C in single sediment horizons (Elsgaard et al., 1994). As in our slurry experiments, sulfate reduction ceased above 102 °C. Another study (Weber and Jørgensen, 2002) confirmed these results and reported maximum SRR of 3350 nmol cm^{-3} d^{-1} at 70 °C. Rates above 500 nmol cm^{-3} d^{-1} where only observed in this study when hydrostatic pressure

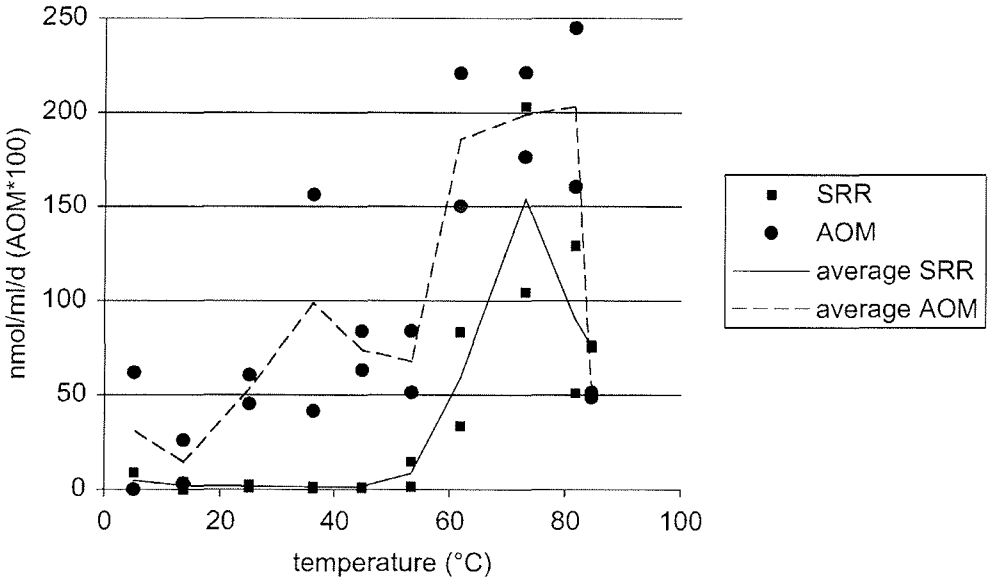

Fig. 1: Temperature optima of SRR and AOM (Exp. 3)

was applied to keep the medium from boiling at high temperatures above 100 °C. At 80 °C and 220 bar, which represents the in situ conditions for our 20 cm sediment core from the hydrothermal vents of the Guaymas basin (2010 m water depth), SRR was around 650 nmol cm^{-3} d^{-1} (Tab. 2). An extreme barophilic reaction of SRR was discovered at higher temperatures and pressures. With a maximum of almost 6700 nmol cm^{-3} d^{-1} at 450 bar and 95 °C SRR was over 40 times higher than in the 1 and 10 bar incubations that rarely exceeded 150 nmol cm^{-3} d^{-1}. These rates are among the highest rates ever observed in a marine setting, comparable to the methane-driven SRR measured in *Beggiatoa* mats at cold seeps (Boetius et al., 2000). In conclusion, the rates and the temperature range of sulfate reduction in our experiments are in agreement with earlier investigations of SRR in Guaymas sediments (e.g. Jørgensen et al., 1990; Jørgensen et al., 1992; Elsgaard et al., 1994; Weber and Jørgensen, 2002). Obviously, the SRR community of the Guaymas vents is dominated by a thermophilic and barophilic population of sulfate reducers. Unfortunately, very little is known about barophilic sulfate reducers, or on pressure effects on sulfate reduction rates in general.

4.2. Comparing temperature optima of anaerobic oxidation of methane and sulfate reduction

It was proposed earlier that the anaerobic oxidation of methane mediated by thermophilic archaeal methanotrophs could be an important process at the Guaymas vents

(Teske et al., 2002). This hypothesis was based on the finding of typical signatures of anaerobic methanotrophic archaea (ANME groups) in surface sediments (0 – 2.5 cm sediment depth) of vented sites (Teske et al., 2002). Clones of the ANME groups dominated the 16S rDNA clone library from these sediments, and high amounts of specific archaeal biomarkers such as archaeol and hydroxyarchaeol were extracted. These biomarkers were depleted in $\delta^{13}C$ to -58 to -89 ‰ (Teske et al., 2002). In comparison, the methane of the vented Guaymas sediments has an isotopic signature of -43 to-51 ‰ $\delta^{13}C$ and is the likely source for the depletion in the archaeal biomarkers. The abundance of ANME clones, archaeal lipids with such isotopic signatures are usually indicative of an active methanotrophic community able to oxidize methane at high rates of several 100 nmol cm^{-3} d^{-1} (Hinrichs and Boetius, 2003; Joye et al., 2003, in press; Michaelis et al., 2002). However, this previous investigation (Teske et al., 2002) was limited to the upper 2 cm of surface sediment, which usually has average temperatures of 3 – 30 °C and is not the typical habitat for thermophiles with growth optima above 45 °C. In a second investigation of the existence of thermophilic methanotrophs in hot Guaymas sediments, the biomarker isotopic signatures of a deeper core sectioned into layers of 0 – 5, 5 – 10 and 10 – 15 cm sediment was determined (Jørgensen et al., 1992). A strong decrease in archaeol, hydroxyarchaeol and other biphytanic acids was found. These lipids decreased by 2 orders of magnitude in abundance from the surface sediments with temperatures < 30 °C to the 10 – 15 cm layer with temperatures of up to 95 °C. Other lipid compounds, namely glycerol dibiphytanyl glycerol tetraethers (GDGTs) were more abundant, and decreased only about 10-fold from the mesophilic surface sediments to the thermophilic deeper layers. The isotopic signature of some GDGTs in the 10 cm horizon was as low as -71 ‰ $\delta^{13}C$, indicative of methanotrophy. These findings led the authors to confirm the existence of thermophilic anaerobic methanotrophic Archaea in the vented Guaymas basin sediments (Jørgensen et al., 1992).

In the present investigation we measured the activity of sulfate-reducing and methane-oxidizing microbial populations in homogenized sediments from a 20 cm core with a thermal gradient of 3 – 130 °C from surface to the bottom of the core. Experimental temperature gradients ranged from 5 – 200 °C (Table 1). SRR and AOM rates were measured after pre-incubating the samples for 1 day (experiment #2) or 7 days (experiment #3) with methane (100 µM). Samples which were pre-incubated only for 1 day in the temperature gradient block (experiment #2) showed no activity or very

low rates of SRR and AOM of around 0.5 – 1 nmol cm^{-3} d^{-1} at any temperature. These rates were barely above detection limit and no clear trend related to the temperature settings could be detected. Apparently, a pre-incubation of 1 day was insufficient for the microorganisms to adjust to the original temperature conditions after the homogenization procedure. Exp. # 1 and 3 show that about one week is needed to obtain a microbial activity similar to what is measured in situ (Weber and Jørgensen, 2002) or ex situ directly after sampling in samples from similar settings (Elsgaard et al., 1994).

In experiment #3 (7 day pre-incubation, 100 µM CH_4) SRR was low at cold to intermediate temperatures ranging from 1 – 10 nmol cm^{-3} d^{-1} at 5 °C to 45 °C (Fig. 1). The maximal value of SRR of 200 nmol cm^{-3} d^{-1} was observed in one subsample incubated at 73 °C. AOM activity was only 1 % of the SRR activity at all temperatures, indicating that another electron donor must have fueled sulfate reduction. Maximal AOM rates of 2.2 – 2.5 nmol cm^{-3} d^{-1} were measured at 62 – 82 °C. In Fig. 1, AOM is scaled up to the SRR activity to compare the effect of temperature on both activities. The temperature trend appears similar in SRR and AOM with increased rates at 45 – 82 °C. However, considering the very low AOM rates, the identification of clear temperature optima is critical. Hence, another experiment (experiment #4) was carried out to test the temperature optimum of AOM in samples pre-incubated for a week at higher methane concentration of ca. 1mM. In this experiment with Guaymas sediments, AOM rates increased to an average of 10 nmol cm^{-3} d^{-1} at temperatures of 30 – 60 °C, but declined at higher temperatures (Fig. 2). Hence, our results suggest a thermophilic optimum for anaerobic oxidation of methane in these sediments. However, compared to the several 100 to 1000 nmol cm^{-3} d^{-1} usually measured in sediment slurries from active cold seeps at similar conditions of methane and sulfate availability (Nauhaus et al., 2002; Treude et al., submitted), the AOM of the Guaymas vent sediments appears rather low. In our experiments, anaerobic oxidation of methane contributed only 1 – 5 % to sulfate reduction rates. In contrast, the AOM/SRR ratio is often close to 1 in cold seep sediments where methane is the dominant carbon source (Nauhaus et al., 2002, Michaelis et al., 2002), although this ratio can be lower in cold seep settings where other carbon sources are available (Joye et al., 2003, in press).

It remains unclear if the ANME-1 and ANME-2 groups detected in the surface sediments of *Beggiatoa* cores are also present in subsurface sediments and responsible for AOM at high temperatures > 30 °C. ANME-2 populations from sediments of Hydrate Ridge showed a rapid decline in activity at temperatures above 20 °C (Nauhaus et al.,

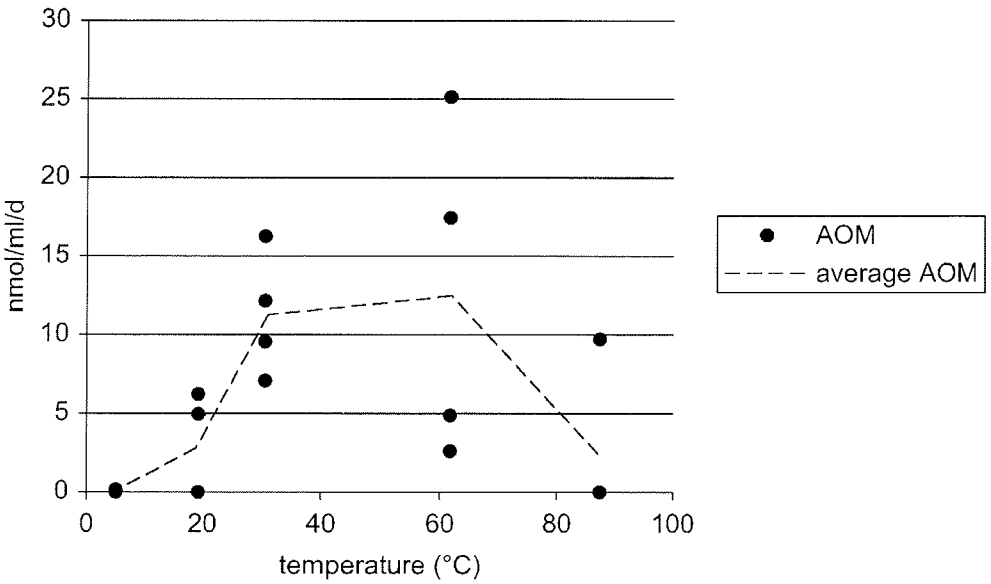

Fig. 2: Temperature optimum of AOM (Exp. 4)

2002), but their ambient temperature in this environment is 5 °C. Taking into account the substantial decrease in biomarker lipids of archaeal methanotrophs with increasing sediment depth (i.e. temperature) observed in previous studies of Guaymas sediments (Reysenbach and Shock, 2002; Teske et al., 2002), this may indicate that the methane rich, hot subsurface sediments are NOT a preferred environment of ANME populations. Regarding our experimental approach, it is possible that the ANME populations inhabiting the surface sediments (Teske et al., 2002) were "diluted" by the deeper sediments void of active ANME during the preparation of slurries from whole sediment cores, thus resulting in a low activity. However, the observed thermophilic optimum of AOM does not support this hypothesis, because the surface populations thrive at temperatures < 20 °C. Another possible explanation for the rather low but thermophilic AOM rates in our experiments could be an unspecific reverse reaction of enzymes of thermophilic methanogens as previously observed in experiments with methanogens (Harder, 1997). On the other hand, there seems to be no obvious reason why thermophilic anaerobic methanotrophs should not have developed to make use of the high methane concentrations in hydrothermal fluids.

4.3. The question of the electron donor for SRR

It was proposed that the natural variety of methane, higher hydrocarbons and volatile fatty acids present at millimolar concentrations in the Guaymas vent sediments serve as substrates for sulfate reduction (Jørgensen et al., 1990). The high rates of sulfate reduction found in undisturbed and unamended Guaymas sediments in high temperature incubations lead to the question of what kind of electron donors are used by the sulfate reducers and how they are replenished. In general, the highest SRR are either found at the sediment surface where freshly deposited organic material is readily available, or in deeper layers where upwardly-moving fluids advect thermogenic substrates (Jørgensen et al., 1992; Jørgensen et al., 1990; Weber and Jørgensen, 2002). Volatile fatty acids (VFA) (Martens, 1990) and a variety of hydrocarbons (Simoneit and Lonsdale, 1982) are produced thermogenically in deeper and hotter (> 100 °C) parts of the sediment and are transported upwards by hydrothermal fluids. These substances may be a carbon source for sulfate reduction in deeper layers. By using an in-situ probe it was shown that there was no acetate and propionate in near-surface sediments. (Martens, 1990). Concentrations start to increase only at depths > 10 cm where temperatures are above 40 °C, suggesting a removal of these VFAs by sulfate reducers. Furthermore, enriching sediments with a nutrient mix of VFA and yeast extract resulted in a substantial increase in SRR in Guaymas sediments suggesting some substrate limitation (Elsgaard et al., 1994). In whole core sediment slurries (10 – 20 cm sediment depth, 70 – 90 °C incubation temperature, atmospheric pressure) SRR of 120 nmol cm^{-3} d^{-1} in unamended sediments were increased several fold by addition of volatile fatty acids. However, acetate concentrations in Guaymas sediments are very variable and range between 10s to > 1000 µM, whereby the maximum concentrations are found in relatively hot sediments (Martens, 1990). Methane concentrations are as high as 12 to 16 mM (Whelan, 1988), and various hydrocarbons, derived from thermal alteration of organic material have been found in high concentrations (Kawka and Simoneit, 1994; Simoneit and Lonsdale, 1982; Simoneit and Schoell, 1995).

In our experiments, the highest SRR ever observed in Guaymas basin sediments were found in sediment slurries incubated for 4 days under high temperatures and high pressures without any additional carbon source. AOM activity was only 1 % of the SRR activity at all temperatures, indicating that another electron donor must have fueled sulfate reduction. In cold seep environments where methane is the main carbon

source, such as Hydrate Ridge and the Black Sea seeps, AOM and SRR are close to a 1:1 ratio and are equally depending on the amount of methane available (Michaelis et al., 2002; Nauhaus et al., 2002). However, in sediments of the Gulf of Mexico, which contain a high load of higher hydrocarbons and petroleum, the decoupling of SRR and AOM can be observed (Joye et al., 2003, in press). Here it was found that in oil-containing sediments, the AOM to SRR ratio was reduced to 1 – 10 %, similar to our results with Guaymas sediments. These findings and the observations of the present study indicate the presence of sulfate reducers able to make use of low and high hydrocarbons, maybe even petroleum. Although thermophilic anaerobic oxidation of methane exists in the subsurface sediments of the Guaymas basin, it is clearly not the dominant carbon cycling process. Future investigations should carry out field research as well as experimental studies combining tracer measurements, biomarker studies and 16S rDNA technologies to identify the thermophilic, barophilic anaerobic hydrocarbon degraders of the Guaymas vents.

5. Acknowledgements

The authors wish to thank Dan Albert for providing samples, Imke Müller for carrying out AOM analyses, Tina Lösekann for sharing unpublished data on microbial diversity, and Beth Orcutt, Samantha Joye and Andreas Teske for fruitful discussions and comments on the manuscript.

5 Pathways of organic carbon turnover in deep sediments from the Peru continental margin

Jens Kallmeyer[1], Timothy G. Ferdelman[1], Tina Treude[1], Bo Barker Jørgensen[1], Ivano W. Aiello[2]

[1]Max Planck Institut for Marine Microbiology
[2]Moss Landing Marine Laboratories

Abstract

Rates of dissimilatory sulfate reduction were measured through radiotracer incubations in numerous sediments samples from the Peru continental Margin, taken during RV Sonne cruise SO 147 and ODP Leg 201. The sulfate reduction rates (SRR) decrease with depth over more than six orders of magnitude. Over the same depth interval the number of bacterial cells, enumerated by acridine orange direct counts drops only over 3 orders of magnitude.

Complementary to the SRR measurements rates of turnover were modeled by based on the porewater profiles of sulfate and methane. Also potential rates of anaerobic oxidation of methane were experimentally determined.

While in some parts of the cores there is good agreement between the different approaches, in many parts the rates differ considerably.

When calculating per-cell SRR the rates cover a range that has not been previously reported in the literature. This wide range may be caused by changes in the community structure or the fraction of active bacteria among the counted cells.

Introduction

Oceanographical setting

The continental shelf off Peru is characterized by strong upwelling between 4 ° and 16 °S. It is one of the most productive oceanic areas with primary productivity between 300 and 3000 g C m^{-2} y^{-1}, which is orders of magnitudes higher than normal ocean productivity of less than 1 g C m^{-2} y^{-1} (e.g. Henrichs, 1992). The upwelling persists year-round, with lowest and highest intensity around January and July, respectively. Four centres of upwelling can be defined, at around 6 °S, 9 °S, 11 °S, and 15 °S (Böning et al., submitted) and references therein)

Inside the upwelling zone about 90 % of the primary production is remineralized in the water column, resulting in oxygen depletion between 80 and 500 m water depth. Inside the OMZ the sediments are usually covered by thick mats of nitrate storing filamentous sulfide oxidizing bacteria of the genus *Thioploca* and *Beggiatoa* (e.g. Ferdelman et al., 1997; Fossing et al., 1995).

Organiclastic vs. methanotrophic SR

Sulfate reduction is the quantitatively most important anaerobic terminal electron acceptor process in marine sediments. At the sediment-water interface, dissolved sulfate concentrations are over 50 times higher than all electron acceptors with higher standard free energies (e.g. nitrate, iron, manganese) together. Those electron acceptors with a higher energy yield are usually depleted within the top few millimeters to meters of the sediment (Froelich et al., 1979).

The importance of sulfate reduction in the degradation of organic matter in the sea-bed has been shown in numerous studies (e.g. Ferdelman et al., 1999; Ferdelman et al., 1997; Fossing, 1990; Fossing and Jørgensen, 1989; Howarth and Giblin, 1983; Iversen and Jørgensen, 1985; Jørgensen, 1982; King, 2001; Knoblauch et al., 1999; Martens, 1993).

Sulfate reduction (SR) can broadly be divided into two main pathways: (1). Organoclastic SR that utilises low molecular weight substrates derived from fermented particulate or dissolved organic matter, and (2) methanotrophic SR that is driven by methane utilising consortia involved in the anaerobic oxidation of methane (AOM) (Boetius et al., 2000; Orphan et al., 2001).
The reactions can be expressed as follows.

Organoclastic SR:	$2\ CH_2O + SO_4^{2-} = 2\ HCO_3^- + H_2S$	Eq. 1
Methanotrophic SR:	$CH_4 + SO_4^{2-} = HCO_3^- + HS^- + H_2O$	Eq. 2

In the upper centimeters to meters of the sediment column, organiclastic SR is normally the dominant anaerobic process for the degradation of organic matter, due to the abundance of easily degradable organic matter. With increasing depth the fraction of recalcitrant organic matter becomes larger and SR decreases (Jørgensen, 1982).

The recalcitrant organic matter that is not utilised by sulfate reducers is then further degraded by different, mostly acetogenic and methanogenic, microorganisms (Parkes et al., 1993). The biologically produced methane diffuses upwards and finally reaches the zone where sulfate is available. In the narrow zone where sulfate and methane overlap, the sulfate-methane transition zone (SMZ), methanotrophic SR takes place. It was shown in several studies, that in this zone a narrow band of high SRR occurs before sulfate is depleted and therefore SR stops (Adler et al., 2000; Hoehler et al.,

1994; Iversen and Jørgensen, 1985; Niewöhner et al., 1998). However, through the influx of brines or lateral fluid flow, sulfate may increase again at greater depth, and in such cases microbial SR can take place again in the presence suitable electron donor available (Böttcher et al., 1999; Böttcher et al., 1998).

Martens and Berner (1974) described the accumulation of methane in marine sediments only after sulfate is approaching depletion. Iversen and Jørgensen (1985) showed the 1:1 stoichiometry of sulfate reduction and methane oxidation in the sulfate-methane transition zone. However, methanotrophic SR remained elusive, as it was not clear which organism is responsible for the reaction. Hoehler et al. (1994) proposed a consortium of several different microorganisms responsible for the process and Boetius et al. (2000) finally identified aggregates that are capable of anaerobic methane oxidation. These clusters consist of archaea that apparently do reverse methanogenesis, surrounded by sulfate reducing bacteria. Orphan et al. (2001) additionally confirmed the methanotrophic metabolism by isotope analysis of the biomass. The isotopic signal of carbon was extremely negative and could only be derived from methane.

Although much progress has been made on the biology of these aggregates, the details of the overall reaction are still not fully understood. The archean metabolic products that are transferred to the sulfate reducers who then produce CO_2 and HS^- are still to be identified, H_2 or acetate being the most possible candidates.

The sulfate-methane transition zone is generally between 0.3 and 1 meter thick but can extend to up to tens of meters. As a rule of thumb Jørgensen et al. (2001) suggest the lower 10 % of the sulfate penetration depth for the estimated thickness of the transition zone. The thickness of the transition zone is surprising, considering the resulting long turnover times. It is still not clear why the process is so sluggish but may partly be explained by the small energy yield of only 25 kJ mol^{-1} under in situ conditions (Valentine and Reeburgh, 2000). In comparison, the reaction $2\ CH_2O + SO_4^{2-} = 2\ HCO^{3-} + H_2S$ yields 77 kJ mol^{-1}.

Radiotracer measurements vs. modelled rates

There are different ways to measure sulfate reduction in sediments, (1) by amending the sediment with $^{35}SO_4^{2-}$ radiotracer e.g. (for a review see King, 2001) or through mathematical modelling based on porewater profiles (e.g. Adler et al., 2000; Berner, 1964; Jørgensen, 1978; Niewöhner et al., 1998).

Each way has its advantages and disadvantages but combined studies that use both approaches are rare (Fossing et al., 2000; Jørgensen et al., 2001). Those studies that used both approaches both come to the conclusion that calculation of consumption or production rates solely based on concentration profiles strongly underestimate the true sulfate reduction rates at the sediment water interface. As Fossing et al. (2000) stated, the major difference between the two approaches is that the modelling approach only provides information about the net sulfate consumption and thereby strongly underestimates processes at the surface, where transport mechanisms other than diffusion may be of quantitative importance. The radiotracer technique on the other hand provides the gross rate of the process.

Many studies that have measured sulfate reduction rates by using $^{35}SO_4^{2-}$ radiotracer have mostly been restricted to the upper centimeters to meters of the seafloor and to sediments with high turnover rates (e.g. Albert, 1985; Ferdelman et al., 1997; Jørgensen et al., 2001). Only few have dealt with radiotracer measurements in deep sediments (for an overview see Parkes et al., 2000). A major problem is the limit of detectability of sulfate reduction. Kallmeyer et al. (submitted) showed that there are certain physicochemical limits for the detection of sulfate reduction with radiotracer. Even with those recent advances in methodology the rates expected from the fluxes of sulfate are on the limit of detectability or even below that.

Models for carbon utilization in marine sediments

D'Hondt et al. (2002) postulated that in the Deep Biosphere (> 1.5mbsf) methanotrophic SR is the dominating terminal electron acceptor process. Their conclusion is based on an in-depth review of available sulfate and methane porewater data from the Ocean Drilling Program (ODP) and its predecessor the Deep Sea Drilling Program (DSDP). They broadly distinguished two different zones:

1) Ocean margins, with sulfate being depleted within meters to tens of meters below seafloor and high CH_4 concentrations.
2) Open ocean settings, with much deeper sulfate penetration and low methane concentrations.

At many open ocean sites high concentrations of sulfate and low concentrations of methane coexist over long depth intervals, a fact that contradicts the commonly

accepted redox sequence. At open ocean sites, where methanotrophic SR can be neglected due to low methane concentrations, the depth-integrated rate of sulfate reduction can be used as a measure of total dissimilatory activity (Canfield, 1991; In ocean margin settings, D'Hondt et al. (2002) postulate that most of the sulfate flux below 1.5 mbsf is used to oxidise upwards diffusing methane. Because there is normally no methane above the sulfate methane transition zone, the total sulfate flux into the sediment can be used as a measure for total carbon turnover in the entire sediment column. Like in some earlier case studies of sulfate reduction coupled to methane oxidation at DSDP sites (Canfield, 1991), the continental slope of Namibia (Niewöhner et al., 1998), and the Amazon Fan (Adler et al., 2000), these findings are all based on flux calculations and numerical modelling. In light of the results of Fossing et al. (2000) and Jørgensen et al. (2001) however, sulfate reduction exclusively based on modelling tends to underestimate the total areal SRR and thereby the total carbon turnover of the sediment.

In our study we present SRR data from the Peru continental margin that stretch through the major part of the sediment column, thereby allowing a detailed study of carbon turnover in the sediment.

Methods and Materials

Sulfate reduction rates

Multicores

The 15 – 30 cm long undisturbed surface sediment cores were taken during R/V SONNE cruise 147 in June 2000. Sulfate reduction rates (SRR) were determined using the whole-core $^{35}SO_4^{2-}$-radiotracer method of (Jørgensen, 1978a). Acrylic tubes (26 mm diameter) were pushed into the sediment and immediately transferred into a temperature controlled incubator for thermal re-equilibration to approximate in-situ temperature. To prevent compaction of the sediment during sub-coring, suction was carefully applied to the headspace. In cases where bacterial mats covered the surface, the diameter of the tube was first cut with a scalpel to prevent dragging down the mats thereby destroying the sedimentary structure.

After the sub-core was temperature re-equilibrated for a few hours, 10 µl of $^{35}SO_4^{2-}$-radiotracer (100 – 200 kBq) was injected in 1 cm intervals through silicone sealed holes in the walls of the tube followed by incubation for 12 to 24 hours. The subcores from

samples of the oxygen minimum zone (OMZ) were stoppered to prevent influx of oxygen into the sample during incubation, other cores with oxygenated bottom waters were left open.

The major advantage of this method is the rapid labelling of the sediment with only minimal mechanical disturbances. Therefore small sedimentary structures like burrows remain intact. This is especially important in cases where *Thioploca* mats cover the sediment surface.

Slicing the cores and placing the slices in 20 % (w/v) zinc acetate (ZnAc) solution terminated incubations. The samples were stored frozen until further analysis in Bremen.

The Gravity cores were also taken during R/V SONNE cruise 147 in June 2000. The cores were not opened lengthwise, like normally done in sedimentological work, but cut in 1 m whole round core (wrc) segments and the ends sealed immediately with plastic caps. The cores were then stored at 4 °C and processed within the next 2 to 3 days. Sampling was done with the core sitting vertically inside a custom-made cutting rig with the sediment pushed out to the top of the liner. With this technique the loss of gasses like H_2S and CH_4 and the introduction of oxygen can be minimized. 5 ml glass tubes with a syringe plunger on one end were introduced into the sediment, pulled out and the open end closed with black rubber stoppers immediately. Care was taken to fill the glass tubes entirely with sediment and not to trap any air bubbles. 10 ml of $^{35}SO_4^{2-}$ radiotracer (about 200 – 400 kBq) were injected into each sample. The samples were incubated for 24 hours at 4 °C in the dark. Incubation is stopped by pushing the sediment into centrifuge tubes, filled with 20 ml of 20% ZnAc.

Peru Leg 201 ODP Cores

Syringe sub-samples from Whole Round Cores were obtained under anoxic, clean conditions in the cold storage room of the JOIDES Resolution. Samples were incubated for 14 to 21 days after labelling with $^{35}SO_4^{2-}$ onboard at near in situ temperatures. Transferring the sediment into 20 % (w/v) zinc-acetate (ZnAc) terminated the incubation. To have a substantial database for the determination of the blank values, in every core between 15 and 25 blank samples were taken. Half of the samples were first mixed with ZnAc and after 30 to 60 minutes radiotracer was added, the other half was first injected with radiotracer and transferred into ZnAc within a few minutes. Both types of blanks were subsequently treated like normal samples.

Separation of radiolabeled reduced sulfur species and analysis

Further sample handling of all samples was done in Bremen according to the cold chromium distillation procedure of Kallmeyer et al. (in prep.). The sample is centrifuged (3500 g for 10 minutes), the supernatant removed and an aliquot is taken off and the amount of radioactivity quantified. The remaining supernatant is kept for further analysis.

Remaining unreacted $^{35}SO_4^{2-}$ is removed form the sample by resuspending the sediment twice in 20 % ZnAc followed by centrifugation. After mixing the sample with 20 ml of 1,2 N, N Dimethyl-Formamide (DMF), technical grade, the slurry is immediately transferred into a 3-neck glass flask and bubbled with N_2 to drive off any oxygen. After 15 minutes 8 ml of 6 N HCl and 16 ml of 1 N $CrCl_2$ solution is added. The total reduced inorganic sulfur species (TRIS, comprised of metal mono- and disulfides, and elemental sulfur) are liberated as H_2S and driven out of solution by bubbling with N_2 for two hours. The outflowing gas is first lead through an aerosol trap filled with 7 ml of 1 N Na-Citrate solution buffered at pH 4 before reaching a final trap filled with 7 ml of 5 % ZnAc, and a drop of Antifoam. In this final trap all hydrogen sulfide precipitates as Zinc sulfide. To ensure complete recovery of the reduced sulfur species, 500 µl of 50 mM ZnS solution was added to each sample.

By comparing the activity of the radiolabelled TRIS to the total sulfate radiotracer a reduction rate can be calculated from Eq. 3, assuming that only a small fraction of the sulfate is reduced during incubation (see Fossing, 1995, for a detailed review).

$$SRR = [SO_4] \times P_{SED} \times \frac{a_{TRIS}}{a_{TOT}} \times 1/t \times 1.06 \times 1000 \qquad \text{Eq. 3}$$

SRR	Sulfate reduction rate (nmol cm^{-3} d^{-1})
$[SO_4]$	sulfate concentration of the porewater of the sediment sample (mmol l-1)
P_{SED}	porosity of the sediment (fraction of 1)
a_{TRIS}	radioactivity of TRIS (cpm or dpm)
a_{TOT}	total radioactivity used (cpm or dpm)
t	incubation time (days)
1.06	correction factor for the expected isotopic fractionation (Jørgensen and Fenchel, 1974)
1000	factor for the change of units from mmol l^{-1} to nmol cm^{-3}

Quantification of radioactivity was done by liquid scintillation counting, using a Canberra Packard Tri-Carb 2500 counter, with a counting window of 4-167 keV and high sensitivity mode turned off. The scintillation cocktail used was Lumasafe Plus (Lumac BV, Holland). Results were given as counts per minute.

A major prerequisite for measuring the extremely low SRR in those samples was a high sensitivity of the detection method in order to distinguish the signal produced by the radiolabelled TRIS from the background.

A mean blank value was subtracted from the counts from each sample to account for background noise not related to sulfate reduction. The mean blank value was determined by taking the average of all blank samples from the respective core. This value was subtracted from the radioactivity found in the distillation trap. The resulting value was only considered to be a truly detected signal when it was higher than three times the standard deviation of the blank. For each sample from ODP Leg 201 a minimum detection limit was calculated because the SRR is not only depending on the ratio between the radioactivity of reduced species over total radioactivity but also on the amount of available sulfate, which changes over depth.

Average SRR were calculated for the MUC samples by averaging all samples from one depth. For the gravity cores and the ODP cores the data were grouped into depth intervals and then the average was taken. For the gravity cores the depth intervals were 0 – 50, 50 – 100, 100 – 200, 200 – 300, 300 – 400, and > 400 cmbsf. For the ODP cores the intervals were 0 – 1, 1 – 2, 2 – 3, 3 – 5, 5 – 10, 10 – 50, 50 – 100, and > 100 mbsf.

Potential rates of anaerobic oxidation of methane (AOM)

Sediment samples were taken out of whole round cores (wrc) with sterile cut-off plastic syringes under an N_2 atmosphere. The sediments (total volume 4 ml per replicate) were transferred into sterile 10 ml serum vials. For each wrc two replicates were taken. The vials were filled with methane-saturated artificial seawater (methane concentration 1.3 mM, sulfate concentration 28 mM) and sealed gas-tight with thick black butyl rubber stoppers. The NaCl concentration of the artificial water was 500, 700 and 1000 mM, respectively, according to in situ concentrations in the sediment, resulting in a salinity of 69, 52 and 43, respectively. For each salinity three controls were taken, i.e. sterile 10 mL serum vials filled solely with artificial seawater and no sediment. ^{14}C-methane tracer (dissolved in water, injection volume 50 µL, activity 0.6 kBq) was injected in all replicates and controls. The vials were carefully turned

Site	depth mbsf	AOM pmol/ml/d	AOM pmol/ml/d
1227	17,1	106,7	114,6
	36,3	75,4	137,9
	55,1	264,9	lost
	75,6	289,9	406,8
	93,8	194,5	172,9
	121,5	447,0	242,9
	0,8	92,3	228,5
	31,5	115,9	79,3
	34,6	119,8	133,9
	38,1	86,1	101,6
1228	20,0	104,3	lost
	20,4	85,2	72,5
	39,8	41,3	55,6
	65,4	44,0	18,7
	114,4	110,7	163,5
	178,0	129,0	45,1
	187,8	35,6	146,7
1229	7,3	164,4	nd
	16,5	nd	nd
	25,8	nd	nd
	42,3	6,7	nd
	60,8	nd	nd
	70,5	nd	14,5
	81,4	nd	nd
	102,0	nd	nd
	120,9	nd	nd
	157,4	nd	nd
	29,9	14,1	nd
	30,1	nd	nd
	32,3	15,0	nd
	30,5	nd	nd
	72,9	18,0	nd
	85,6	nd	nd
	89,2	lost	nd
1230	6,6	nd	nd
	8,0	nd	nd
	8,4	nd	nd
	9,4	nd	nd
	10,9	nd	nd

Tab. 1: Experimentally determined rates of potential anaerobic oxidation of methane. nd = not detectable

upside-down to equally distribute the tracer without disturbing the sedimentary structure of the sediment pieces. Samples and controls were incubated for 134 days at 12 °C. After the incubation, samples and controls were stopped and analyzed for the rate of AOM by gas chromatography, ^{14}C-methane combustion and ^{14}C-CO_2 diffusion method according to Treude et al. (submitted). The results are given in Tab. 1

Analysis for methane and sulfate

On board JOIDES the sulfate and methane concentrations were determined. For methane determination 3 ml of sediment was placed into a 20 ml glass serum vial filled with 5 ml of 1 M NaOH followed y headspace analysis. Measurements were made after 20 min., 6 h., 1 or 1.5 day, and 2.5 days. For our interpretations we only used the 1 or 1.5 day results. The concentration of dissolved sulfate in the porewater was determined by ion chromatography.

Modelling of consumption and production rates.

We used the one-dimensional numerical modelling program PROFILE of Berg et al. (1998). The model simulates the depth distribution of dissolved ions and calculates consumption or production rates based on measured pore water concentration and porosity. It divides the sediment column into equally sized units with constant consumption rates and simulates the concentration profiles, thereby providing an objective selection of the minimum number of zones necessary to produce the best fit of the concentration profile. Two of the four boundary conditions (flux and concentration at top and bottom, respectively) have to be defined, the other two are calculated by the program.

The model assumes steady-state conditions for its calculations. Because in some cores the upper parts did not represent steady-state conditions they have been omitted from the calculations. It was assumed that all transport took place by molecular diffusion only and therefore bioirrigation could be excluded. Fossing et al. (2000) state that bioirrigation can effect sulfate reduction and methane oxidation down to several meters depth, but it can be ruled out for this study, as the cores are much longer. We also assumed that no lateral transport due to fluid flow occurred.

Sediment diffusion coefficients D_S were calculated for Methane and Sulfate according to Low (1981) from the measured porosities

$$D_S = D/(1 + 3(1-f) \quad \text{Eq. 4}$$

D_S = Sediment diffusion coefficient
D = Diffusion coefficient in water
f = Porosity

For the samples from ODP Leg 201, the molecular diffusion coefficient was corrected for each core based on the in-situ temperature of the top and the bottom of the core. It was assumed that the thermal gradient is linear with depth. All sites had a considerable low thermal gradient and in no case the temperature reached 25 °C.

Based on the concentration profiles of other redox-sensitive elements, like Iron and Manganese, we ruled out re-oxidation of sulfide to sulfate and therefore excluded production of sulfate from the calculations. Methane is actively produced and consumed, therefore both processes were included in the calculations.

The porosity data were taken on board the ship. In cases where no porosity data corresponding to a porewater sample was available, it was calculated by linear regression from the two adjacent datapoints. The boundary conditions and other parameters used for the modelling are given in Table 2.

Sulfate reduction rates per cell

All SRR samples were divided in depth intervals, regardless of their origin (MUC, GC, ODP). The depth intervals chosen were 0–0.01, 0.01–0.05, 0.05–0.1, 0.5–1, 1–5, 5–10, 10–50, 50–100 mbsf. A maximum and minimum SRR was defined by the 95 % confidence level of all samples in a given interval. The standard deviation could not be used because the data scatter over several orders of magnitude and the standard deviation was larger than the average value.

Based on the AODC counts of (Parkes et al., 2000) rates of per-cell sulfate reduction were calculated. Equation 5 describes the general distribution of bacterial cells counted by AODC with 95 % upper and lower prediction limit at depth (Parkes et al., 2000).

$$\text{Log}_{10} \text{ bacterial cells} = 7.89 \pm 1 - 0.57 \ \text{Log}_{10} \text{ Depth (m)} \quad \text{Eq. 5}$$

SRR 1225	1226	1227	1228	1229 top	1229 bottom	1230	
100	130	0	635	1115	8615	0	Depth at top of calculation domain (cm)
30670	41770	4291	18660	3500	12475	1500	Depth at bottom of calculation domain (cm)
29422	30100	x	16754	x	x	x	Concentration at top (μM)
x	x	x	x	x	x	x	Flux at top (nmol cm $^{-2}$ s^{-1})
27626	25150	0	30921	0	0	0	Concentration at bottom (μM)
x	x	0	x	0	0	0	Flux at bottom (nmol cm $^{-2}$ s^{-1})
8	12	12	12	12	12	12	Max number of equally spaced zones in interpretation
1.3-6.6	1.7-23.7	8.6-16.4	13.7-19	13.4-15.6	15.6-19.9	1.75-3.19	Temperature range (^{o}C)

AOM 1227	1228	1229 top	1229 bottom	1230	
130	30	0	6640	0	Depth at top of calculation domain (cm)
4790	18655	3965	9340	1060	Depth at bottom of calculation domain (cm)
7.5	1900	1.56	x	0	Concentration at top (μM)
0	x	x	x	0	Flux at top (nmol cm $^{-2}$ s^{-1})
x	1560	180.67	17.45	x	Concentration at bottom (μM)
x	x	x	0	x	Flux at bottom (nmol cm $^{-2}$ s^{-1})
10	10	12	12	4	Max number of equally spaced zones in interpretation (1 to 12)
8.6-16.4	13.7-19	13.4-15.6	15.6-19.9	1.75-3.19	Temperature range (^{o}C)

Tab. 2: Boundary conditions used for the numerical modeling.

By dividing the maximum SRR through the minimum bacterial number and vice versa, the maximum and minimum per cell SRR was calculated. The fraction of sulfate reducing bacteria from the total bacterial population was assumed to be 15 %. This percentage is derived from the work of Llobet-Brossa et al. (2002) on intertidal sediments from the Wadden Sea and of Ravenschlag et al. (2000) on Arctic sediments. To which degree these studies can be transferred to the deep biosphere is not yet clear, however this value was used as it is the only one available. Even if the fraction of sulfate reducers was much different, it would only shift the results and not change the overall range of the data.

Results

General distribution of sulfate reduction rates over depth

When plotting all available sulfate reduction rates (SRR) from the Peru continental margin, a decrease with depth over seven orders of magnitude can be seen (Fig. 1) This decrease is larger than the decrease of the number of total bacterial cells (only about 3 orders of magnitude), counted by acridine orange direct counting (AODC). At each given depth, SRR scatter over about four to five orders of magnitude.

SRR in the multicorer (MUC) samples range over ca. 4 orders of magnitude, with the lowest and highest values in the range of < 1000 pmol cm^{-3} d^{-1} and > 1,000,000 pmol cm^{-3} d^{-1}, respectively. Sulfate was detectable in all MUC samples. The differences in the rates over depth appear to be only small, but when calculating an average of all available data at a given depth (Fig. 1), a strong decrease of the rates over the first 3 cm can be seen (note the log scale on the x-axis). While the 0 – 1 cm interval has an average SRR of > 500,000 pmol cm^{-3} d^{-1}, in the 2 – 3 cm interval SRR have decreased by 80 % to only 100,000 pmol cm^{-3} d^{-1}. Between 3 and 10 cm depth the average SRR show only a slight decrease. In the depth-range that is covered by both MUC and gravity cores (GC), the rates overlap. The slow decrease continues in the gravity cores, although with less scatter, which can be attributed to the smaller

Fig. 1: Sulfate reduction rates in sediments from the Peru continental margin, measured with $^{35}SO_4^{2-}$ radiotracer. The multicorer and gravity corer samples do not include samples from sulfate-methane transition zones, while the ODP samples include samples from methane-sulfate transition zones. The dashed lines indicate the upper and lower boundary of the distribution of bacterial cells counted by acridine orange direct counting (AODC) at the 95 % confidence interval.

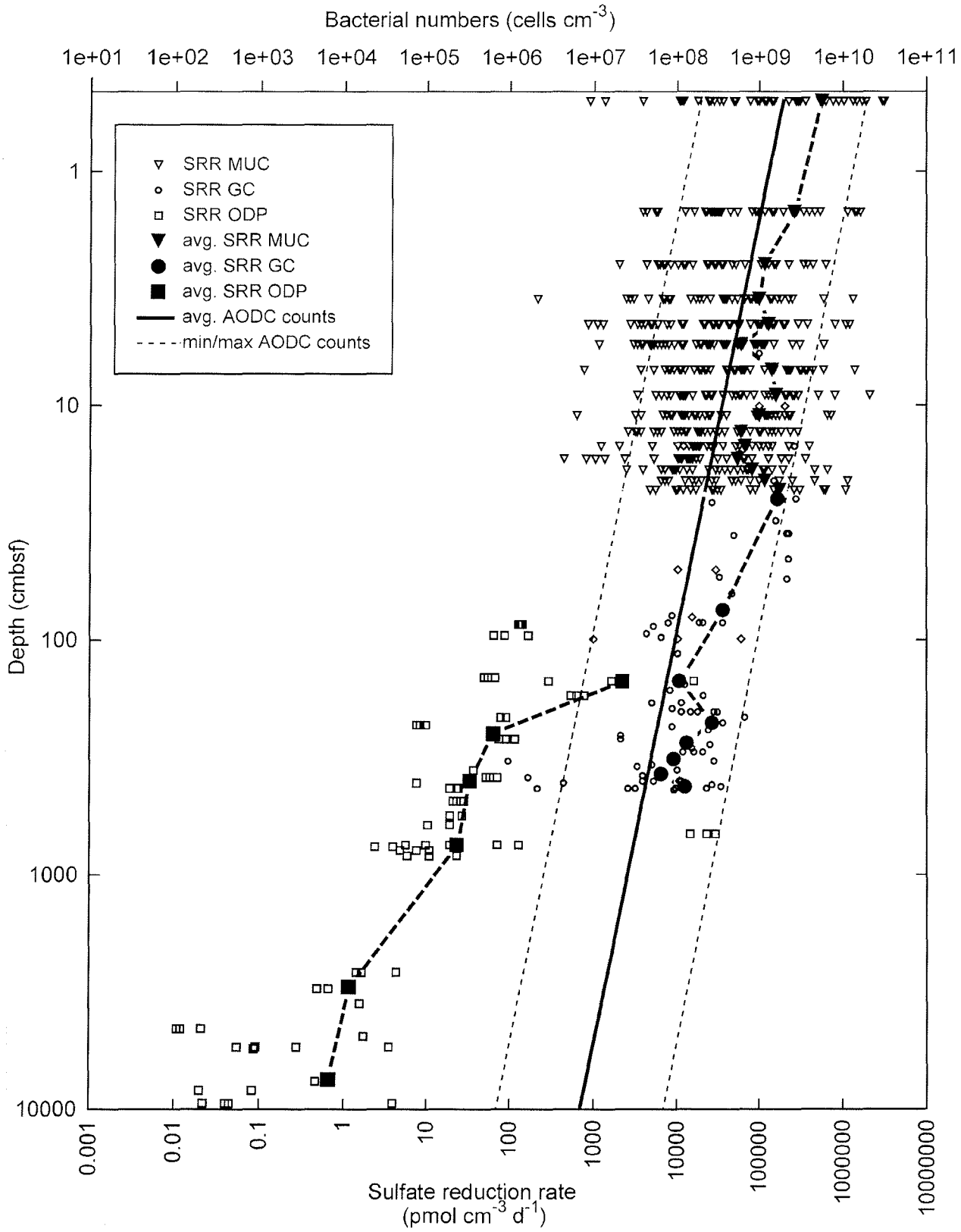
Bacterial numbers (cells cm-3)
1e+01
1e+02
1e+03
1e+04
1e+05
1e+06
1e+07
1e+08
1e+09
1e+10
1e+11
SRR MUC
SRR GC
SRR ODP
avg. SRR MUC
avg. SRR GC
avg. SRR ODP
avg. AODC counts
min/max AODC counts
Depth (cmbsf)
1
10
100
1000
10000
0.001
0.01
0.1
1
10
100
1000
10000
100000
1000000
10000000
Sulfate reduction rate
(pmol cm-3 d-1)

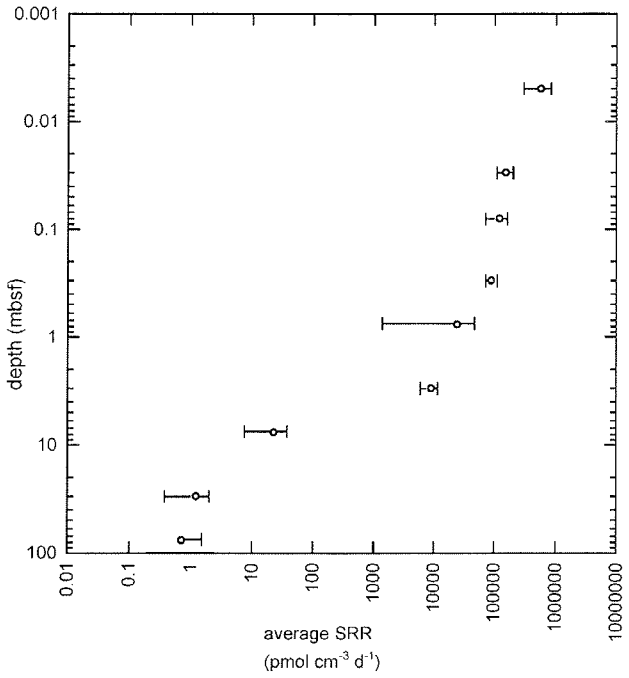

Fig. 2: Distribution of sulfate reduction rates over depth. The error bars show the range of SRR at a 95 % confidence level. There is a significant drop in SRR below 0.5 mbsf.

number of available samples. In the gravity cores methane was found in low concentrations (single µM) in all samples and sulfate was present in all samples as well. No sulfate-methane transition zone was sampled with the MUC or GC.

The depth range of the gravity cores and the cores taken during Leg 201 of the JOIDES Resolution (ODP cores) overlaps between ca. 1 and 4 mbsf. However, in this region the rates in the ODP cores are orders of magnitude lower and show a much stronger decrease with depth than the MUCs and GCs. While the SRR of the MUC and gravity corer GC samples follow the same trend as the number of bacterial cells, the SRR of the ODP cores are considerably off-set from the rates found in GC and MUC samples . The SRR decrease much stronger with depth than the bacterial cells.

When grouping the radiotracer SRR measurements into depth segments and calculating the range of SRR at the 95 % confidence level it can clearly be seen that there is significant drop between the surface interval (0 – 0.01 mbsf) and the deeper parts. Below 0.01 mbsf SRR stay almost constant down to 0.5 mbsf before dropping again significantly between 0.5 and 10 mbsf . Below 10 mbsf no significant change in rates can be observed (Fig. 2).

Measured SRR in ODP cores

By using the new cold chromium distillation technique of Kallmeyer et al. (submitted) SRR lower than 1 pmol cm^{-3} d^{-1} can be measured. Still, many of the radiotracer measurements fall below the minimum detection limit. Sulfate reduction was detected mostly in the upper parts of the cores with some scattered signal in the deeper parts.
It was surprising that in the sulfate-methane transition zones most SRR measurements were below the detection limit, although the potential rates of AOM measured by $^{14}CH_4$ radiotracer and the modeling results indicate considerably high activity.

The measured SRR are affected by inhomogeneous samples, causing scatter of the data. Moreover they only give information about one specific point in the sediment column.

For ODP Leg 201 samples we calculated areal sulfate reduction rates for each lithological unit based on a detailed sedimentological examination. By this way we were able to discriminate units of high turnover from those with low or no activity at all and therefore obtained a more precise picture of the distribution of microbial activity in the deep biosphere. However, lithological information alone was not sufficient in all cases to define zones of microbial activity. If, for example, sulfate was depleted inside a lithological unit, the depth of depletion was used as a boundary for the calculation. By using the lowest and highest measured sulfate reduction rate inside the respective lithological unit, the minimum and maximum areal sulfate reduction was calculated. In cases where there were radiotracer measurements below the detection limit, the minimum areal sulfate reduction rate was defined as zero. Also a median areal sulfate reduction rate was calculated by using the median value of the measured SRR in the respective lithological unit. We used a median instead of an average as a median value gives a more representative value in cases where the data scatter over several orders of magnitude.

Modelling based on the porewater profiles, suggested sulfate reduction rates that in many parts of the cores were below the minimum detection limit of the radiotracer technique. This provided an explanation why in certain intervals no SRR was detected with radiotracer.

Like for the SRR measured with the radiotracer technique, depth integrated areal rates were calculated from the modelled data to provide a better comparison between the two approaches. The results of the measurements and the modelling are given in Table 3. Figure 3 to 6 show for each of the ODP Leg 201 Peru margin sites (A) the

Fig. 3: Site 1227

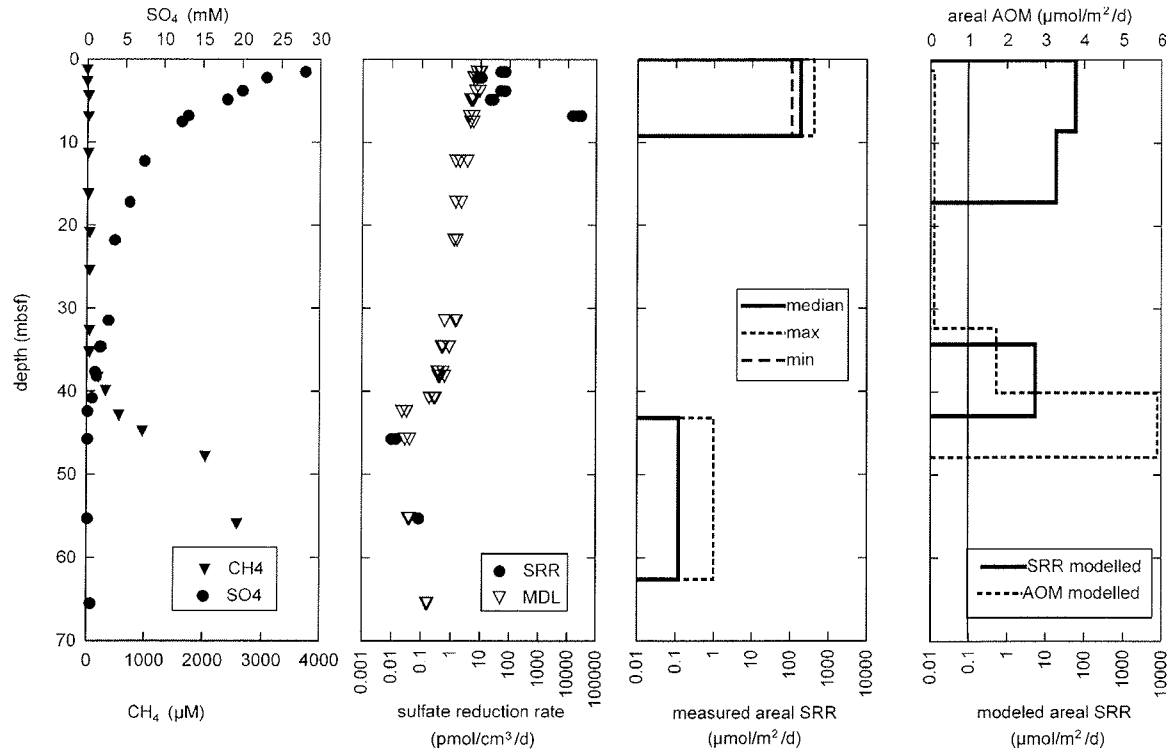

Fig. 4: Site 1228

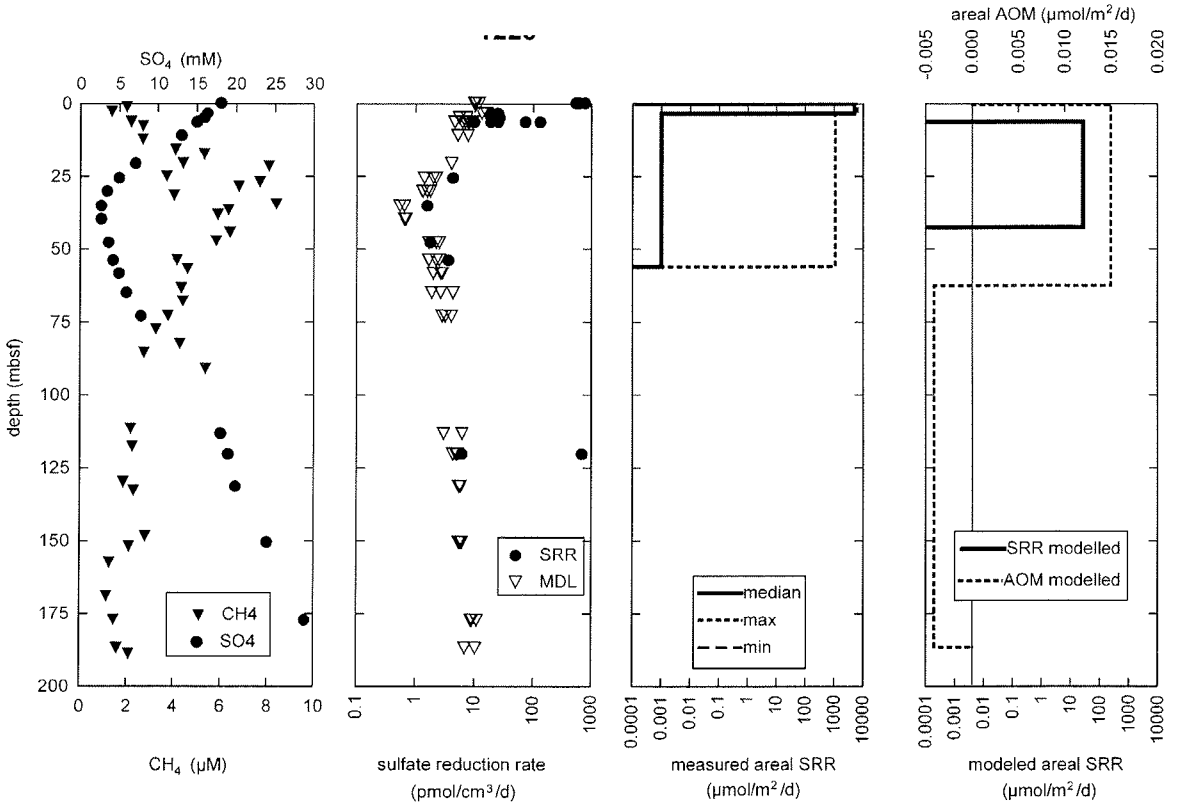

Fig. 3 to 6: The main parameters of the cores taken during ODP Leg 201 on the Peru continental margin that are discussed in the text.
A) Sulfate and methane concentrations in the porewater
B) Rates of sulfate reduction measured by $^{35}SO_4^{2-}$ radiotracer (circles), in cases where no SRR was detected, the minimum detection limits is shown (triangles)

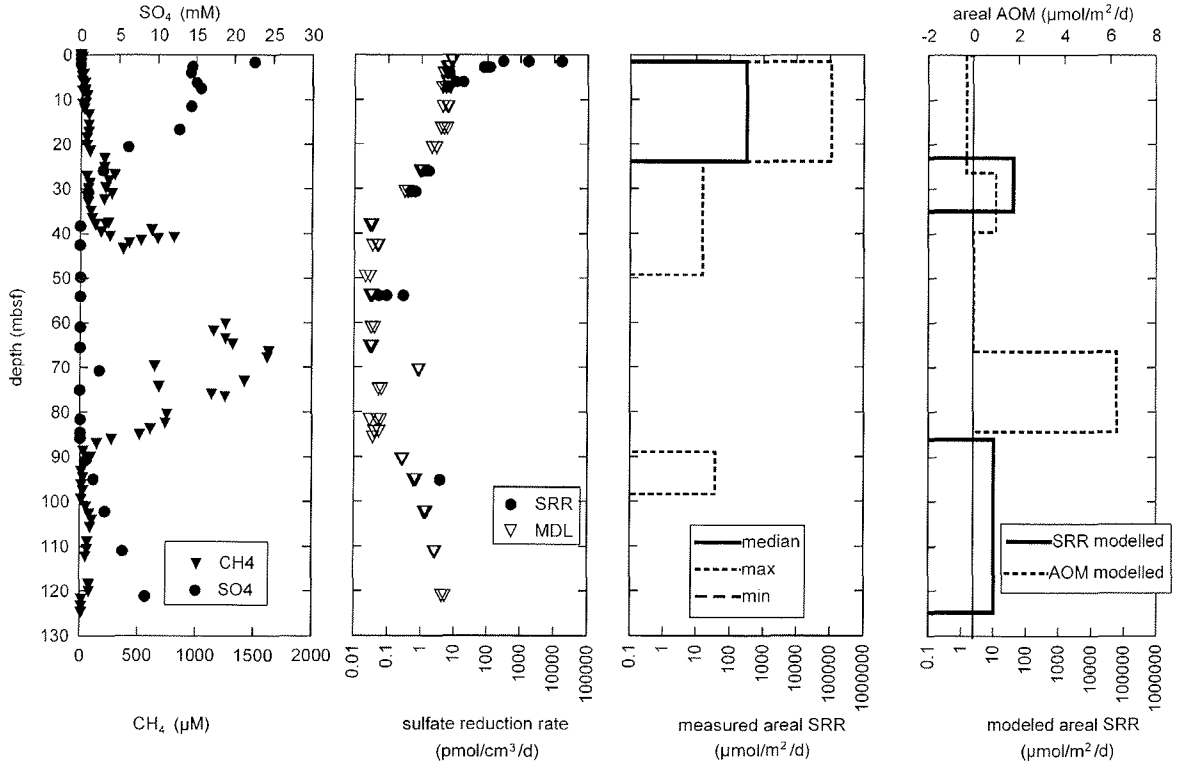

Fig. 5: Site 1229

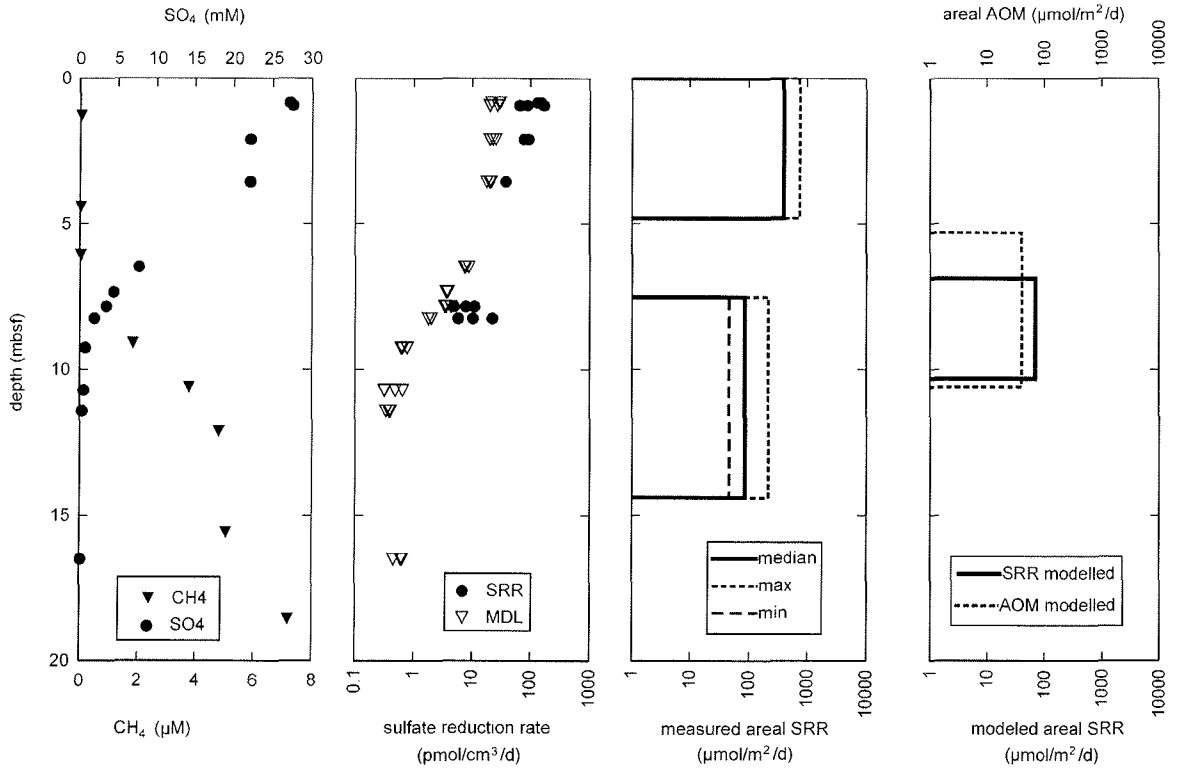

Fig. 6: Site 1230

C) Areal sulfate reduction rate calculated for each lithological unit. The results of (B) were used for the calculations

D) Modeled areal rates of sulfate reduction and anaerobic oxidation of methane calculated (see text for details)

porewater concentration profiles of methane and sulfate, (B) the SRR measured with the radiotracer technique and the minimum detection limit for samples where no SRR was detected, the areal sulfate reduction rates based on (C) the measured SRR and (D) the model results.

Site 1227

The cores from this site show a porewater profile for sulfate and methane that is typical for ocean margin sediments (Fig. 3A). Sulfate decreases steadily from the surface down to about 42 mbsf, methane shows an almost mirror profile. After its first appearance at about 35 mbsf it rapidly increases downwards to supersaturation with values > 2000µM. Due to degassing no estimates about the in-situ methane concentration in the deeper parts of the core can be made.

With the radiotracer technique only one zone of organiclastic SR at the surface (0 to 7 mbsf) can clearly be identified (Fig. 3B). SRR are in the range of single to hundreds of pmol cm^{-3} d^{-1}, but one sample at 6 m shows values that are about two orders of magnitude higher, up to 30,000 pmol cm^{-3} d^{-1}. This signal can not be discarded as a sampling or handling error as it was found in all 3 replicates.

Directly in the sulfate-methane transition (32 to 42 mbsf) no SR was detected, but below this zone some single samples show detectable activity at three depths (42, 55, 80 mbsf). The two upper depths (42 and 55 mbsf) belong to the same lithological unit in which the sulfate methane transition is located. We therefore have used those two samples as an estimate for the maximum SRR inside the SMZ.

The potential rates of AOM show measurable activity over the entire length of the core. From the top down to 40 mbsf the rates are rather uniformly in the range of 100 pmol cm^{-3} d^{-1} but at the depth where the sulfate-methane transition is located the values increase to about 450 pmol cm^{-3} d^{-1} and show higher scatter.

The measured SRR are in part supported by the modelling results. Based on the porewater sulfate concentration, the model suggests two zones of sulfate consumption, one SR zone at the surface and one at the SMZ. However, the model suggests a top SR zone that reaches much deeper into the sediment, from the surface down to 27 mbsf. The second zone is located at 37 to 43 mbsf.

When using the porewater methane profile, only one zone of activity is identified, stretching from 32 to 48 mbsf. This is expectable as a net consumption of methane takes place only inside the SMZ.

The calculated areal SRR for the organiclastic zone, based on either measured or modelled values are somewhat comparable when omitting the zone from 6 to 7.5 mbsf. This narrow zone alone would account for over 99 % of all SR in the entire core when included in the calculation. This zone of high activity was omitted from Figure 3C. In Table 2 values are given for with and without inclusion of this zone.

Based on the radiotracer measurements the areal SRR in the organoclastic zone (0 to 9.2 mbsf) is in the range of 110 to 412 µmol m^{-2} d^{-1} with a median value of 189 µmol m^{-2} d^{-1}. The model results based on the sulfate profile suggest an organiclastic zone from 0 to 17.16 mbsf with an areal SRR of 79 µmol m^{-2} d^{-1}.

For the methanotrophic zone there is very good agreement among the model results but not between the modelled and the radiotracer measurements. When either using the methane or sulfate concentrations for modelling, the areal rate is 5.9 or 5.5 µmol m^{-2} d^{-1}, respectively. The thickness of the methanotrophic zone is in the same range, however slighty shifted in its position, 32 to 48 mbsf when based on methane and 37 to 43 mbsf when based on sulfate.

The radiotracer measurements give a different picture, not only in the areal SRR but also in position and thickness of the methanotrophic zone. The lithological unit in which sulfate reduction was measured, stretches from 43 to 63 mbsf. When assuming homogeneous activity throughout the entire lithological unit, the areal rate is in the range of 0.1 to 1 µmol m^{-2} d^{-1}.

Site 1228

A feature of site 1228 is the influx of a sulfate bearing brine from below, causing reverse gradients in the bottom part of the core (Fig. 4A). Sulfate and methane are both present throughout the entire core. Sulfate concentration decreases rapidly from 29 mM at the surface to about 17.8 mM at 1 mbsf before decreasing more slowly to a minimum of 2.5 mM at around 35 meters. Below this depth it increases again steadily to a maximum value of > 30 mM at the bottom of the core. It is not clear what causes this abrupt change at 1mbsf. The methane concentration is low throughout the entire core (max. 9 µM) and its profile over depth shows scatter. The shape of the profile mimics the H_2S profile. Highest CH_4 concentrations are found at 25 to 35 mbsf, decreasing steadily to 1 to 2 µM in both directions.

1227	measured areal SRR per unit				
	from	to	min	median	max
	mbsf	mbsf	µmol $m^{-2}d^{-1}$	µmol $m^{-2}d^{-1}$	µmol $m^{-2}d^{-1}$
organiclastic	0	9,2	110 (21684)	189 (34257)	412 (45707)
intermediate	9,2	43,2	0	0	0
methanotrophic	43,2	62,6	0,11	0,12	1
	modelled areal SRR				
	from	to			
	mbsf	mbsf	µmol $m^{-2}d^{-1}$		
organiclastic	0	17,2	79		
intermediate	10,2	34,4	2,15E-15		
methanotrophic	34,4	42,9	5,5		
	modelled areal AOM				
	from	to			
	mbsf	mbsf	µmol $m^{-2}d^{-1}$		
organiclastic	1	32,3	0,1		
intermediate	32,4	40,1	1,7		
methanotrophic	40,1	47,9	5,9		

1228	measured areal SRR per unit				
	from	to	min	median	max
	mbsf	mbsf	µmol $m^{-2}d^{-1}$	µmol $m^{-2}d^{-1}$	µmol $m^{-2}d^{-1}$
organiclastic	0	3,5	0	5075	6413
methanotrophic	3,5	55,9	0	0,001	1091
	modelled areal SRR				
	from	to			
	mbsf	mbsf	µmol $m^{-2}d^{-1}$		
organiclastic	0	8,5	60,3		
intermediate	8,5	42,4	38,5		
methanotrophic	42,4	186,6	0		
	modelled areal AOM				
	from	to			
	mbsf	mbsf	µmol $m^{-2}d^{-1}$		
organiclastic	0,3	62,4	-0,01		
methanotrophic	62,4	186,5	0,004		

Tab. 3: Modeled and measured areal sulfate reduction rates and position of zones of microbial activity.

1229	measured areal SRR per unit				
	from	to	min	median	max
	mbsf	mbsf	μmol $m^{-2}d^{-1}$	μmol $m^{-2}d^{-1}$	μmol $m^{-2}d^{-1}$
organiclastic	1,5	23,9	0	320	109240
methanotrophic 1	23,9	49,3	0	0	15,6
intermediate	49,3	88,9	0	0	0
methanotrophic 2	88,9	98,4	0	0	37,3
	modelled areal SRR				
	from	to			
	mbsf	mbsf	μmol $m^{-2}d^{-1}$		
organiclastic	11,15	23,1	0		
methanotrophic 1	23,1	35,0	42,3		
intermediate	35,0	86,2	0		
methanotrophic 2	86,15	124,8	10,32		
	modelled areal AOM				
	from	to			
	mbsf	mbsf	μmol $m^{-2}d^{-1}$		
organiclastic	0	26,4	-0,32		
methanotrophic 1	26,4	39,7	0,99		
intermediate	39,65	66,4	0		
methanotrophic 2	66,4	84,4	6,27		

1230	measured areal SRR per unit				
	from	to	min	median	max
	mbsf	mbsf	μmol $m^{-2}d^{-1}$	μmol $m^{-2}d^{-1}$	μmol $m^{-2}d^{-1}$
organiclastic	0	4,8	0	397,5	750,1
intermediate	4,8	7,8	0	0	0
methanotrophic	7,8	12,0	46,4	85,9	214,4
	modelled areal SRR				
	from	to			
	mbsf	mbsf	μmol $m^{-2}d^{-1}$		
organiclastic	0	6,9	0		
methanotrophic	6,9	10,3	69,0		
	modelled areal AOM				
	from	to			
	mbsf	mbsf	μmol $m^{-2}d^{-1}$		
organiclastic	0	5,3	0,01		
methanotrophic	5,3	10,6	40,4		

In the top three meters very high SRR were measured, with values up to 1000 pmol cm^{-3} d^{-1} (Fig. 4B). Below this high activity zone SR was still detectable down to about 50 mbsf but the measured values were very close to the detection limit or below. Below 50 mbsf only one single datapoint showed detectable activity. This point was discarded because drilling disturbances occurred in this interval. The potential rates of AOM show no correlation with the sulfate reduction radiotracer measurements, the porewater profile and the modelling results. The potential AOM rates decrease from 20 mbsf to 65 mbsf steadily from around 100 pmol cm^{-3} d^{-1} to 30 pmol cm^{-3} d^{-1}. Deeper the potential rates increase to values > 150 pmol cm^{-3} d^{-1} but show high scatter.

The calculated methane concentration profile only poorly fits the measured data because of the high scatter in the measurements. Therefore the methane production and consumption profile should be treated with caution. The sulfate-based model suggests SR only in the top part of the core, between 5 and 40 mbsf. The methane-based model suggests methane consumption to take place much deeper, between 60 and 180 mbsf.

The areal SRR, calculated from the $^{35}SO_4^{2-}$ radiotracer measurements, show high variation because of the scatter in the measured data (Fig. 4C). In the high activity zone at the top (0 – 3.5 mbsf), areal SRR range from 0 to > 6000 µmol m^{-2} d^{-1}, with median values of about 5000 m^{-2} d^{-1}. Between 3.5 and 55.9 mbsf activity is still scattered but with lower absolute numbers, ranging from 0 to > 1000 µmol m^{-2} d^{-1}, with a median value of 0.001 µmol m^{-2} d^{-1}.

Based on the sulfate concentration profile, the model suggests a zone of SR reaching from the sediment surface down to 42.4 mbsf with a total areal SRR of 78.8 µm ol m^{-2} d^{-1} (Fig. 4D).

The model calculations for AOM do not show any significant activity, in the interval from 62.4 to 186.5 mbsf an areal consumption of 0.004 µmol m^{-2} d^{-1} is suggested.

Due to the high scatter of the measured SRR it is difficult to compare the data, but they fall roughly into the same range. The position of the organiclastic SR zone is quite similar, the model suggests a somewhat smaller zone than suggested by the measured data. The very low methane concentrations and the resulting extremely low rates of methanotrophic SR suggest that neither methanogenesis nor methanotrophic process are significant at this site.

Site 1229

Like at site 1228 there is an upward diffusing sulfate-bearing brine. However, sulfate is depleted between 35 and 80 mbsf (Fig. 5A). Methane reaches high concentrations (up to 1500 µM) inside the zone of sulfate depletion and diffuses upwards and downwards, therefore two methane-sulfate transition zones (SMZ) are observed, at around 35 and 85 mbsf, respectively. At the top of the sulfate depleted zone an erosion surface was observed. Around the same depth where sulfate re-appears, there is a zone with numerous dolomite and phosphorite concretions. No methane samples were taken between 48 and 65 mbsf because of poor core recovery and drilling disturbances. In this zone a minimal re-appearance of sulfate was observed. This reappearance was regarded as a sampling error and therefore the samples were discarded.

Like in 1228, very high SRR are found at the top part of the core (0 – 6 mbsf), with values > 10,000 pmol cm^{-3} d^{-1} (Fig. 5B). Further down, rates are close to the detection limit or even below and in most cases only some of the replicates show detectable activity.

Only in the upper sulfate-methane transition SR was clearly detected, while in the lower one only single samples showed detectable SR. A few scattered single samples show detectable SR below the lower SMZ, but in no case more with more than one replicate.

The potential AOM rates show some evidence for increased AOM activity in the two transition zones. With the exception of one sample at 7.2 mbsf, activity was only measurable in samples from the two SMZ. All other samples did not show any activity.

The upper section of the core (0 – 10 mbsf) was excluded from the model because it does not represent steady-state conditions. Based on the sulfate and methane concentration data the model suggests consumption to take place in both transition zones. The modelling results show that the rates to be expected from the porewater profiles are in the range of the MDL or even below (Fig. 5C).

The areal rates based on the measured values show extreme scatter in the top part (1.5 to 23.0 mbsf) with minimum, median, and maximum values of 0, 320, and 109,000 µmol m^{-2} d^{-1}, respectively. Below this section areal rates are zero except in the two sulfate-methane transition zones, resulting in maximum rates of 15.6 µmol m^{-2} d^{-1} and 37.3 µmol m^{-2} d^{-1} for the upper and lower zone, respectively (Fig. 5D).

The location of the top of the upper methanotrophic zone is very similar for both models and the measurements, at around 23 mbsf. However, each approach suggests

a different lower boundary, ranging from 35mbsf for the sulfate-based model over 39 mbsf for the methane-based model to 49.3 mbsf for the SRR measurements. The modelled rates also differ considerably, 42.3 µmol m^{-2} d^{-1} when based on sulfate and 0.99 µmol m^{-2} d^{-1} when based on methane. The $^{35}SO_4^{2-}$ radiotracer incubations suggests a maximum areal rate of 15.5 µmol m^{-2} d^{-1}, minimum and media values are bot zero.

Like for the upper zone, there are also great differences in the position and total thickness of the lower methanotrophic zone. The position suggested from the methane-based model (66.4 to 84.4 mbsf) does not even overlap with the one suggested by the sulfate-based model (86.2 to 124.8 mbsf) or the measured values (88.9 to 98.4 mbsf). The measured maximum areal rates for both transition zones are comparable to the model results, 15.6 and 37.3 µmol m^{-2} d^{-1} for the upper and lower zone, respectively.

Site 1230

Site 1230 is located in the Peru Trench in > 5000 m water depth and the sediments bear gas-hydrates. Sulfate decreases steadily from 28 mM at the sediment-water interface to zero at around 15 mbsf. Methane first appears at around 5 mbsf and increases rapidly to values > 5 mM. There is a pronounced SMZ between 6 and 9 mbsf, where both methane and sulfate are present in concentrations > 1 mM (Fig. 6A).

With the radiotracer technique sulfate reduction was detected in two intervals, one from the top down to 4.8 mbsf, the second one at 8 to 9 mbsf (Fig. 6B). The two horizons with detectable SR were composed of diatom-rich silty clays and quartz rich diatom oozes, respectively. In between, where no sulfate reduction was detected, there was a contrasting lithology, composed of foraminifer oozes. The sulfate gradient is almost linear in the top SR zone, with even a slight downward curve. This almost linear gradient is in contradiction with the considerably high rates (up to > 100 pmol cm^{-3} d^{-1}), suggesting that processes other than transport through molecular diffusion are replenishing the sulfate pool in the sediment.

For the organiclastic zone (0 – 4.8 mbsf) the areal SRR based on the radiotracer method are between 0 and 750 µmol m^{-2} d^{-1} with a median value of 397 µmol m^{-2} d^{-1}, while the model did not detect any activity because of the linearity of the sulfate gradient (Fig. 6 C, D).

interval	center	average SRR	95% prediction	AODC cells	Per cell rate		
			limit+/-		minimum	average	maximum
mbsf	mbsf	pmol $cm^{-3} d^{-1}$	pmol $cm^{-3} d^{-1}$	cells cm^{-3}	mol $cell^{-3} y^{-1}$	mol $cell^{-3} y^{-1}$	mol $cell^{-3} y^{-1}$
0-0.01	0,01	562888	267303	2,0E+09	3,7E-14	7,0E-13	1,0E-11
0.01-0.05	0,03	155422	45881	7,0E+08	3,8E-14	5,4E-13	7,0E-12
0.05-0.1	0,08	117903	45606	4,2E+08	4,2E-14	6,9E-13	9,5E-12
0.1-0.5	0,30	92214	20691	1,9E+08	9,2E-14	1,2E-12	1,4E-11
0.5-1	0,75	24349	22965	1,1E+08	3,0E-15	5,3E-13	1,0E-11
1-5	3	8682	2772	5,1E+07	2,8E-14	4,1E-13	5,5E-12
5-10	7,5	22,5	15	3,0E+07	6,4E-17	1,8E-15	3,0E-14
10-50	30	1,18	0,80	1,4E+07	6,8E-18	2,1E-16	3,5E-15
50-100	75	0,72	0,80	8,2E+06	ND	2,1E-16	4,5E-15

Tab. 4: Calculated per-cell sulfate reduction rates, based on the assumption that all AODC counted cells are active and 15 % of the population are sulfate reducers. See text for description.

For the sulfate-methane transition zone there is considerably good agreement between the model results based on sulfate or methane on the one hand and the measured values on the other. All three approaches suggest similar rates. Based on sedimentological data, the lithological unit in which the SMZ is located stretches from 7.8 to 20.5 mbsf but sulfate is depleted at around 12 mbsf, therefore the thickness of the methanotrophic zone can not be estimated from the lithological data alone but through both sedimentological and geochemical parameters. When using sedimentological data alone to calculate an areal SRR the values would be much too high.

When using both the lithological and geochemical information to re-define the methanotrophic zone, it stretches from 7.8 mbsf to 12 mbsf while the numerical model suggests 6.9 – 10.3 mbsf and 5.3 – 10.6 mbsf based on sulfate and methane, respectively.

The areal SRR of the re-defined methanotrophic zone, is 35 to 160 µmol $m^{-2} d^{-1}$, with a median value of 64 µmol $m^{-2} d^{-1}$, while the sulfate and methane based models suggest 69 and 40 µmol $m^{-2} d^{-1}$, respectively.

Potential rates of AOM was not detected in any sample, although they should be highest here.

All measured potential rates of anaerobic oxidation of methane (AOM) are presented in Table 1.

Per-cell sulfate reduction rates

The results are shown in Table 4. The range between the minimum and maximum average rates found in all samples from the Peru continental margin is six orders of magnitude. For each depth segment the range of data at the 95 % confidence level was calculated.

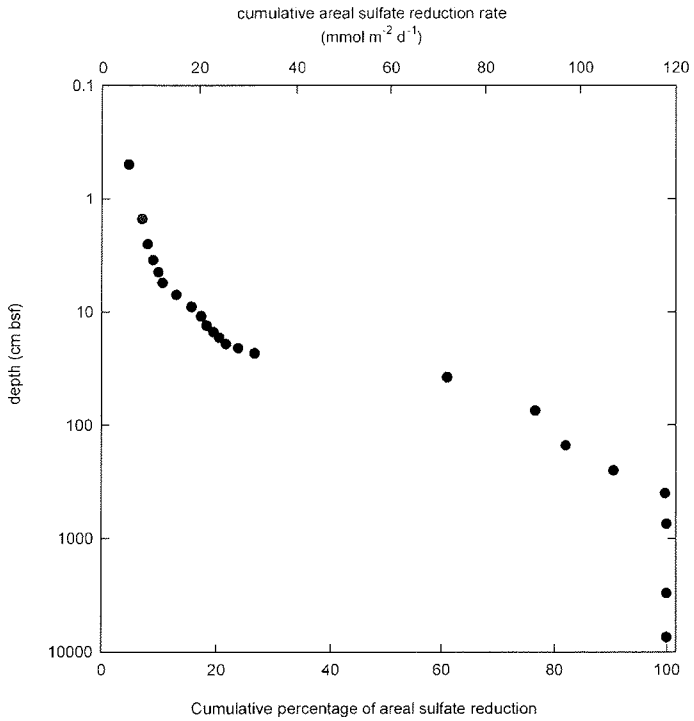

Fig. 7: Cumulative areal sulfate reduction rates, based on the average SRR values shown in Fig. 2 A. Note the different scales on the upper and lower X-axis.

The distribution of bacterial cells counted by AODC over depth can be described by Eq. 5

$$\text{Log}_{10} \text{ bacterial cells} = 7.89 - 0.57 \ (\text{Log}_{10} \text{ depth}) \qquad \text{Eq. 5}$$

The range of the data is +/- one order of magnitude at the 95 % confidence level (Parkes et al., 2000).

We assumed that all bacteria counted by AODC were active and that 15 % of all cells are sulfate reducers. For each depth interval we divided the average SRR by the number of bacterial cells to calculate average per-cell rate was calculated. Based on the 95 % confidence levels, we also calculated minimum and maximum per-cell rates. Too few datapoints were available at depths > 100 mbsf to give a representative average SRR. Therefore all calculations have been limited to a maximum depth of 100 mbsf.

The per-cell rates found in the upper 5 mbsf stay almost constant over depth with a mean value of 10^{-14} to 10^{-13} mol cell^{-1} y^{-1}. Deeper the per-cell rates drop

to 2.7 * 10^{-16} mol $cell^{-1}$ y^{-1} between 5 and 10 mbsf before declining to around 3 * 10^{-17} mol $cell^{-1}$ y^{-1}. The minimum and maximum rates are between one and two orders of magnitude.

Cumulative areal rates

Figure 7 shows the cumulative sulfate reduction rate based on the average SRR shown in Fig. 1. About 20 % of the sulfate reduction takes place in the upper 10 cm. The upper meter accounts for 80 % of the total sulfate reduction. At 4 mbsf, 99.8 % of all sulfate reduction has already proceeded. The deeper hundreds of meters altogether do not account for more than fractions of a percent.

Discussion

Two pathways of sulfate reduction can be found in sediments from the Peru continental margin,

1) With organic matter as a carbon source (organiclastic SR)
2) With methane (methanotrophic SR or AOM).

Among others, Morita (2000) and Parkes et al. (1993) discuss the possibility of Hydrogen being a major energy source in the deep biosphere. The quantities of hydrogen found in Peru margin sediments are by far not high enough (< 1 nM) to account for the turnover of the much larger amounts of sulfate, therefore the vast majority,if not even all, sulfate reduction in these sediments can be attributed to organiclastic or methanotrophic SR.

The scatter of the SRR data over four to five orders of magnitude at each depth can partly be explained by differences of organic matter availability as a function of productivity of the overlying waters, waterdepth etc.

For the upper centimeters to meters of the sediment, the high scatter in the rates can be explained by differences in the availability of organic matter rather than its total concentration. In a detailed study about the composition of the organic matter and the sulfate reduction rates found in the MUCs used in this study Niggemann et al. (2002) found that there is no correlation between the amount of organic carbon and SRR. The percentage of labile and therefore easily degradable organic compounds like chlorophyll shows a much better correlation with sulfate reduction rates. However, when compared with other oceanic regions, the sulfate reduction rates and

the C_{ORG} contents are all generally high, reaching up to 2µmol cm^{-3} d^{-1} and up to 17% C_{ORG} respectively. These rates and C_{ORG} contents are among the highest reported for sediments. For sediments off the coast of Chile Schubert et al. (2000) showed that the fraction of labile material rather than total organic carbon content control SRR. Both studies were limited to the upper centimeters of the sediment as they only dealt with MUC samples.

According to the model calculations of D'Hondt et al. (2002), methane should be the dominant electron donor for sulfate reduction in the deeper parts of the sediment column (> 1.5 mbsf). Our radiotracer measurements do not support this assumption. Therefore the question has to be addressed how representative the radiotracer measurements and numerical models are.

With the exception of very few studies that employed benthic lander systems (Weber et al., 2001) , SRR are measured ex-situ. When measuring SRR ex-situ the effects of sample handling have to be considered with care. There has been considerable debate about the effects of decompression on the rates of microbial activity in deep-sea samples. The literature reports effects in both directions, either increasing (e.g. Jannasch and Taylor, 1984) or decreasing rates (Bianchi and Garcia, 1993), or little to no effect (Martens et al., 1998). Ferdelman et al. (1999) give an overview about the work on pressure effects with special emphasis on sulfate reduction and conclude, that decompression has no clear effect on sulfate reduction. Weber et al., (2001), conclude that based on their results they cannot give a consistent explanation for the differences between SRR measured in situ and in the laboratory.

While several studies have addressed the effects of different composition and therefore bioavailability of the organic matter on SRR (e.g. Niggemann et al., 2002, Schubert et al., 2000), the effects of different methane concentrations on SRR are much harder to investigate (Nauhaus et al., 2002). Decompression has a major effect on the the availability of methane because its solubility is depending on its partial pressure. Methane saturation at 4 °C, 35‰ salinity, and 1 atm, is about 1.65 mM (Yamamoto et al., 1976). Reliable methane concentration values can only be obtained from those parts of the cores where the in situ concentration does not exceed the saturation at 1 bar. In parts with higher concentrations, degassing and bubble formation upon retrieval lead to a scattered CH_4 profile. Because of degassing, the in-situ partial pressure and therefore the availability of methane to the sulfate reducing bacteria can only be estimated. In samples from sulfate-methane transition zones the measured

rates are consistently lower than those calculated by the sulfate-based model; the lack of methane has apparently a decreasing effect on the methanotrophic SRR. Nauhaus et al. (2002) showed on samples from gas hydrate bearing sediments where methane was the sole electron donor, that SRRs increase with increasing methane partial pressure. Without the determination of the in situ methane partial pressure and the possibility to incubate samples under in situ conditions radiotracer incubations may not be representative.

The results of Treude et al. (in prep.) suggest that inside the transition zone anaerobic oxidation of methane (AOM) takes place not equally distributed over the entire transition zone but only in a very narrow zone. In samples from the Chile Continental Margin they found that the vast majority of AOM proceeds in an interval of less than 10 cm. At the border of this zone rates increase by several orders of magnitude within 2 – 4 cm. In case the same is occurring in the ODP cores, it is highly unlikely that this zone will be hit when sampling in intervals > 1 m.

In most ODP cores no SR was detected in the sulfate-methane transition zones when using the radiotracer method. In several cases the modeled rates were lower than the minimum detection limit of the radiotracer method. Due to the degassing in the supersaturated parts of the cores it is impossible to obtain exact methane porewater concentration profiles that could be used for modeling. Upon degassing bubble formation and expansion of the sediment can cause a significant redistribution of the sediment, thereby also affecting the sulfate distribution in the core. Porewater sulfate concentrations still seem to be a more robust parameter for modeling sulfate reduction rates as they are less affected by degassing than methane. Re-oxidation of sulfide during porewater pressing and handling can bias the sulfate concentration. In all cores discussed in this study great care was taken to avoid any artifacts due to sample handling. In cases where electron donors other than methane are available, a distinction between the different pathways of sulfate reduction can not be made.

When comparing the radiotracer measurements with the model results a general trend can be observed. In the upper parts of the cores the model tends to underestimate rates.

The differences between the modeled and the measured results can be explained by the fact that the model provides information about the net rate, while the radiotracer measures the gross rate.

The net rate is the amount of production or consumption that is necessary to account for the change in the concentration gradient over a given depth interval. Many models assume that the only transport mechanism is molecular diffusion. When modeling reaction close to the sediment-water interface other transport processes like advection have to be quantified and incorporated into the model, which can be difficult to achieve. In cases where sulfide re-oxidation of reduced species or advective transport takes place, the concentration gradient can be linear, indicating no net consumption of sulfate although radiotracer incubations show high rates of sulfate reduction.

The gross rate gives information about the total turnover of a compound. By using a radiotracer, one can follow the pathway of a compound through the entire chain of transformations. and its distribution in the different pools. However, the gross rate does not provide information about the net concentration changes of the respective compound. Both parameters complement each other.

In ODP site 1230 for example, the sulfate gradient is linear from the surface down to about 7.5 mbsf, before it a sharp turn occurs and concentration reaches zero at around 10 mbsf. Methane appears around 6 mbsf and reaches supersaturation at around 10 mbsf. Therefore the sulfate-methane transition zone is located between 6 and 10 mbsf. The linear gradient between 0 and 7.5 mbsf suggests that sulfate is not consumed in this interval. However, radiotracer measurements show high SRR of up to 100 pmol cm^{-3} d^{-1} between 0 and 2.5 mbsf, which is even higher than what has been suggested by the model for the sulfate-methane transition zone. Apparently bioturbation and/or advective transport delivers enough sulfate or sulfide oxidizing compounds into the sediment to maintain the linear gradient despite the active sulfate consumption. The porewater concentration profile of sulfide does not show elevated values in the upper 2.5 mbsf. Sulfide oxidation can play an important role in such ecosystems thereby providing another way of maintaining high levels of sulfate concentration despite high consumption. In shallower water-depths nitrate storing sulfide oxidizing bacteria can have a major impact on sediment sulfur geochemistry (Ferdelman et al., 1997; Fossing, 1990; Schmaljohann et al., 2001). In the upper part of the cores, numerical models generally fail to predict SRR as other processes that are hard or impossible to quantify (advective transport, bioturbation, bioirrigation) affect the net sulfate turnover.

An advantage of models is that they are less susceptible against sample manipulation. Especially degassing makes it very difficult to assess methanotrophic SR with radiotracer incubations, as most of the carbon source has vanished even before the incubation has started. It is still almost impossible to conduct an entire incubation at in situ methane partial pressure, despite great technical advances in recent times.

The detection limit of the radiotracer technique is determined by several physical and chemical parameters that can be influenced by the user only to a certain extend. Even by using the most sensitive method available (Kallmeyer et al., submitted) there is a certain minimum detection limit below which no sulfate reduction can be detected. In parts of the core where turnover is lower than the MDL of the radiotracer method, the model is still able to calculate rates of consumption.

Per-cell rate

The decrease of the average SRR with depth over about six orders of magnitude can not be explained with a decrease in availability of suitable electron acceptors. The total number of bacterial cells decreases only over three to four orders of magnitude. The per-cell sulfate reduction rates calculated from the average SRR and the bacterial distribution data of Parkes et al. (2000) show that there is a large span of six orders of magnitude between the maximum and minimum rates. In the depth range that is covered by the MUCs and GCs (< 5 mbsf) this range is comparable with the results of Canfield et al. (2000) who found per cell rates in the range of $3 * 10^{-14}$ to $2.5 * 10^{-11}$-mol $cell^{-1}$ y^{-1}. An interesting feature is the little shift of the per-cell rates over depth. Any actually occurring shift may be covered by the large span of the data but the reduction in the number of bacteria and the reduction in SRR follow almost the same trend, resulting in a constant per-cell rate when assuming no changes in the fraction of sulfate reducers. The assumed 15 % fraction of SRBs on the total bacterial population represents a maximum value found in surface sediments (Llobet-Brossa et al., 2002; Ravenschlag et al., 2000) and may not be representative of the deep biosphere. But even when the fraction of sulfate reducers would be somewhat different from that value, the resulting rates would still fall roughly in the same range as the results of (Canfield et al., 2000).

While down to 5 mbsf the average per-cell SRR are in the same range as the values of Canfield et al. (2000) the deeper parts of the sediment show a much lower per-cell rate. Below 5 mbsf the rates drop sharply by several orders of magnitude to values

of $3*10^{-17}$ mol $cell^{-1}$ y^{-1}. The question arises what causes these much lower SRR in the ODP cores, both in direct measurements and on a per-cell level. Several scenarios arise:

1) In the deeper parts of the sediment a large fraction of the bacteria that have been counted are not viable, they either "rest" in a dormant state, or are dead but not degraded. The question about the proper sampling and counting techniques when assessing bacterial numbers in the deep biosphere is beyond the scope of this paper. Only few studies calculated average doubling time of cells at great depth. In a study of bacterial populations in sapropels from the Mediterranean Sea Parkes et al. (2000) calculated cell division times of ca. 105 kyr, and a population doubling time of 0.92 Myr. The findings of Vreeland et al., (2000) suggest that bacteria can rest for long periods of time, up to millions of years, before becoming active again when the right conditions appear. Parkes et al. (2000) found 8.3 % dividing cells in sapropels of the Mediterranean. It is difficult to use the fraction of dividing cells to estimate the percentage of the viable population. If a significant fraction of the cells are dead, why are they not degraded? Bacterial necromass would represent an available carbon source. One possible explanation would be the limitation of pore space, preventing active cells from reaching the dead ones. But still extracellular enzymes should be capable of reaching the dead cells in case there is any connection between the pores. If there were no connections at all, i.e. the dead cells rest in closed pores, how did the bacteria get into the pores and how could they survive for any length of time? We can therefore assume that it is well possible that only a fraction of the total number of counted bacteria are actually active cells. However, quantification is at least problematic.

2) The fraction of sulfate reducers decreases dramatically with depth but the per-cell rate of sulfate reduction remains more or less constant. This scenario arises the question what metabolism do the other cells have? The most important control parameter for sulfate reducers is, of course, the availability of sulfate. The work of Parkes et al. (2000) suggests that acetogenesis and methanogenesis are taking place at great depth and it is reasonable to assume that a certain change in the microbial community structure happens but it remains questionable that a dramatic change over several orders of magnitude takes place. Up to now only few studies about the community structure of marine sediments that especially focused on sulfate reducers were carried

out (Llobet-Brossa et al., 2002; Llobet-Brossa et al., 1998; Ravenschlag et al., 2000). To which degree these findings are comparable with the deep biosphere is not clear. The experimentally determined upper and lower limits of per-cell SRR show a range of about four orders of magnitude (Canfield et al., 2000). The span of SRR found in samples of from the Peru Margin appears too large to be explained entirely by a shift in the community structure. Therefore, if the per-cell rates reported by Canfield et al. (2000) represent the absolute maximum range, then a shift in the community structure of about two orders of magnitude is necessary to explain the SRR found in the Peru continental margin.

3) The fraction of sulfate reducers stays constant, but the per cell rate decreases by several orders of magnitude. Literature data report rates for pure cultures and from natural environments in the range of 10^{-15} to 10^{-12} mol cell^{-1} y^{-1} (see Canfield et al., 2000) and references therein). Based on our calculations the per cell rates are in the range of 10^{-14} to 10^{-11} mol cell^{-1} y^{-1} at the surface and 10^{-18} to 10^{-15} mol cell^{-1} y^{-1} at greater depth. While at the surface the rates found in Peru margin sediments are in the same range as the literature data, the rates are considerably lower at depth. In many cases the rates derived by numerical modeling are lower than the minimum detection limit of the radiotracer method. As we can deduct from the sulfate concentration profile that sulfate reduction actually happens, it is reasonable to assume that the modeling results rather than the radiotracer measurements represent the true per-cell rates. The sulfate reduction rates that are based on radiotracer measurement may represent a maximum estimate rather than average rates.

We based the calculation of per-cell sulfate reduction rates on several assumptions

1) The fraction of sulfate reducers stays uniformly at 15 % over the entire depth (based on the work of Ravenschlag et al. (2000) and Llobet-Brossa et al. (2002).
2) All AODC-counted cells are active, most probably only a certain fraction of the cells is active and viable but as we do not have information about the fraction of viable cells we use the AODC counts.
3) The SRR measured by radiotracer represent in-situ rates. In cases where the radiotracer technique was not able to detect any sulfate reduction, the model results suggest rates that were below the detection limit of the radiotracer method. The radiotracer measurements may therefore represent maximum rates.

When comparing the per-cell rates calculated for Peru margin sediments they roughly fall into the same range as the rates reported by Canfield et al. (2000). Therefore sulfate-reducing microorganisms in the deep biosphere do not have to be adapted to rates of metabolic activity that are much lower that what has already been described from natural sediments and pure cultures. Although rates of sulfate reduction as low as the minimum rates calculated in this work have not yet been reported for any sulfate-reducing microorganism, they are not too far away from values reported in the literature and can therefore not completely ruled out. We still do not know enough about the community structure and the metabolic capabilities of life in the deep biosphere to make a more precise estimate of the true rates of sulfate reduction.

Carbon turnover due to sulfate reduction in Peru Margin sediments

When calculating the cumulative sulfate reduction rate over depth (Fig. 7) it becomes obvious that the vast majority of carbon is turned over in the upper few meters. As in the upper 4 mbsf, 99.8 % of all sulfate reduction has already proceeded and the deeper hundreds of meters altogether do not account for more than fractions of a percent, we can assume that organiclastic SR is the main pathway for sulfate reduction in this sediment column. In all cases where we have sampled sulfate-methane transition zones, they were located deeper than 10 mbsf, and therefore methane is usually not available in significant quantities in the upper few meters. Even in the deeper parts where methane can play an important role as an electron donor in narrow intervals, its contribution to the total carbon turnover budget is small because of the limited thickness of the sulfate-methane transition zone.

Conclusions

Carbon turnover through sulfate reduction in sediments from the Peru continental margin appears to proceed mainly with sedimentary organic matter as a carbon source, rather than methane. In certain narrow intervals methane can be a significant electron donor but its overall contribution to sulfate reduction is rather small.

When using the porewater concentration profiles as a basis for numerical modeling it appears as if the fraction of sulfate that is used for anaerobic oxidation of methane is much larger. This is mostly caused by an underestimation of organiclastic sulfate reduction in shallow sediment depth.

Acknowledgements

The authors wish to thank the crews and the participating scientists on Sonne cruise 147 and JOIDES Resolution Leg 201 for help and expert handling of the samples and providing additional data. Kirsten Neumann, Sabine Knipp, and Astrid Rohwedder helped with the processing of the sulfate reduction rate samples.

6 Inorganic and sulfur isotope geochemistry of Holocene Peruvian upwelling sediments

H. Philipp Böning[1], Michael E. Böttcher[2], Bernhard Schnetger[1], Jens Kallmeyer[2], Cornelia Kriete[3], and Hans-Jürgen Brumsack[1]

Submitted to Geochimica et Cosmochimica Acta

This manuscript was not included, as it only deals with surface sediments and does not fit into the scope of this thesis. The manuscript can be provided upon request.

[1]Institute for Chemistry and Biology of the Marine Environment (ICBM), Carl von Ossietzky University of Oldenburg, P.O. Box 2503, D-26111 Oldenburg, Germany
[2]Max Planck Institute for Marine Microbiology, Celsiusstrasse 1, D-28359 Bremen, Germany
[3]Federal Institute for Geosciences and Natural Resources (BGR), Stilleweg 2, D-30655 Hannover, Germany

Abstract

16 short sediment cores from the upper edge, within and below the oxygen minimum zone (OMZ) off Peru were recovered during cruise 147 of R/V Sonne. The sediments were analysed for major elements (Si, Ti, Al, Mg, Ca, Na, K, P) and trace elements (Ag, As, Ba, Bi, Co, Cd, Cr, Cu, Mn, Mo, Ni, Pb, Re, Sb, Tl, U, V, Y, Zn, Zr), as well as organic carbon and reduced sulfur (essentially pyrite), the stable sulfur isotope composition ($\delta^{34}S$) of pyrite, sulfate reduction rates (SRR) and $^{206}Pb/^{207}Pb$ ratios. Pore waters were analyzed for dissolved sulfate/sulfide and $\delta^{34}S$ of sulfate.

The mean terrigenous component of Peruvian upwelling sediments is close to an andesitic composition. Most samples show slight increases in biogenic silica (diatoms) and some exhibit distinct carbonate enrichments (foraminifera). High TOC and P contents are due to enhanced primary productivity and the presence of phosphorites, high sedimentation rates and corresponding organic matter preservation under a strong OMZ. Strong $\delta^{34}S$ depletions in pyrite ($\delta^{34}S$ values as light as –49 ‰) indicate intense bacterial isotope fractionation. In all cores highest SRR are observed in top 5 cm where pore water sulfate concentrations vary little due to resupply of sulfate by sulfide oxidation and/or diffusion of sulfate from bottom water. Nutrient-type trace elements are highly (Ag, Ni) and extremely (Cd) enriched in the sediments due to association with plankton, high sedimentation rates and fixation as sulfides (Cd) or association with organic matter (Ni). Ag transfer to the sediments may be governed by productivity and/or bottom water concentrations (scavenging onto particles). Ba concentrations only exceed the geogenic level in cores of greater water depth implying the preservation of barite and confirming the water depth depending distribution pattern of Ba. Pb, Bi, besides Cu, Zn are significantly enriched in near-coastal sites and may have been contributed by anthropogenic activity. With upcore increasing Pb/Al ratios $^{206}Pb/^{207}Pb$ ratios decrease suggesting an increasing admixture of isotopically lighter Pb most likely related to mining/industrial activity. Redox-sensitive elements are significantly (U, As, Sb) and highly (Re, Mo) enriched. Diffusion of these elements from the water column into sub/anoxic sediments followed by reduction seems to be an important step for accumulation. Re/Mo ratios indicate anoxic conditions for OMZ sites and suboxic conditions for sites below the OMZ. Despite of their different sources Mo and Cd are well correlated, implying the same early diagenetic response to sulfidic conditions. Redox-sensitive Mn and Co are significantly depleted in the sediments most likely due to mobilization from particles settling through the OMZ rather than

diffusion from reducing sediments. A comparison of different upwelling sediments yields that trace metal contents from Peruvian and Namibian sediments exceed those from Oman and Gulf of California.

7 Conclusions

The aim of this thesis was to get a better understanding of sulfate reduction in the deep biosphere. In order to do so a new distillation procedure was developed that allows the recovery of very small amounts of radiolabeled sulfide, thereby reducing the minimum detection limit to much lower levels.

By using the new technique, sulfate reduction rates (SRR) were measured in almost 700 samples from the Peru continental margin, ranging from the sediment-water interface down to several hundred meters. This dataset of unpreceeded resolution allowed for a detailed study of the controls and effects of sulfate reduction. Additionally SRR, rates of methanogenesis, and anaerobic oxidation of methane (AOM) were mathematically modeled, based on the porewater concentration profiles. Although the new distillation technique allowed the detection of sulfate reduction rates of > 1pmol cm^{-3} d^{-1} many measurements were below the detection limit, especially in the deeper parts of the cores.

Over the upper few meters the decrease of SRR follows the same trend as the decrease of the number of enumerated bacterial cells, counted by AODC. In the deeper part however, the sulfate reduction rates decrease much stronger than the number of bacterial cells. The reasons for this remain elusive and several possible scenarios arise. Either the fraction of viable cells decreases, or the fraction of sulfate reducers or the per-cell sulfate reduction rate. Based on data about the community structure of surface sediments, per-cell rates were calculated for the Peru margin sediments and the resulting rates are similar to values reported in the literature. This is remarkable, as it would suggest that the microorganisms in deeper sediment layers do not need to have a highly specialized metabolism to survive in the deep biosphere. Another interesting observation was the apparently low contribution of anaerobic methane oxidation to the total sulfate reduction and therefore total carbon remineralization. Contrary to D'Hondt et al. (2002) the data from the Peru continental margin suggest that in sediment depths > 1.5 mbsf the majority of sulfate is used to oxidize organic matter other than methane. More than 80 % of all sulfate reduction takes place in the upper meter, where methane is usually not available.

Another development during this thesis was a high-pressure thermal gradient block in which multiple samples can be incubated at pressures of up to 500 bar and over a wide range of temperatures, covering more than the entire biological range. With this

block the effect of pressure and temperature on biological activity can be determined in a single experiment.

Sediment from the hydrothermal vent area of Guaymas Basin was used in these experiments. Similar to previous studies it was shown that the sulfate reducing community has a thermophilic to hyperthermophilic temperature optimum. Upon application of in-situ pressure (220 bar) the rates increase by over an order of magnitude. This strong pressure effect has not previously been described for Guaymas Basin sediments. In another experiment with these sediments rates of anaerobic oxidation of methane were measured over a wide range of temperatures. Up to now the only sites where this process has been directly measured were considerably cold (< 10 °C). From molecular and biomarker studies there was indirect evidence for anaerobic oxidation of methane to proceed in the mesophilic or even thermophilic temperature range. Here we present the first direct rate measurements of anaerobic oxidation of methane in the thermophilic temperature range. However, the vast majority of sulfate reduction proceeds with carbon sources other than methane.

Sulfate reduction can not only be mediated by microorganisms but also through thermochemical reactions. Thermochemical sulfate reduction (TSR) was not observed in any of the experiments. This in most probably due to the fact that the rates of TSR are much slower than those of biological sulfate reduction (BSR) and the experiments were not specifically designed for the detection of TSR.

The findings of this study do not only provide new insights into the biogeochemical cycles of carbon and sulfur in deep sediments, they might also be used for a better interpretation of the geologic record. As anaerobic oxidation methane has now been shown for meso- to thermophilic environments, the interpretation of fossil hydrothermal vent deposits has to take AOM into consideration. In seep deposits autogenic carbonates derived from AOM have been found in many locations. Michaelis et al. (2002) already suggested that AOM is an ancient process and perhaps one of the earliest metabolic pathways. In light of the now widely believed theory that life may have evolved around hydrothermal vents (see Reysenbach and Shock, 2002, for a review) the fact that AOM can proceed at elevated temperatures adds another piece of evidence to this theory. Although methane is not the dominating carbon source for sulfate reduction in Guaymas Basin, in cases where no other electron donor is available AOM might be the quantitatively most important process.

The rapidly expanding field of deep biosphere research has already had a major impact on the concepts of global biogeochemical cycles. However, many questions remain unsolved as the techniques are still in their infancy and the wider implications of the results already produced are still not fully understood.

8 Outlook and recommendations for future work

In order to be able to proceed further in the field of deep biosphere research the development of new and the refinement of existing methods has to be an integral part of science in this field.

Due to the low metabolic rates the methods currently used for measuring turnover rates are not sensitive enough in many cases. The new method for sulfate reduction rate measurements has most probably reached the physical limits of this approach. Other methods however may still have potential for refinements (^{14}C incorporation techniques, beta-imaging, etc.). Molecular genetics and compound specific isotope analysis might reveal new insights into the processes and pathways in the deep biosphere.

Sampling and sample handling is another field where vast improvements still have to be made. Currently there are no systems available that allow the retrieval, handling and processing of a sample without de-pressurization. Without such a system the investigation of sediments harboring strictly barophilic organisms is almost impossible.

Leaving the practical problems aside, a few points that might be of use to get a better understanding of the biogeochemistry of the deep biospshere are:

- Determination of the fraction of viable and/or active bacteria in deep sediments.
- Better quantification of other important metabolic pathways (e.g. acetogenesis, methanogenesis)
- Test of hydrogen as a energy source in the deep biosphere
- Estimation of the quantitative importance of AOM in hydrothermal vent systems with different amounts of available organic matter
- Search for traces of hydrothermal AOM in fossil hydrothermal vent systems to track back this process over Earth's history

9 References

Adler M., Hensen C., Kasten S., and Schulz H. D. (2000) Computer simulation of deep sulfate reduction in sediments of the Amazon Fan. International Journal of Earth Sciences 88, 641-654.

Albert D. B. (1985) Sulfate reduction and iron sulfide formation in sediments of the Pamlico River estuary, North Carolina. PhD, University of North Carolina.

Aller R. C. and Rude P. D. (1988) Complete oxidation of solid phase sulfides by manganese and bacteria in anoxic marine sediments. Geochimica et Cosmochimica Acta 52, 751-765.

Amelin Y., Lee D.-C., Halliday A. N., and Pidgeons R. T. (1999) Nature of the Earth's earliest crust from hafnium isotopes in single detrital zircons. Nature 399, 252-255.

Amurskii G. I., Goncharov E. S., Zhabrev I. P., and Solov'ev N. H. (1977) Genesis of H_2S-containing Natural Gases of Oil and Gas Basins. Soviet Geology 5, 56-68.

Appel P. W. U. and Moorbath S. (1999) Exploring the Earths oldest geological record in Greenland. EOS 80(23), 257.

Baker B. J., Moser D. P., MacGregor B. J., Fishbain S., Wagner M., Fry N. K., Jackson B., Speolstra N., Loos S., Takai K., Sherwood Lollar B., Fredrickson J., Balkwill D., Onstott T. C., Wimpee C. F., and Stahl D. A. (2003) Related assemblages of sulphate-reducing bacteria associated with ultradeep gold mines of South Africa and deep basalt aquifers of Washington State. Environmental Microbiology 5(4), 267-277.

Berg P., Risgaard-Petersen N., and Rysgaard S. (1998) Interpretation of measured concentration profiles in sediment pore water. Limnology and Oceanography 43(7), 1500-1510.

Berner R. A. (1964) An idealized model of dissolved sulfate distribution in recent sediments. Geochimica et Cosmochimica Acta 28, 1497-1503.

Bianchi A. and Garcia J. (1993) In stratified waters the metabolic rate of deep-sea bacteria decreases with decompression. Deep Sea Research 1 40(8), 1703-1710.

Bildstein O., Worden R. H., and Brosse E. (2001) Assessment of anhydrite dissolution as the rate-limiting step during thermochemical sulfate reduction. Chemical Geology 176, 173-189.

Bizarro M., Baker J. A., Haack H., Ulfbeck D., and Rosing M. (2003) Early history of Earth's crus-mantle system inferred from hafnium isotopes and chondrites. Nature 421(421), 931-933.

Bjerrum C. J. and Canfield D. E. (2002) Ocean productivity before about 1.9 Gyr ago limited by phosphorus adsorption onto iron oxides. Nature 417, 159-162.

Blöchl E., Rachel R., Burggraf S., Hafenbradl D., Jannasch H. W., and Stetter K. O. (1997) Pyrolobus fumarii, gen. and sp. nov., represents a novel group of archaea, extending the upper temperature limit for life to 113°C. Extremophiles 1, 14-21.

Boetius A., Ravenschlag K., Schubert C. J., Rickert D., Widdel F., Giesecke A., Amann R., Jørgensen B. B., Witte U., and Pfannkuche O. (2000) A marine microbial consortium apparently mediating anaerobic oxidation of methane. Nature 407, 623-626.

Böning H. P., Böttcher M. E., Schnetger B., Kallmeyer J., Kriete C., and Brumsack H.-J. (submitted) Inorganic and sulfur isotope geochemistry of Holocene Peruvian upwelling sediments. Cheochimica et Cosmochimica Acta.

Böttcher M. E., Bernasconi S. M., and Brumsack H.-J. (1999) 32. Carbon, sulfur, and oxygen isotope Geochemistry of interstitial waters from the Western Mediterranean. In Proceedings of the Ocean Drilling Program, Scientific Results, Vol. 161 (ed. R. Zahn, M. C. Comas, and A. Klaus), pp. 413-421.

Böttcher M. E., Brumsack H.-J., and de Lange G. J. (1998) 29. Sulfate reduction and related stable isotope (34S, 18O) variations in interstitial waters from the Eastern Mediterranean. In Proceedings of the Ocean Drilling Progam, Scientific Results, Vol. 160 (ed. A. H. F. Robertson, K.-C. Emeis, C. RIchter, and A. Camerlenghi), pp. 365-373.

Brasier M. D., Green O. R., Jephcoat A. P., Kleppe A. K., Van Kranendonk M. J., Lindsay J. F., Steele A., and Grassineau N. V. (2002) Questioning the evidence for Earth's oldest fossils. Nature 416, 76-81.

Brock T. D. and Madigan M. T. (1984) Biology of Microorganisms. Prentice Hall.

Brocks J. J., Logan G. A., Buick R., and Summons R. E. (1999) Archean Molecular Fossils and the Early Rise of Eukaryotes. Science 285, 1033-1036.

Buick R., Thornett J. R., McNaughton N. J., Smith J. B., Barley M. E., and Savage M. (1995) Record of emergent continental crust ~3.5 billion years ago in the Pilbara craton of Australia. Nature 375, 574-577.

Burggraf S., Jannasch H. W., Nicolaus B., and Stetter K. O. (1990) Archaeoglobus profundus sp. nov., Represents a New Species within the Sulfate-reducing Archaebacteria. Systemantic and Applied Microbiology 13, 24-28.

Canfield D. E. (1989) Sulfate reduction and oxic respiration in marine sediments: Implications for organic carbon preservation in euxinic environments. Deep-Sea Research 36(1), 121-138.

Canfield D. E. (1991) Sulfate reduction in deep-sea sediments. American Journal of Science 291, 177-188.

Canfield D. E. (1998) A new model for Proterozoic ocean chemistry. Nature 396, 450-454.

Canfield D. E., Habicht K. S., and Thamdrup B. (2000) The Archean Sulfur Cycle and the Early History of Atmospheric Oxygen. Science 288, 658-661.

Canfield D. E. and Raiswell R. (1999) The Evolution of the Sulfur Cycle. American Journal of Science 299(7-9).

Canfield D. E., Raiswell R., Westrich J. T., Reaves C. M., and Berner R. A. (1986) The use of chromium reduction in the analysis of reduced inorganic sulfur compounds in sediments and shales. Chemical Geology 54, 149-155.

Canfield D. E. and Teske A. (1996) Late Proterozoic rise in atmospheric oxygen concentration inferred from phylogenetic and sulphur-isotope studies. Nature 382, 127-132.

Cann J. R. and Strens M. R. (1982) Black smokers fuelled by freezing magma. Nature 329, 104.

Cline J. D. (1969) Spectrophotometric Determination of Hydrogen Sulfide in Natural Waters. Limnology and Oceanography 14, 454-458.

Cornwell J. C. and Morse J. W. (1987) The characterization of iron sulfide minerals in anoxic marine sediments. Marine Chemistry 22, 193-206.

Cowen J. P., Giovannoni S. J., Kenig F., Johnson H. P., Butterfield D., Rappe M. S., Hutnak M., and Lam P. (2003) Fluids from Aging Ocean Crust That Support Microbial Life. Science 299, 120-123.

Cross M., Manning D., Bottrell S., and Worden R. (submitted) Thermochemical Sulphate Reduction (TSR): Experimental Determination of Reaction Kinetics and Implications of the Observed Reaction Rates for Petroleum Reservoirs. Organic Geochemistry.

Cross M. M. (1999) Rates and Mechanisms of Thermochemical Sulfate Reduction. PhD, University of Manchester.

Cypionka H. (1989) Characterization of sulfate transport in Desulfovibrion desulfuricans. Archives of Microbiology 152(3), 237-243.

Cypionka H. (1994) Sulfate transport. Methods in Enzymology 243, 3-14.

D'Hondt S., Rutherford S., and Spivack A. J. (2002) Metabolic Activity of Subsurface Life in Deep-Sea Sediments. Science 295, 2067-2069.

Duan W.-M., Coleman M. L., and Pye K. (1997) Determination of reduced sulphur species in sediments- an evaluation and modified technique. Chemical Geology 141, 185-194.

Einsele G., Gieskes J. M., Curray J., Moore D., M., Aguayo E., Aubry M.-P., Fornari D., Guerrero J., Kastner M., Kelts K., Lyle M., Matoba Y., Molina-Cruz A., Niemitz J., Rueda J., Saunders A., Schrader H., Simoneit B., and Vacquier V. (1980) Intrusion of basaltic sills into highly porous sediments and resulting hydrothermal activity. Nature 283, 441-445.

Elsgaard L., Isaksen M. F., Jørgensen B. B., Alayse A.-M., and Jannasch H. W. (1994) Microbial sulfate reduction in deep-sea sediments at the Guaymas Basin hydrothermal vent area: Influence of temperature and substrates. Geochimica et Cosmochimica Acta 58(16), 3335-3343.

Ferdelman T. G., Fossing H., Neumann K., and Schulz H. D. (1999) Sulfate reduction in surface sediments of the southeast Atlantic continental margin between 15°38'S and 27°57' S (Angola and Namibia). Limnology and Oceanography 44(3), 650-661.

Ferdelman T. G., Lee C., Pantoja S., Harder J., Bebout B., M., and Fossing H. (1997) Sulfate reduction and methanogenesis in a Thioploca-dominated sediment off the coast of Chile. Geochimica et Cosmochimica Acta 61(15), 3065-3079.

Fischer A. T. and Becker K. (1991) Heat flow, hydrothermal circulation and basalt intrusions in the Guaymas Basin, Gulf of California. Earth and Planetary Science Letters 103, 84-99.

Fossing H. (1990) Sulfate reduction in shelf sediments in the upwelling region off Central Peru. Continental Shelf Research 10(4), 355-367.

Fossing H. (1995) 35S-Radiolabeling to probe biogeochemical cycling of sulfur. In Geochemical Transformations of Sedimentary Sulfur, Vol. 612 (ed. M. A. Vairavamurthy and M. A. A. Schoonen). American Chemical Society.

Fossing H., Ferdelman T. G., and Berg P. (2000) Sulfate reduction and methane oxidation in continental margin sediments influenced by irrigation (South-East Atlantic off Namibia). Geochimica et Cosmochimica Acta 64(5), 897-910.

Fossing H., Gallardo V. A., Jørgensen B. B., Hüttel M., P. N. L., Schulz H., Canfield D. E., Forster S., Glud R. N., Gundersen J. K., Küver J., Ramsing N. B., Teske A., Thamdrup B., and Ulloa O. (1995) Concentration and transport of nitrate by the mat-forming sulphur bacterium Thioploca. Nature 374, 713-715.

Fossing H. and Jørgensen B. B. (1989) Measurements of bacterial sulfate reduction in sediments: Evaluation of a single-step chromium reduction method. Biogeochemistry 8, 205-222.

Fossing H. and Jørgensen B. B. (1990) Isotope exchange reactions with radiolabeled sulfur compounds in anoxic seawater. Biogeochemistry 9(3), 223-245.

Froelich P. N., Klinkhammer G. P., Bender M. L., Luedtke N. A., Heath G. R., Cullen D., Dauphin P., Hammond D., Hartman B., and Maynard V. (1979) Early oxidation of organic matter in pelagic sediments of the eastern equatorial Atlantic: suboxic diagenesis. Geochimica et Cosmochimica Acta 43, 1075-1090.

Goldhaber M. B. and Orr W., L. (1995) Kinetic controls on thermochemical sulfate reduction as a source of sedimentary H2S. In Geochemical Transformations of Sedimentary Sulfur, Vol. 612 (ed. M. A. Vairavamurthy and M. A. A. Schoonen), pp. 467. American Chemical Society.

Gundersen J. K., Jørgensen B. B., Larsen E., and Jannasch H. W. (1992) Mats of giant sulfur bacteria on deep-sea sediments due to fluctuating hydrothermal flow. Nature 360, 454-456.

Habicht K. S. and Canfield D. E. (2001) Isotope fractionation by sulfate-reducing natural populations and the isotopic composition of sulfide in marine sediments. Geology 29(6), 555-558.

Habicht K. S., Gade M., Thamdrup B., Berg P., and Canfield D. E. (2002) Calibration of Sulfate Levels in the Archaean Ocean. Science 298, 2372-2374.

Hansen J. W., Thamdrup B., and Jørgensen B. B. (2000) Anoxic incubation of sediment in gas-tight plastic bags: A method for biogeochemical process studies. Marine Ecology Progress Series 208, 273-282.

Harder J. (1997) Anaerobic methane oxidation by bacteria employing 14C-methane uncontaminated with 14C-carbon monoxide. Marine Geology 137, 13-23.

Henrichs S. M. (1992) Early diagenesis of organic matter in marine sediments: progress and perplexity. Marine Chemistry 391, 119-149.

Hinrichs K.-U. and Boetius A. (2003) The anaerobic oxidation of methane: new insights in microbial ecology and biogeochemistry. In Ocean Margin Systems (ed. G. Wefer, D. Billett, D. Hebbeln, B. B. Jørgensen, M. Schlüter, and T. van Weering). Springer.

Hoehler T. M., Alperin M. J., Albert D. B., and S. M. C. (1994) Field and Laboratory studies of methane oxidation in an anoxic marine sediment: Evidence for a methanogen-sulfate reducer consortium. Global Geochemical Cycles 8(4), 451-463.

Honma H. (1996) High ammonium content in the 3800 Ma Isua supracrustal rocks, central West Greenland. Geochimica et Cosmochimica Acta 60(12), 2173-2178.

Hovland M., Hill A., and Stokes D. (1997) The structure and geomorphology of the Dashgil mud volcano, Azerbaijan. Geomorphology 21, 1-15.

Howarth R. W. and Giblin A. (1983) Sulfate reduction in the salt marshes at Sapelo Island, Georgia. Limnology and Oceanography 28(1), 70-82.

Hsieh Y. P. and Yang C. H. (1989) Diffusion methods for the determination of reduced inorganic sulfur species in sediments. Limnology and Oceanography 34(6), 1126-1130.

Iversen N. and Jørgensen B. B. (1985) Anaerobic methane oxidation rates at the sulfate-methane transition in marine sediments from Kattegat and Skagerrak (Denmark). Limnology and Oceanography 30(5), 944-955.

Jannasch H. W., Nelson D., C., and Wirsen C. O. (1989) Massive natural occurrence of unusually large bacteria (Beggiatoa sp.) at a hydrothermal deep-sea vent site. Nature 342, 834-836.

Jannasch H. W. and Taylor C. D. (1984) Deep-Sea Microbiology. Annual Reviews in Microbiology 38, 487-514.

Jannasch H. W., Wirsen C. O., Molyneaux S. J., and A. L. T. (1988) Extremely Thermophilic Fermentative Archaebacteria of the Genus Desulfurococcus from Deep-Sea Hydrothermal Vents. Applied and Environmental Microbiology 54(5), 1203-1209.

Jørgensen B. B. (1978a) A Comparison of Methods for the Quantification of Bacterial Sulfate Reduction in Coastal Marine Sediments 1. Measurement with radiotracer techniques. Geomicrobiology Journal 1(1), 11-27.

Jørgensen B. B. (1978b) A Comparison of Methods for the Quantification of Bacterial Sulfate Reduction in Coastal Marine Sediments 2. Calculation from mathematical models. Geomicrobiology Journal 1(1), 29-47.

Jørgensen B. B. (1978c) A Comparison of Methods for the Quantification of Bacterial Sulfate Reduction in Coastal Marine Sediments 3. Estimation from chemical and bacteriological field data. Geomicrobiology Journal 1(1), 49-64.

Jørgensen B. B. (1982a) Ecology of the sulfur cycle with special referene to anoxic-oxic interfaces. Philosophical Tranactions of the Royal Society of London B298, 543-561.

Jørgensen B. B. (1982b) Mineralization of organic matter in the sea bed-the role of sulphate reduction. Nature 296, 643-644.

Jørgensen B. B. (1990) A Thiosulfate Shunt in the sulfur Cycle of Marine Sediments. Science 249, 152-154.

Jørgensen B. B., Bang M., and Blackburn T. H. (1990a) Anaerobic mineralization in marine sediments from the Baltic Sea-North Sea transition. Marine Ecology Progress Series 59, 39-54.

Jørgensen B. B. and DesMarais D. J. (1986) Competition for sulfide among colorless and purple sulfur bacteria in cyanobacterial mats. FEMS Microbiology Ecology 38(3), 179-186.

Jørgensen B. B. and Fenchel T. (1974) The Sulfur Cycle of a Marine Sediment Model System. Marine Biology 24, 189-201.

Jørgensen B. B., Isaksen M. F., and Jannasch H. W. (1992) Bacterial sulfate reduction above 100 °C in deep-sea hydrothermal vent sediments. Science 258, 1756-1757.

Jørgensen B. B., Weber A., and Zopfi J. (2001) Sulfate reduction and anaerobic methane oxidation in Black Sea sediments. Deep Sea Research 1 48, 2097-2120.

Jørgensen B. B., Zawacki L. X., and Jannasch H. W. (1990b) Thermophilic bacterial sulfate reduction in deep-sea sediments at the Guaymas Basin hydrothermal vent site (Gulf of Califonia). Geochimica et Cosmochimica Acta 37, 695-710.

Joye S. B., Boetius A., Orcutt B. N., Montoya J. P., Schulz H. N., Erickson M. J., and Lugo S. (2003, in press) The anaerobic oxidation of methane and sulfate reduction in sediments from Gulf of Mexico cold seeps. Chemical Geology.

Kallmeyer J., Ferdelman T. G., Jansen K.-H., and Jørgensen B. B. (2003) A high-pressure thermal gradient block for investigating microbial activity in multiple deep-sea samples. Journal of Microbiological Methods 1846, 1-8.

Kawka O. E. and Simoneit B. R. T. (1994) Hydrothermal pyrolisis of organic matter in Guaymas Basin: I. Comparison of hydrocarbon distributions in subsurface sediments and seabed petroleums. Organic Geochemistry 22(6), 947-978.

King G. M. (2001) Radiotracer Assays (35S) of Sulfate Reduction Rates in Marine and Freshwater Sediments. In Methods in Microbiology, Vol. 30. Academic Press.

Kiyosu Y. and Krouse H. R. (1990) Thermochemical resuction and the abiogenic reduction of sulfate by acetic acid in the presence of native sulfur. Geochemical Journal 27, 49-57.

Knoblauch C., Jørgensen B. B., and Harder J. (1999) Community Size and Metabolic Rates of Psychrophilic Sulfate-Reducing Bacteria in Arctic Marine Sediments. Applied and Environmental Microbiology 65(9), 4230-4233.

Lasaga A. C. and Kirkpatrick R. J. (1981) Kinetics of geochemical processes. In Reviews in Mineralogy, Vol. 8, pp. 398. Mineralogical Society of America.

Lin L.-H., Onstott T. C., Lippmann J., Ward J., Hall J., and Sherwood Lollar B. (2002) Radiogenic H2 in continental crust: A potential energy source for microbial metabolism in deep biosphere. Geochimica et Cosmochimica Acta, special supplement 66(15A), A457.

Llobet-Brossa E., Rabus R., Böttcher M. E., Könneke M., Finke N., Schramm A., Mezer R. L., Grötzschel S., Rosselo-Mora R., and Amann R. (2002) Community structure and activity of sulfate-reducing bacteria in an intertidal surface sediment: a multi-method approach. Aquatic Microbial Ecology 29, 211-226.

Llobet-Brossa E., Rossello-Mora R., and Amann R. (1998) Microbial Community Composition of Wadden Sea Sediments as Revealed by Fluorescence In Situ Hybridization. Applied and Environmental Microbiology 64(7), 2691-2696.

Lonsdale P. and Becker K. (1985) Hydrothermal plumes, hot springs, and conductive heat flow in the Southern Trough of Guaymas Basin. Earth and Planetary Science Letters 73, 211-225.

Low P. F. (1981) Principles of ion diffusion in clays. In Chemistry in the Soil Environment, Vol. 40, pp. 31-45. Amercian Society for Agronomy.

Luther G. W. I. (1987) Pyrite oxidation and reduction: Molecular orbital theory considerations. Geochimica et Cosmochimica Acta 51(12), 3193-3199.

Machel H. G. (2001) Bacterial and thermochemical sulfate reduction in diagenetic settings-old and new insights. Sedimentary Geology 140, 143-175.

Magenheim A. J. and GIeskes J. M. (1992) Hydrothermal discharge and alteration in near-surface sediments from the Guaymas Basin, Gulf of California. Geochimica et Cosmochimica Acta 56, 2329-2338.

Martens C. S. (1990) Generation of short chain organic acid anions in hydrothermally altered sediments of the Guaymas Basin, Gulf of California. Applied Geochemistry 5(1/2), 71-76.

Martens C. S. (1993) Recycling efficiencies of organic carbon, nitrogen, phosphorus and reduced sulfur in rapidly depositing coastal sediments. In Interaction of C, N, P and S Biogeochemical Cycles and Global Change, Vol. 14 (ed. R. Wollast, F. T. Mackenzie, and I. Chou), pp. 379-400. Springer-Verlag.

Martens C. S., Albert D. B., Alperin M. J., Taylor C. D., and J. C. E. (1998) Shipboard and in-situ measurements of sulfate reduction in upper slope sediments at 36° 20'N to 35°25'N north of Cape Hatteras, NC (USA). EOS, Trans. Am. Geophys. Union Ocean Sci. Mtg. Suppl. 79, OS183.

Martens C. S. and Berner R. A. (1974) Methane Production in the Interstitial Waters of Sulfate-Depleted Marine Sediments. Science 185, 1167-1169.

Martens C. S. and Klump J. V. (1984) Biogeochemical cycling in an organic-rich coastal marine basin 4. An organic carbon budget for sediments dominated by sulfate reduction and methanogenesis. Geochimica et Cosmochimica Acta 48(10), 1987-2004.

Martin W. and Russel J. (2002) On the origins of cells: a hypothesis for the evolutionary transitions from abiotic geochemistry to chemoautotrophic procaryotes, and from procaryotes to nucleated cells. Phil. Trans. R. Soc. Lond. B. 358, 59-85.

Michaelis W., Seifert R., Nauhaus K., Treude T., Thiel V., Blumenberg M., Knittel K., Gieseke A., Peterknecht K., Pape T., Boetius A., Amann R., Jørgensen B. B., Widdel F., Peckmann J., Pimenov N. V., and Gulin M. B. (2002) Microbial Reefs in the Black Sea fueled by anaerobic oxidation of methane. Science 297, 1012-1015.

Morita R. Y. (2000) Is H2 the universal energy source for long-tern survival? Microbial Ecology 38, 307-320.

Morita R. Y. and ZoBell C. E. (1955) Occurrence of bacteria in pelagic sediments collected during the Mid-Pacific Expedition. Deep-Sea Research 3, 6-73.

Mottl M. J., Holland H. D., and Corr R. F. (1979) Chemical exchange during hydrothermal alteration of basalt by seawater-II. Experimental results for Fe, Mn, and sulfur species. Geochimica et Cosmochimica Acta 43, 869-884.

Nauhaus K., Boetius A., Krüger M., and Widdel F. (2002) In vitro demonstration of anaerobic oxidation of methane coupled to sulphate reduction in sediment from a marine gas hydrate area. Environmental Microbiology 4(5), 296-305.

Niewöhner C., Hensen C., Kasten S., Zabel M., and Schulz H. D. (1998) Deep sulfate reduction completely mediated by anaerobic methane oxidation in

sediments of the upwelling area off Namibia. Geochimica et Cosmochimica Acta 62(3), 455-464.

Niggemann J., Kallmeyer J., and SChubert C. (2002) Sediments in the Peruvian upwelling region: Organic matter composition and sufate reduction rates. Geochimica et Cosmochimica Acta 66(15 A, Suppl. 1), A555.

Nisbet E. G. and Sleep N. H. (2001) The habitat and nature of erly life. Nature 409, 1083-1091.

Ohmoto H. and Lasaga A. C. (1982) Kinetics of reactions between aqueous sulfates and sulfides in hydrothermal systems. Geochimica et Cosmochimica Acta 46, 1727-1745.

Orcutt B. N., Boetius A., Lugo S., MacDonald I. R., and Samarkin V. A. (2003, in press) Life at the Edge of Methane Ice: Microbial Cycling of Carbon and Sulfur in Gulf of Mexico Gas Hydrates. Chemical Geology.

Orphan V. J., House C. H., Hinrichs K.-U., McKeegan K. D., and DeLong E. (2001) Methane-Consuming Archaea Revealed by Directly Coupled Isotopic and Phylogenetic Analysis. Science 293, 484-487.

Orr W. L. (1992) Rate and mechanism of non-biological sulfate reduction. 95th Annual Geological Society of America Meeting.

Parkes R. J., Cragg B. A., Bale S. J., Getliff J. M., Goodman K., Rochelle P. A., Fry J. C., Weightman A. J., and Harvey S. M. (1994) Deep bacterial biosphere in Pacific Ocean sediments. Nature 371, 410-413.

Parkes R. J., Cragg B. A., Getliff J. M., Harvey S. M., Fry J. C., Lewis C. A., and Rowland S. J. (1993) A quantitative study of microbial decomposition of biopolymers in Recent sediments from the Peru Margin. Marine Geology 113, 55-66.

Parkes R. J., Cragg B. A., and Wellsbury P. (2000) Recent studies on bacterial populations and processes in subsea-floor sediments: A review. Hydrogeology Journal 8, 11-28.

Peckmann J., Gischler E., Oschmann W., and Reitner J. (2001a) An Early Carboniferous seep community and hydrocarbon-derived cabonates from the Harz Mountains, Germany. Geology 29(3), 271-274.

Peckmann J., Goedert J. L., Thiel V., Michaelis W., and Reitners J. (2002) A comprehensive approach to the study of methane-seep deposits from the Lincoln Creek Formation, western Washington State, USA. Sedimentology 49, 855-873.

Peckmann J., Reimer A., Luth U., Luth C., Hansen B. T., Heinicke C., Hoefs J., and Reitner J. (2001b) Methane-derived carbonates and authigenic pyrite from

the northwestern Black Sea. Marine Geology 177, 129-150.

Phelps T. J., Murphy E. M., Pfiffner S. M., and White D. C. (1994) Comparison between geochemical and biological estimates of subsurface microbial activities. Microbial Ecology 28, 335-349.

Ravenschlag K., Sahm K., Knoblauch C., Jørgensen B. B., and Amann R. (2000) Community Structure, Cellular rRNA Content, and Activity of Sulfate-Reducing Bacteria in Marine Arctic Sediments. Applied and Environmental Microbiology 66(8), 3592-3602.

Reysenbach A.-L. and Shock E. (2002) Merging Genomes with Geochemistry in Hydrothermal Ecosystems. Science 296, 1077-1082.

Schippers A. and Jørgensen B. B. (2001) Oxidation of pyrite and iron sulfide by manganese dioxide in marine sediments. Geochimica et Cosmochimica Acta 65(6), 915-922.

Schippers A. and Jørgensen B. B. (2002) Biogeochemistry of pyrite and iron sulfide oxidation in marine sediments. Geochimica et Cosmochimica Acta 66(1), 85-92.

Schmaljohann R., Drews M., Walter S., Linke P., von Rad U., and Imhoff J. F. (2001) Oxygen-minimum zone sediments in the northeastern Arabian Sea off Pakistan: a habitat for the bacterium Thioploca. Marine Ecology Progress Series 211, 27-42.

Schopf J. W., Kudryavtsev A. B., Agresti D. G., Wdowiak T. J., and Czaja A. D. (2002) Laser-Raman imagery of Earth's earliest fossils. Nature 416, 73-76.

Schouten S., Wakeham S. G., Hopmans E. C., and Sinninghe Damste J. S. (2003) Biogeochemical Evidence that Thermophilic Archaea Mediate the Anaerobic Oxidation of Methane. Applied and Environmental Microbiology 69(3), 1680-1686.

Schubert C. J., Ferdelman T. G., and Strotmann B. (2000) Organic matter composition and sulfate reduction rates in sediments off Chile. Organic Geochemistry 31, 351-361.

Schulz H. D., Dahmke A., Schinzel U., Wallmann K., and Zabel M. (1994) Early diagenetic processes, fluxes, and reaction rates in sediments of the South Atlantic. Geochimica et Cosmochimica Acta 58(9), 2041-2060.

Schulz H. N., Brinkhoff T., Ferdelman T. G., Hernandez Marine M., Teske A., and Jørgensen B. B. (1999) Dense Populations of a Giant Sulfur Bacterium in Namibian Shelf Sediments. Science 284, 493-495.

Shen Y., Buick R., and Canfield D. E. (2001) Isotopic evidence for microbial sulphate reduction in the early Archean era. Nature 410, 77-80.

Simoneit B. R. T. and Lonsdale P. F. (1982) Hydrothermal petroleum in mineralized mounds at the seabed of Guaymas Basin. Nature 295, 198-202.

Simoneit B. R. T. and Schoell M. (1995) Carbon isotope systematics in individual hydrocarbons in hydrothermal petroleums from the Guaymas Basin, Gulf of California. Organic Geochemistry 23(9), 857-863.

Simpson G. (1996) Oil, water, and gas from carbonate, Devonian reservoirs of Alberta, emphasis on thermochemical sulfate reduction. The origins of sulphur in natural gas and liquid hydrocarbons.

Skoog D. A. and Leary J. J. (1992) Principles of Instrumental Analysis. Saunders College Publishing.

Skyring G. W. (1987) Sulfate Reduction in Coastal Ecosystems. Geomicrobiology Jounral 5(3/4), 295-374.

Sorokin Y. I. (1962a) Experimental investigation of bacterial sulfate reduction in the Black Sea using S-35. Microbiology (Engl. transl.) 31, 329-335.

Sorokin Y. I. (1962b) Experimental investigations of bacterial sulfate reduction in the Black Sea using 35-S. Microbiology (Engl. transl.) 31, 329-335.

Stasiuk L. D. (1996) Reflected light optical properties and micro textures of pyrobitumens from Upper Devonian Leduc Formation: evidence for oil-gas transformations disrupted by possible late stage TSR alteration. The origins of sulphur in natural gas and liquid hydrocarbons.

Stetter K. O. (1988) Archaeoglobus fulgidus gen. nov. sp. nov.: a New Taxon of extremely Thermophilic Archaebacteria. Systematic and Applied Microbiology 10, 172-173.

Teske A., Hinrichs K.-U., Edgcomb V., de Vera Gomez A., Kysela D., Sylva S. P., Sogin M. L., and Jannasch H. W. (2002) Microbial Diversity of Hydrothermal Sediments in the Guaymas Basin: Evidence for Anaerobic Methanotrophic Communities. Applied and Environmental Microbiology 68(4), 1994-2007.

Thamdrup B., Finster K., Hansen J. W., and Bak F. (1993) Bacterial Disproportionation of Elemental Sulfur Coupled to Chemical Reduction of Iron and Manganese. Applied and Environmental Microbiology 59(1), 101-108.

Toland W. G. (1960) Oxidation of organic compounds with aqueous sulfate. Journal of the American Chemical Society 82, 1911-1916.

Treude T., Boetius A., Knittel K., Wallmann K., and Jørgensen B. B. (submitted) Anaerobic oxidation of methane above gas hydrates (Hydrate Ridge, OR). Submitted to Marine Ecology Progress Series.

Trudinger P. A., Chambers L. A., and Smith J. W. (1985) Low-temperature sulphate reduction: biological versus abiological. Canadian Journal of Earth Sciences 22, 1910-1918.

Ulrich G. A., Krumholz L. R., and Suflita J. M. (1997) A rapid and simple method for estimating sulfate reduction activity and quantifying inorganic sulfides. Applied and Environmental Microbiology 63(4), 1627-1630.

Valentine D. L. and Reeburgh W. S. (2000) New perspectives on anaerobic methane oxidation. Environmental Microbiology 2(5), 477-484.

Vreeland R. H., Rosenzweig W. D., and Powers D., W. (2000) Isolation of a 250 million-year-old halotolerant bacterium from a primary salt crystal. Nature 407, 897-900.

Wade M. (1968) Preservation of soft-bodied animals in Precambrian sandstones at Ediacara, South Australia. Lethaia 1(3), 238.

Weber A. and Jørgensen B. B. (2002) Bacterial sulfate reductio in hydrothermal sediments of the Guaymas Basin, Gulf of California, Mexico. Deep Sea Research I 49, 827-841.

Weber A., Riess W., Wenzhoefer F., and Jørgensen B. B. (2001) Sulfate reduction in Black Sea sediments: in situ and laboratory radiotracer measurements from the shelf to 2000 m depth. Deep Sea Research 1 48, 2073-2096.

Wenzhöfer F. and Glud R. N. (2002) Benthic carbon mineralization in the Atlantic: a synthesis based on in situ data from the last decade. Deep Sea Research I 49, 1255-1279.

Whelan J. A. (1988) Origins of methane in hydrothermal systems. Chemical Geology 71(1), 183-198.

Whelan J. K., Oremland R., Tarafa M., Smith R., Howarth R., and Lee C. (1985) Evidence for sulfate-reducing and methane producing microorganisms in sediments from sites 618, 619, and 622. ODP 767-775.

Widdel F. (1988) Microbiology and ecology of sulfate- and sulfur-reducing Bacteria. In Ecology of anaerobic microorganisms (ed. A. Zehnder), pp. 469-585.

Worden R. H. and Smalley P. C. (1996) H2S-producing reactions in deep carbonate reservoirs: Khuff Formation, Abu Dhabi. Chemical Geology 133, 157-171.

Worden R. H., Smalley P. C., and Oxtoby N. H. (1996) The effects of thermochemical sulfate reduction upon formation water salinity in carbonate reservoirs. Geochimica et Cosmochimica Acta 60(20), 3925-3931.

Worden R. H., Smallez P. C., and Cross M. M. (2000) The influence of rock fabric and mineralogy on thermochemical sulfate reduction: Khuff Formation, Abu

Dhabi. Journal of Sedimentary Research 70(5), 1210-1221.

Worthmann U. G., Bernasconi S. M., and E. B. M. (2001) Hypersulfidic deep biosphere indicates extreme sulfur isotope fractionation during single-step microbial sulfate reduction. Geology 29(7), 647-650.

Yamamoto S., Alcauskas J. B., and Crozier T. E. (1976) Solubility of methane in distilled water and seawater. Journal of Chemical and Engineering Data 21(1), 78-80.

Zhabina N. N. and Volkov I. I. (1978) A method of determination of various sulfur compounds in sea sediments and rocks. In Environmental biogeochemistry and geomicrobiology (ed. W. E. Krumbein), pp. 735-745. Ann Arbor Sci.

Zhao H., Wood A. G., Widdel F., and Bryant M. P. (1988) An extremely thermophilic Methanococcus from a deep sea hydrothermal vent and its plasmids. Archives of Microbiology 150, 178-183.

ZoBell C. E. (1952) Bacterial Life at the Bottom of the Phillipne Trench. Science 115, 507-508.

Danksagung

Herrn Professor Bo Barker Jørgensen sei für die Vergabe und Begutachtung der Arbeit gedankt.
Herrn Professor Jörn Peckmann danke ich für die Übernahme des Zweitgutachtens.
Ein ganz großes Dankeschön geht an Tim Ferdelman für die Betreuung meines Projekts. Mit vielen Diskussionen und Anregungen hat er sehr zum Gelingen der Arbeit beigetragen.
Ohne die tatkräftige Hilfe von Kirsten Neumann und den anderen TA's der Biogeochemie hätten viele Sachen nicht so gut geklappt.
Ein großes Dankeschön geht an Paul Färber, Georg Herz, Volker Meyer, Alfred Kutsche, Jens Langreder, Axel Nordhausenund Harald Osmers von den Werkstätten des MPI, die immer ein offenes Ohr für meine manchmal recht extravaganten Ideen hatten und mir immer wieder geholfen haben wenn meine handwerklichen Fähigkeiten nicht ausreichten.
Ohne die Kommentare und Ideen der Co-Autoren wäre wohl keines der Paper in dieser Form entstanden, dafür danke ich Henrik Fossing, Andreas Weber, Karl-Heinz Jansen, Antje Boetius und Ivano Aiello.
Für die vielen kleinen Kommentare, Korrekturen, Randbemerkungen und Unterstützung geht ein dickes Dankeschön an Eli und Hans.
Natürlich dürfen auch die anderen Doktoranden nicht unerwähnt bleiben, insbesondere Tina, Niko und Jutta.
Dank gebührt meinen Mitfahrern und den Mannschaften auf den Forschungsschiffen auf denen die Proben für diese Arbeit gesammelt wurden und all den anderen Menschen, die auf die eine oder andere Weise zum gelingen dieser Arbeit begetragen haben.
Kai Hövelmann sei gedankt für das liebevolle Umsorgen meiner feuchten Pfleglinge wenn ich mal wieder unterwegs war.
Dafür, daß er es schon so lange mit mir aushält und meine eigenwillige Zeitplanung zwar nicht immer gebilligt so doch akzeptiert hat geht ein großes Dankeschön an Frank Hagemann. Außerdem gebührt ihm Dank für das Layout der Arbeit.
Meinen Eltern danke ich für die vielen Jahr der Unterstützung, obwohl sie bei vielen Sachen nicht wussten, ob es Sinn macht. Ohne sie wäre ich heute nicht da wo ich jetzt bin.